MINNESOTA GEOLOGICAL SURVEY
Harvey Thorleifson, *Director*

REEXAMINATION OF THE MINNESOTA RIVER VALLEY SUBPROVINCE WITH EMPHASIS ON NEOARCHEAN AND PALEOPROTEROZOIC EVENTS

David L. Southwick

Report of Investigations 69
ISSN 0076-9177

UNIVERSITY OF MINNESOTA
Saint Paul — 2014

REEXAMINATION OF THE MINNESOTA RIVER VALLEY SUBPROVINCE WITH EMPHASIS ON NEOARCHEAN AND PALEOPROTEROZOIC EVENTS

This publication is accessible from the home page of the Minnesota Geological Survey (http://www.mngs.umn.edu as a PDF file readable with Acrobat Reader 5.0.

Date of release: February, 2014

Recommended citation

Southwick, D.L., 2014, Reexamination of the Minnesota River valley subprovince with emphasis on Neoarchean and Paleoproterozoic events: Minnesota Geological Survey Report of Investigations 69, 52 p.

Minnesota Geological Survey
2642 University Avenue West
Saint Paul, Minnesota 55114-1057

Telephone: 612-627-4780
Fax: 612-627-4778
E-mail address: mgs@umn.edu
Web site: http://www.mngs.umn.edu

ISSN 0076-9177

CONTENTS

FIGURES

TABLES

NOTE ON MEASUREMENTS USED IN THIS REPORT

Although the metric system is preferred in scientific writing, certain measurements are still routinely made in English customary units; for example, distances on land are measured in miles and depths in drill holes are measured in feet. Preference was given in this report to retaining the units in which measurements were made. To assist readers, conversion factors for some of the common units of measure are provided below.

English units to metric units:

To convert from	to	multiply by
inch	millimeter	25.40
inch	centimeter	2.450
foot	meter	0.3048
mile	kilometer	1.6093

Metric units to English units:

To convert from	to	multiply by
millimeter	inch	0.03937
centimeter	inch	0.3937
meter	foot	3.2808
kilometer	mile	0.6214

REEXAMINATION OF THE MINNESOTA RIVER VALLEY SUBPROVINCE WITH EMPHASIS ON NEOARCHEAN AND PALEOPROTEROZOIC EVENTS

David L. Southwick

ABSTRACT

The Minnesota River valley subprovince (MRV) is a fragment of Mesoarchean continental crust that was sutured to the southern margin of the Superior craton about 2,600 m.y. ago. The suturing event induced widespread regional metamorphism and local anatexis in a dominantly orthogneissic crust and ended with the emplacement of numerous granite plutons. In the Paleoproterozoic era the MRV was a tectonically rigid part of the cratonic foreland with respect to Penokean (geon 18), Yavapai (geon 17), and Mazatzal (geon 16) accretionary events. As such, it was affected by crustal extension and the emplacement of mafic dikes associated with the ca. 2,070 Ma opening of the pre-Penokean ocean. Subsequently, internal shear zones that had formed during Neoarchean docking of the MRV crustal block were reactivated in response to stresses applied during cycles of Paleoproterozoic stretching and subsequent compression from the south and southeast. Most of this reactivation is inferred to have taken place between 2,000 and 1,750 Ma. The Minnesota segment of the Great Lakes tectonic zone, the Neoarchean suture, was not significantly reactivated, whereas the Appleton shear zone and the Yellow Medicine shear zone both were. Six sets of mafic dikes were emplaced in the interval between 2,070 and ca. 1,750 Ma. Two sets that were emplaced early in the interval are the southwesternmost members of the pre-Penokean Kenora–Kabetogama/Fort Frances dike swarm. Two and perhaps four younger dike sets were emplaced during a period of vigorous crustal heating and magmatic activity that affected much of the MRV in early- to mid-geon 17. Numerous plugs and small plutons also were emplaced in early- to mid-geon 17. These intrusions range in composition from peridotite to granite and are comparable to rock types within and satellitic to the East-Central Minnesota batholith; they are most abundant in the eastern and southern parts of the MRV, relatively near the inferred Penokean and Yavapai tectonic fronts. Transtensional stress during the extensional stage of the Mazatzal orogenic cycle generated differential subsidence of crust south of the Yellow Medicine shear zone and produced en echelon fault-bounded depressions that became depocenters filled by supermature clastic sediment ancestral to the Sioux Quartzite. The Sioux Quartzite was deposited, lithified, and hydrothermally altered over a prolonged time interval that may have begun as early as ca. 1,730 and ended as recently as ca. 1,280 Ma.

PURPOSE AND SCOPE

The Precambrian rocks that crop out along the Minnesota River have attracted interest for generations. Geologists and topographers travelling with mid-nineteenth century military expeditions recorded their observations in expedition reports, and later N.H. Winchell published a summary of the geologic conditions in the counties of southwestern Minnesota that has become a classic example of late 19th century scientific reporting (Winchell and Upham, 1888). J.A. Grant (1972) remarked in his summary paper on the geology of Minnesota River valley that the outcrops there provide just a "tantalizing glimpse" of a complex Precambrian terrane that cannot be seen away from the valley because it is almost totally covered by Phanerozoic sedimentary strata.

The present contribution is a synthesis of new and previously published information on the geology of a Precambrian terrane now known as the Minnesota River valley subprovince of the Superior Province of the Canadian Shield (terminology of Card, 1990). The rocks of the subprovince reveal a long record of continental growth and development. The subprovince consists predominantly of Mesoarchean quartzofeldspathic gneiss and migmatite and large intrusions of Neoarchean tonalite and granite. It also contains numerous Paleoproterozoic intrusions and a variety of shear zones and faults that are inferred to have been active in the Paleoproterozoic era. The latest stages of Paleoproterozoic tectonism affected the depositional history, alteration, and deformation of the Sioux Quartzite, a tightly cemented, supermature quartz arenite that unconformably overlies various Archean and Paleoproterozoic crystalline rocks that form the primary foundation of the subprovince. In the interest of clarity and brevity, the acronym MRV will hereafter refer to the geologic subprovince, and the geographic name Minnesota River valley will refer to the physiographic feature in the present landscape. Also, the term Superior craton will be used in place of Superior Province.

The research published on the MRV in the past 60 years has dealt primarily with the Archean components of the terrane. The less abundant Paleoproterozoic rocks have received only sporadic study and much of the record of this research is dispersed in locally focused reports by the Minnesota Geological Survey, dormant Minnesota Geological Survey files, and university theses. The updated summary presented here incorporates much of this relatively obscure information, and also includes the findings from topical studies completed since the most recent integrated summary of MRV geology was compiled (Bauer and Himmelberg, 1993). The interpretations presented are heavily dependent on regional aeromagnetic and gravity data that allow the MRV to be "seen" well beyond the narrow strip of outcrops along the Minnesota River. Many of the conclusions are tentative due to limited outcrop, scarcity of drill-hole samples, and variably inadequate petrologic, geochemical, and geochronologic databases. Suggestions for future research are distributed throughout with the expectation that some of them will eventually be followed.

REGIONAL CONTEXT

Collectively, several recent geologic, geochemical, geophysical, and geochronologic studies have shown that Archean rocks near the southern margin of the Superior craton were significantly involved in Paleoproterozoic tectonism (Holm and others, 2005; Schmitz and others, 2006; Chandler and others, 2007; Holm and others, 2007; NICE Working Group, 2007; Schulz and Cannon, 2007; Van Schmus and others, 2007). Moreover, it is becoming increasingly clear that far-field events associated with Yavapai (geon 17) and Mazatzal (geon 16) tectonism affected previously accreted Penokean (geon 18) and older terranes as the Laurentian continent grew southward (Fig. 1). The Archean core of the MRV apparently withstood these repeated accretionary assaults without acquiring deformational fabrics or regional metamorphic imprint. A specific conclusion particularly relevant to the present synopsis is the recognition that the east end of the MRV was an east-facing promontory (present directions) of tectonically stiff continental crust that deflected structural trends of the Penokean orogen from east–west to south–southwest as the putative pre-Penokean ocean closed in mid-geon 18 (Fig. 2; Chandler and others, 2007; Schulz and Cannon, 2007).

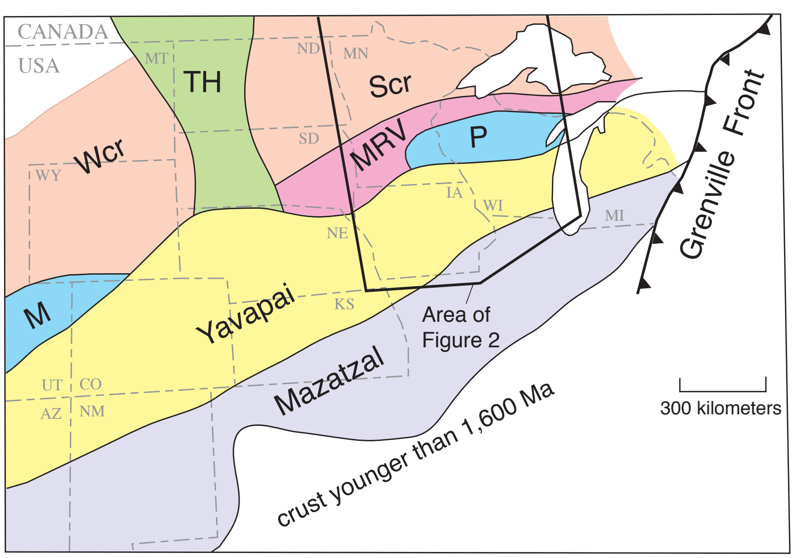

Figure 1. Regional Precambrian terrane map of the north-central United States showing the position of the Minnesota River valley subprovince (MRV) relative to the age-distinguished Paleoproterozoic belts that constitute the south flank of the Laurentian craton. The area mapped as Penokean (P) contains isotopically juvenile crust that was accreted to the Superior craton in geon 18; Penokean-age and older foreland deposits that were emplaced upon the margin of the Superior craton are not shown. Scr = Superior craton (Archean), Wcr = Wyoming craton (Archean), TH = Trans-Hudson orogen, M = Mojave terrane. The area shown in Figure 2 is outlined.

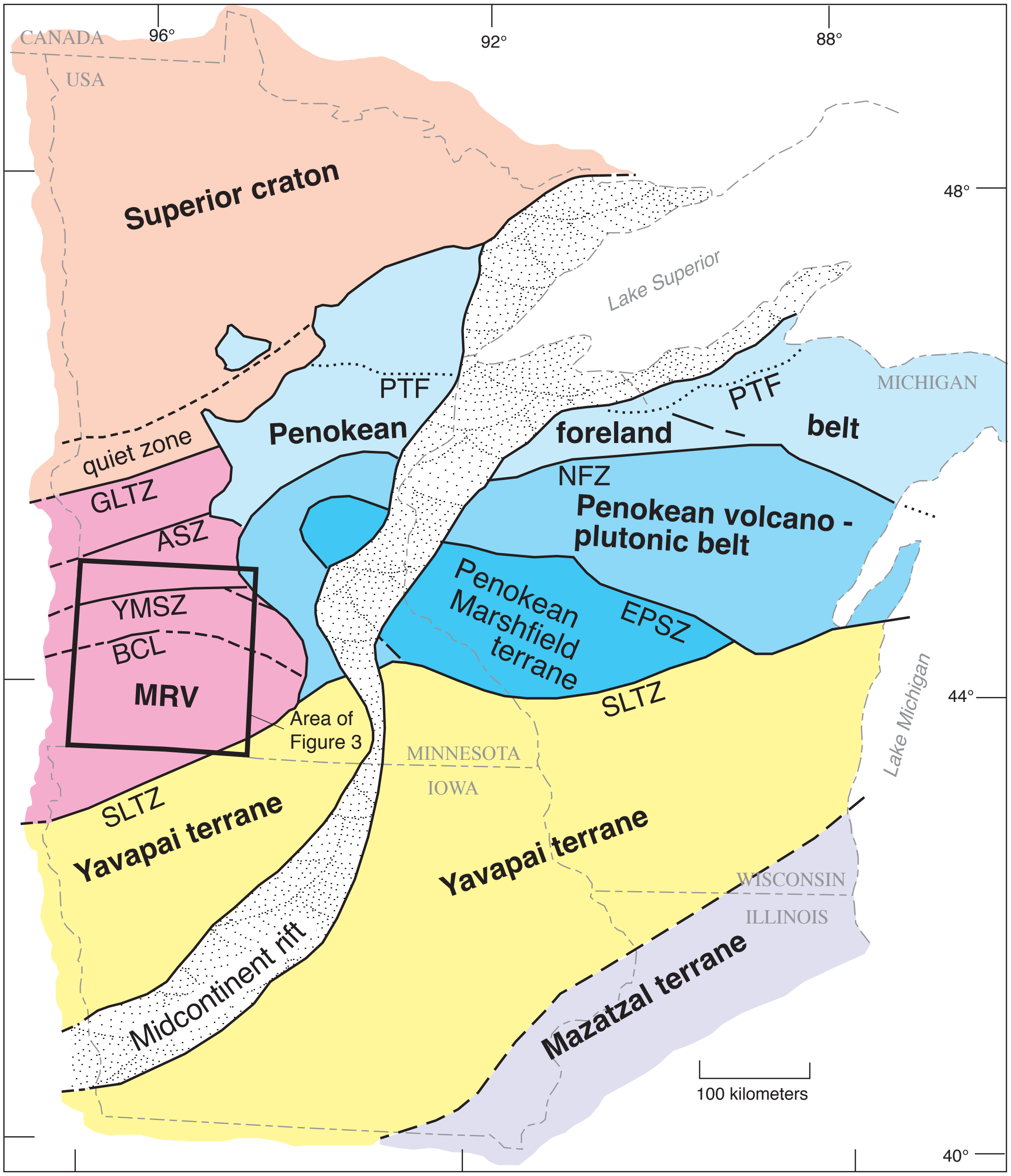

Figure 2. Tectonic sketch map of the west end of the Penokean orogen and its Archean foreland. The dominantly Mesoarchean MRV occupies a foreland promontory opposite a poorly defined recess in the Penokean tectonic front. GLTZ = Great Lakes tectonic zone, ASZ = Appleton shear zone, YMSZ = Yellow Medicine shear zone, BCL = Brown County lineament, SLTZ= Spirit Lake tectonic zone, NFZ = Niagara fault zone, EPSZ = Eau Pleine shear zone, PTF = Penokean tectonic front. Map modified from NICE Working Group (2007; their Fig. 3). The area shown in Figure 3 is outlined.

Although the MRV was essentially stable and passive during active Paleoproterozoic tectonism on the east, south, and west, it was invaded by many relatively small and scattered igneous bodies that range in composition from granite to peridotite and in age from 2.07 to 1.79 Ga and possibly younger. Furthermore, it responded to external tectonic stress by faulting internally, mainly along pre-existing zones of weakness. The geophysics-dependent subsurface geologic map of southwestern Minnesota (Fig. 3; Southwick, 2002) presents the regional geologic picture. The 2002 map incorporated earlier outcrop mapping in the Minnesota River valley (Lund, 1956; Himmelberg, 1968; Grant, 1972), the results of widely scattered scientific and mineral-exploration core drilling (Southwick and others, 1993 and previously unpublished data), and field mapping of critical areas by the author. The geochronologic framework pertinent to the geologic map at the time of its publication included data from Hanson and Himmelberg (1967), Doe and Deleveaux (1980), Goldich and Wooden (1980), and Goldich and others (1980a). More precise ages published by Bickford and others (2006) and Schmitz and others (2006) have significantly sharpened the temporal framework of the MRV, especially for the Archean components, and are cited in lieu of earlier age determinations wherever applicable. Table 1 summarizes the newer age determinations and other previously published ages that are cited later in this report.

The bedrock geology portrayed in Figure 3, based on the 2002 compilation (Southwick, 2002), has been updated in a statewide bedrock compilation (Jirsa and others, 2011) that utilized reprocessed aeromagnetic and gravity data over southwestern Minnesota (Chandler and Lively, 2007). The principal revisions pertain to the Mesoarchean components of the MRV terrane in which geophysically traceable units of relatively more mafic gneiss can now be distinguished regionally from more felsic gneiss. This added detail does not materially affect the regional validity of the simplified map of Figure 3 or the conclusions relating to the Neoarchean and Paleoproterozoic history of the terrane as developed in the present report.

ARCHEAN COMPONENTS

Regional setting and internal subdivisions

The extensive literature pertaining to the Archean rocks of the MRV has been thoroughly summarized by Bauer and Himmelberg (1993), Bickford and others (2006), and Schmitz and others (2006). The discussion here and in sections that follow is limited to the structural and lithologic aspects of the Archean rocks that affected or were affected by Neoarchean processes and subsequent Proterozoic events.

Figure 4 shows the position of the MRV relative to neighboring subprovinces within the characteristically belted southern part of the Superior craton. The MRV consists primarily of Mesoarchean gneiss and Neoarchean granitic intrusions whereas the Wawa, Quetico, and Wabigoon subprovinces contain large tracts of deformed Neoarchean volcanic, volcaniclastic, and epiclastic rocks in addition to voluminous intrusions of tonalite, granite, and other granitic rock types. The contrasts between the MRV and the Wawa subprovince in rock type, age, regional metamorphic grade, and structural style have been recognized for many years and are well described in the literature (Morey and Sims, 1976; Sims and others, 1987; Sims and Day, 1993; Holm and others, 2007). A further difference, less commonly emphasized, is in seismic parameters of the deep crust. Wide-angle seismic reflection data obtained by Boyd and Smithson (1993) indicate a crustal thickness of 49 kilometers (30 miles) and an average P-wave velocity of 6.8 kilometers (4.2 miles) per second for the central MRV. These values contrast with a crustal thickness of 35 to 40 kilometers (22 to 25 miles) and an average P-wave velocity of about 6.5 kilometers (4 miles) per second for the rest of the Superior craton as determined from data acquired at sites distributed across the craton in Canada (Chulick and Mooney, 2002). It is assumed that the average thickness and velocity values apply to the Wawa subprovince in central Minnesota. The thicker and denser MRV crust as compared to the crust of the Wawa subprovince probably explains the behavior of the MRV as a foreland bulwark during Penokean tectonic accretion. It also may have been the determining cause of the contrasting patterns of Paleoproterozoic dike swarms in the MRV and Wawa terranes that are discussed later in this report.

The contact between the MRV and Wawa subprovinces is the Great Lakes tectonic zone, which is regarded as a crustal-scale north-dipping shear zone and probable Neoarchean tectonic suture (Southwick and Chandler, 1996). Seismic reflection data acquired by COCORP (Consortium on Continental Reflection Profiling) across the Great Lakes tectonic zone and interpreted by Gibbs and others (1984) and Smithson and others (1986) reveal a prominent set of reflectors

Figure 3. Simplified geologic map of southwestern Minnesota modified from Southwick (2002), showing the inferred distribution of Precambrian rock units beneath a nearly continuous cover of Paleozoic and Mesozoic strata and Quaternary glacial deposits. YMSZ = Yellow Medicine shear zone, BCL = Brown County lineament, SLTZ= Spirit Lake tectonic zone. The area shown in Figure 6 is outlined (dashed line).

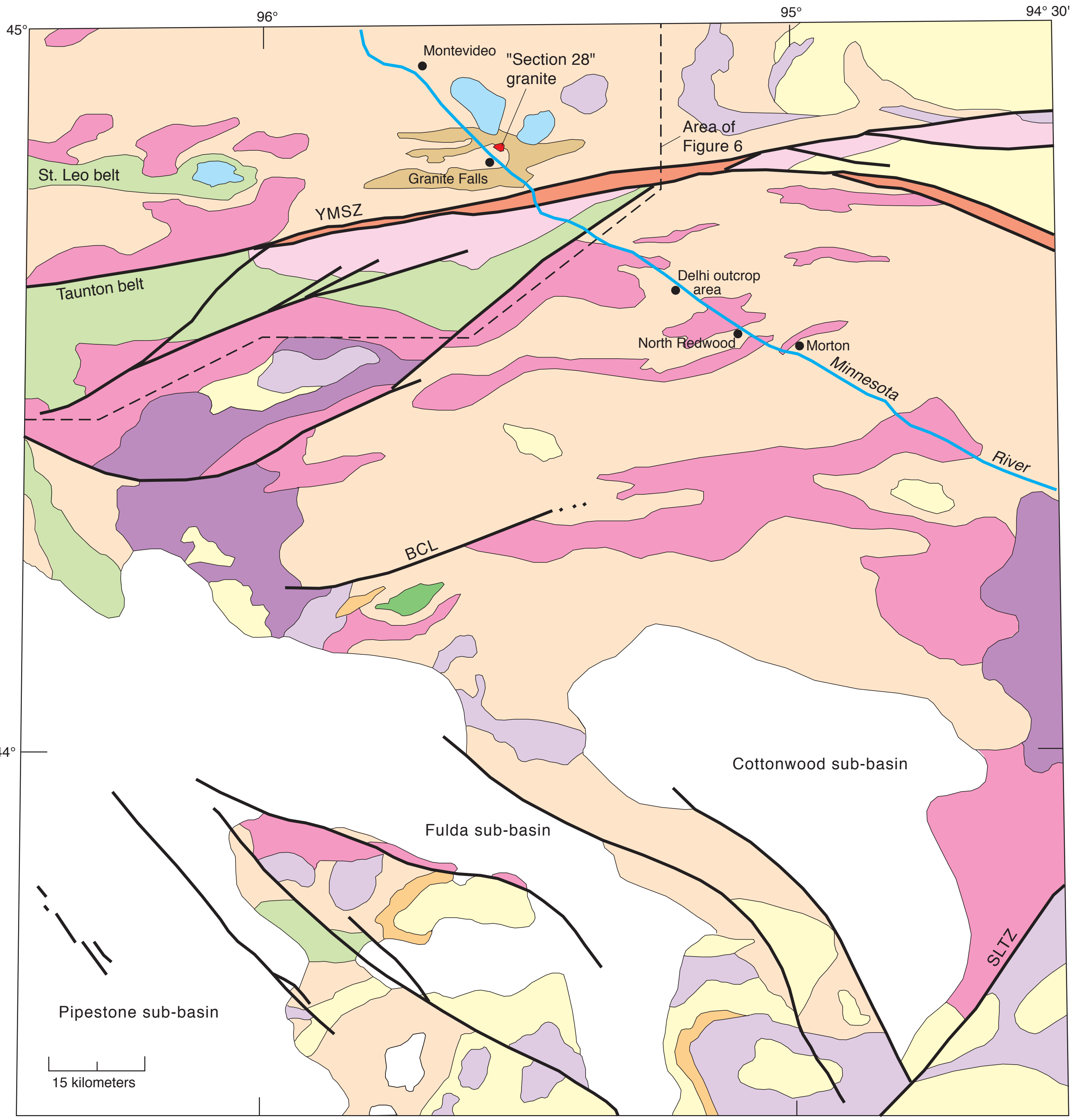

EXPLANATION OF MAP UNITS

Paleoproterozoic

- Sioux Quartzite
- Skarn and igneous intrusion (carbonatite or lamproite?) associated with the Garvin geophysical anomaly.
- Magnetic granitoid rock; forms border phase of zoned plutons and scattered small intrusions.
- Granite, monzogranite, granodiorite, monzonite, and related plutonic rocks
- Tonalite, quartz diorite, diorite, and related intermediate plutonic rocks. Includes some gabbro.
- Gabbro
- "Section 28" granite

Neoarchean

- Sheared rock in major fault zones.
- Leucogranite
- Granite and monzogranite; the Sacred Heart and Fort Ridgeley granites and related intrusions.
- Tonalite
- Intermediate to ultramafic metavolcanic and hypabyssal rocks; unit also includes felsic metavolcanic rocks and iron-formation.

Mesoarchean

- Paragneiss composed of mafic, pelitic, and psammitic layers.
- Chiefly quartzofeldspathic orthogneiss; includes some amphibolite, pyroxene granulite, and micaceous paragneiss.

Table 1. Summary of previously published age determinations cited in this report. See the original sources for analytical details and principal facts.

Sample number	Block location	Rock type	U-Pb age	Mineral	Analyst	Published source	Comments
Mesoarchean orthogneiss complex							
MRV-1	Montevideo	granodioritic gneiss	3,485 ± 10	Zr core	Bickford	Bickford and others (2006)	Relatively uniform gneissose component of complex gneiss outcrop
			3,080 ± 4	Zr rim			
MRV-7	Montevideo	granodioritic gneiss	3,496 ± 9	Zr core	Bickford	Bickford and others (2006)	Most abundant gneiss variety in large quarry
			2,606 ± 4	Zr rim			
MRV96-25	Morton	tonalite gneiss	3,422 ± 1	Zr	Schmitz	Schmitz and others (2006)	Compositionally uniform gray gneiss, "Vicksburg" type
MRV-4	Morton	migmatitic gneiss	3,516 ± 17	Zr	Bickford	Bickford and others (2006)	Flamboyant "rainbow" gneiss, grain population 1
			3,360 ± 9	Zr			Grain population 2
			2,595 ± 2	Zr rim			Data from outermost rims of both populations
MRV-6	Morton	migmatitic gneiss	3,529 ± 3	Zr	Bickford	Bickford and others (2006)	Flamboyant "rainbow" gneiss, grain population 1
			3,356 ± 10	Zr			Grain population 2
Mesoarchean or Neoarchean (?) paragneiss							
MRV-9&10	Montevideo	granulitic paragneiss	2,619 ± 20	Zr	Bickford	Bickford and others (2006)	Date interpreted to mark peak metamorphism
MRV96-13	Montevideo	granulitic paragneiss	2,609 ± 1	Mz	Schmitz	Schmitz and others (2006)	Date interpreted to mark peak metamorphism
UB-035B	Benson	granulitic paragneiss in Ortonville granite	2,594 ± 1	Mz	Schmitz	Schmitz and others (2006)	Enclave in granite; date interpreted to mark peak metamorphism
Mesoarchean granitic and intermediate intrusives ("adamellite 1" and related)							
MRV-3	Montevideo	gneissose biotite granite	3,385 ± 11	Zr	Bickford	Bickford and others (2006)	Interpreted as dating an intrusion
MRV-5	Morton	tonalite/granodiorite gneiss	3,377 ± 19	Zr	Bickford	Bickford and others (2006)	Massive rock interpreted as an intrusion
Late Mesoarchean intrusives							
MRV-8	Montevideo	mafic gneiss	3,141 ± 2	Zr	Bickford	Bickford and others (2006)	Interpreted as dating an intrusion into feldspathic gneiss
Neoarchean granitoid plutons and associated minor intrusions							
MRV96-33	Benson	Ortonville monzogranite	2,603 ± 2	Mz	Schmitz	Schmitz and others (2006)	Weakly deformed phase of pluton
MRV96-28	Benson	Ortonville granite	2,591 ± 7	Mz	Schmitz	Schmitz and others (2006)	Undeformed phase
MRV-13	Morton	Sacred Heart granite	2,604 ± 5	Zr	Schmitz	Schmitz and others (2006)	Weakly foliated main phase of pluton
MRV99-4	Morton	Sacred Heart granite	2,603 ± 1	Zr	Schmitz	Schmitz and others (2006)	Weakly foliated main phase of pluton
MRV96-7	Morton	Sacred Heart alkali syenite	2,592 ± 1	Xe	Schmitz	Schmitz and others (2006)	Border phase
MRV96-27	Morton	aplite	2,590 ± 1	Mz	Schmitz	Schmitz and others (2006)	Dike that intrudes "Vicksburg" tonalite gneiss
MRV96-26	Morton	adamellite	2,600 ± 0.4	Zr	Schmitz	Schmitz and others (2006)	"Adamellite-2" of Wooden and others (1980)
SQ-8	Jeffers (?)	gneissic tonalite	2,624 ± 57	Zr	Van Schmus	Southwick (1994)	Drill sample located close to Morton–Jeffers block boundary
Paleoproterozoic intrusive and volcanic rocks							
MS-MRV-8	Morton	tholeiitic diabase	2,067 ± 0.7	Zr	Schmitz	Schmitz and others (2006)	Large dike south of Franklin
SX-60PEB	Unknown	rhyolite	1,902 ± 55	Zr	Wallin	Southwick (1994)	Pebbles in Sioux Quartzite; also see Wallin and Van Schmus (1988)
SQ-5	Jeffers (?)	quartz monzonite	1,792 ± 31	Zr	Peterman	Southwick (1994)	Rock petrologically similar to unit in East-Central Minnesota batholith

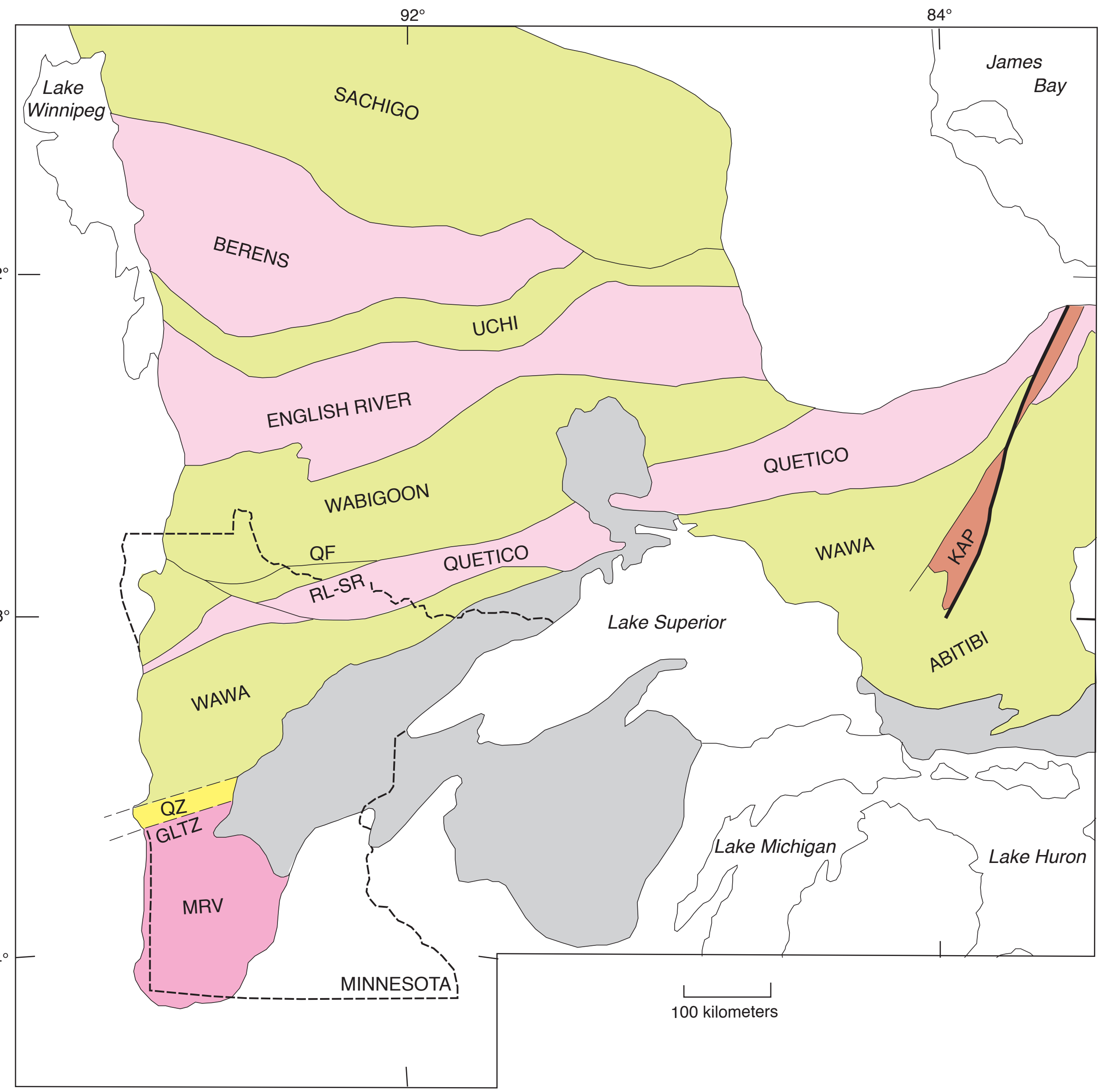

Figure 4. Sketch map of the western Superior craton highlighting the location of the MRV with respect to other subprovinces and selected faults mentioned in the text. The Wawa, Abitibi, Wabigoon, Uchi, and Sachigo subprovinces consist mainly of greenstone-belt metavolcanic rocks and intrusions of tonalite and granite. The Quetico and English River subprovinces consist mainly of metasedimentary schist, migmatite, and granite. The Berens subprovince consists mainly of plutonic granitoid rocks. The Kapuskasing zone (KAP) consists mainly of mid-crustal gneissic rocks. QZ = the magnetic "quiet zone" at the southern margin of the Wawa subprovince. QF and RL-SR designate the Quetico and Rainy Lake–Seine River faults, respectively. Gray shading represents areas of Proterozoic rocks. Uncolored areas represent Paleozoic and Mesozoic sedimentary rocks.

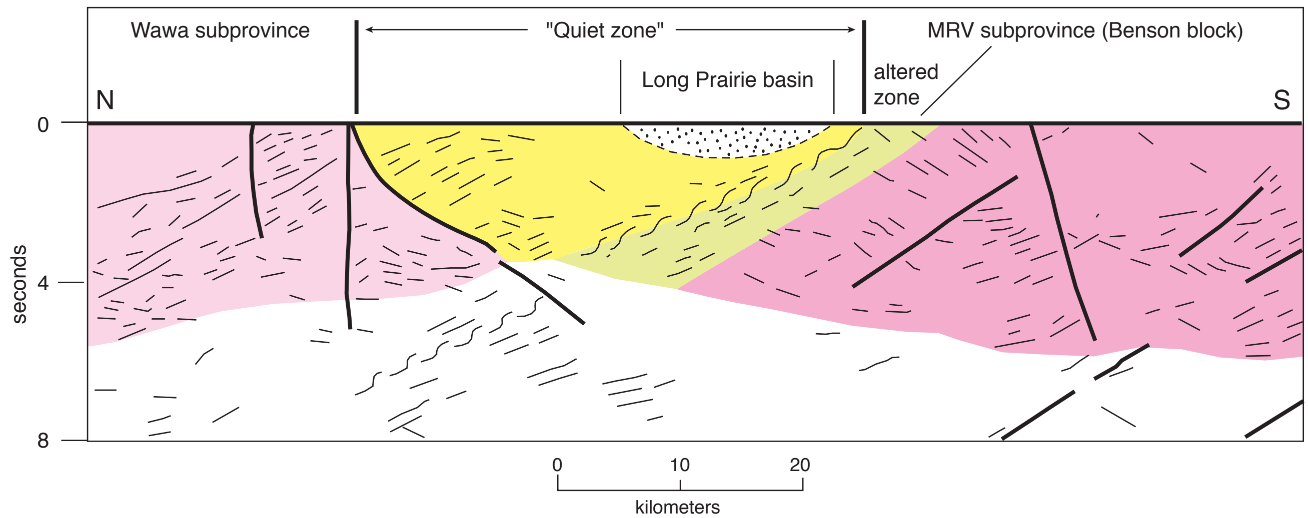

Figure 5. Seismic reflection section across the Great Lakes tectonic zone approximately along longitude 93° W. in central Minnesota. Heavy wavy lines indicate the reflector interpreted to be the principal suture zone. Light lines indicate less prominent reflectors near and parallel to the main suture zone and reflectors of various orientations throughout the section. Section modified from Gibbs and others (1984).

that dips about 35° north and extends to mid-crustal depth (Fig. 5). This set of reflectors is interpreted to be the seismic expression of the principal Great Lakes tectonic zone shear zone. The seismic investigations also show several less prominent north-dipping reflectors in MRV crust south of and beneath the Great Lakes tectonic zone. These are interpreted provisionally as second-order shears related to MRV–Wawa suturing. Two-dimensional models calculated from aeromagnetic and Bouguer gravity data on transects normal to the Great Lakes tectonic zone yield a shear-zone geometry that closely matches the seismic results (Southwick and Chandler, 1996).

The Minnesota segment of the Great Lakes tectonic zone apparently did not experience appreciable Penokean or younger tectonic adjustment, although solid verification of this is precluded by the absence of bedrock outcrops or adequate drill-hole information in the critical area of interest. However, mineral ages obtained from the Michigan segment, which trends approximately along the Penokean tectonic front (Fig. 2), indicate a history of reactivation in geons 18 and 17 (Tohver and others, 2007).

Three north-dipping shear zones divide the MRV into four crustal blocks (Figs. 2, 6, 11; Southwick and Chandler, 1996). The compelling evidence for this block and shear zone architecture is geophysical; the shear zones stand out as pronounced linear features on enhanced potential-field images. The Yellow Medicine shear zone separates the Montevideo block from the Morton block and is the most prominent and best documented of the interior breaks. Ductile and brittle shear fabrics in rocks located close to the main shear-zone trace have been observed in drill core and outcrop. The Appleton shear zone, formerly called the Appleton geophysical lineament (Southwick and Chandler, 1996), separates the Benson block from the Montevideo block. It is well defined geophysically and is substantiated as a shear zone by observed shear fabrics in widely scattered drill core taken in and near the belt of linear geophysical anomalies. The boundary between the Morton and Jeffers blocks (the Brown County lineament of Schaap, 1989) is less well documented. It is reasonably well defined by linear geophysical gradients, but because it is not exposed in outcrop and has not been adequately sampled by drilling, no direct evidence of shearing has been obtained along it. Some segments of this boundary may be intrusive contacts of Neoarchean granite against older gneiss (Southwick and Chandler, 1996; Southwick, 2002), a possibility based on analogy with field observations reported in other cratons

Figure 6. Geologic map of the Yellow Medicine shear zone, the Taunton belt, and flanking areas. Note the alignment of the St. Leo metavolcanic belt with the south limb of the Granite Falls antiform and the folded iron-formation at the west end of the Taunton belt where exploration hole E-1 was drilled. See Figure 3 for location and regional context.

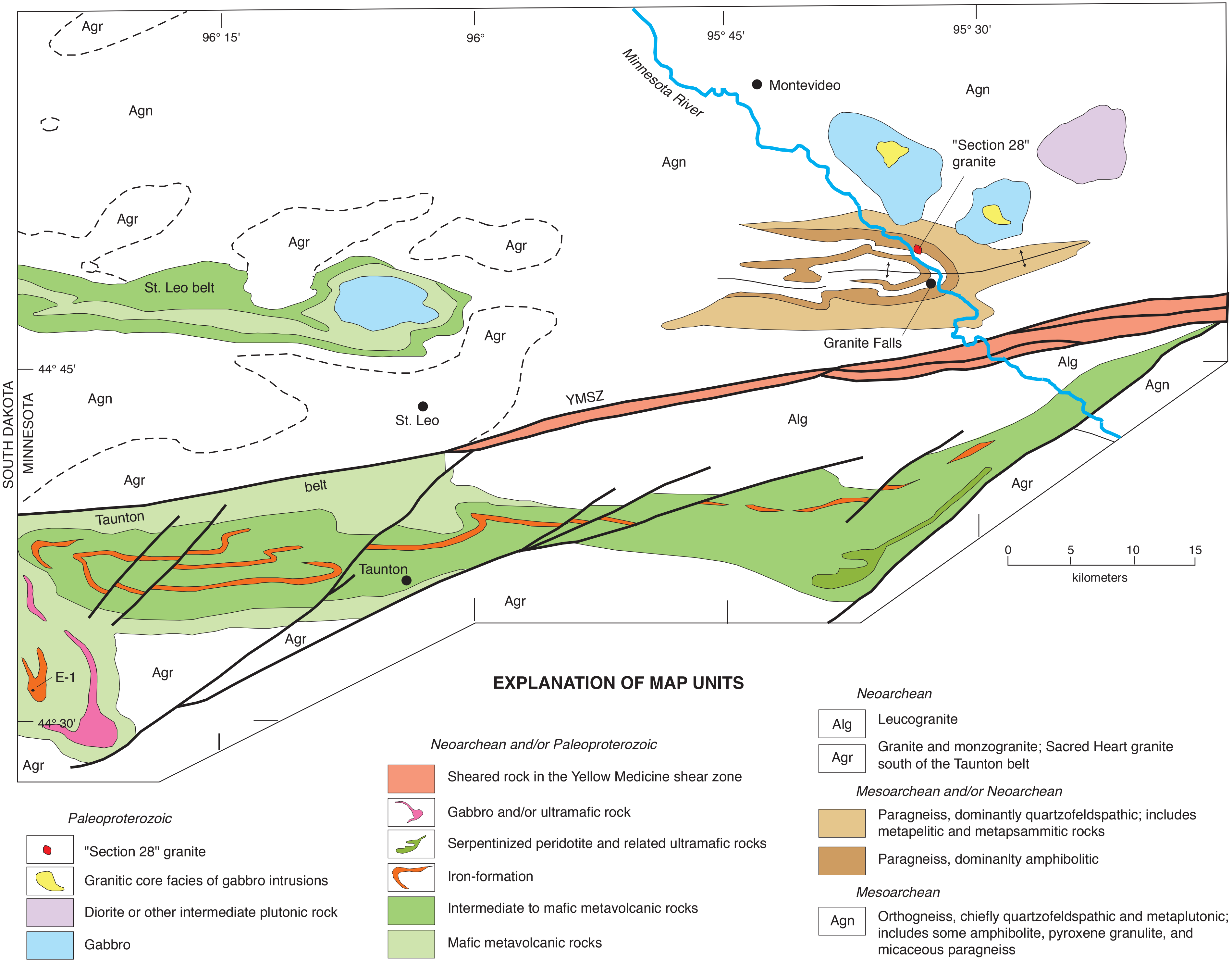

96° 15'
96°
95° 45'
95° 30'
44° 45'
44° 30'
SOUTH DAKOTA
MINNESOTA
Minnesota River
Montevideo
"Section 28" granite
Granite Falls
St. Leo belt
St. Leo
Taunton belt
Taunton
YMSZ
E-1
Agn
Agr
Alg
0
5
10
15
kilometers
EXPLANATION OF MAP UNITS
Neoarchean
Alg Leucogranite
Agr Granite and monzogranite; Sacred Heart granite south of the Taunton belt
Mesoarchean and/or Neoarchean
Paragneiss, dominantly quartzofeldspathic; includes metapelitic and metapsammitic rocks
Paragneiss, dominanlty amphibolitic
Mesoarchean
Agn Orthogneiss, chiefly quartzofeldspathic and metaplutonic; includes some amphibolite, pyroxene granulite, and micaceous paragneiss
Neoarchean and/or Paleoproterozoic
Sheared rock in the Yellow Medicine shear zone
Gabbro and/or ultramafic rock
Serpentinized peridotite and related ultramafic rocks
Iron-formation
Intermediate to mafic metavolcanic rocks
Mafic metavolcanic rocks
Paleoproterozoic
"Section 28" granite
Granitic core facies of gabbro intrusions
Diorite or other intermediate plutonic rock
Gabbro

where well exposed Archean gneiss terranes contain many examples of granite-gneiss contact zones that localized subsequent episodes of ductile to brittle shearing. The block-bounding shear zones, including the Great Lakes tectonic zone, are interpreted to be Neoarchean structures that developed when continental rocks of the MRV were accreted to the southern margin of the growing Superior craton (Southwick and Chandler, 1996). Evidence for their Paleoproterozoic reactivation will be developed in the section on structural and tectonic considerations.

Marginal zones of the Mesoarchean core

Alteration zone at the north margin

Some bedrock at the north margin of the MRV, within a few kilometers of the Great Lakes tectonic zone, displays evidence of pervasive epidote-chlorite alteration (Boerboom, 2007). The extent, age, and origin of this regional alteration remain unknown, due mainly to the lack of sufficient drill-hole coverage, but the proximity of the altered rocks to the Great Lakes tectonic zone suggests that hydrothermal fluids channeled by the Great Lakes tectonic zone and subsidiary structures (Fig. 5) may have played a role. The same type of alteration affected rocks north of the Great Lakes tectonic zone, in the so-called "magnetic quiet zone" along the southern margin of the Wawa subprovince. The origin of the quiet zone is itself an interesting question, the answer to which may involve regional bedrock alteration. A speculative possibility is that hydrothermal fluids circulating above the north-dipping Great Lakes tectonic zone may have altered original Fe-Ti oxides and silicate minerals to feebly magnetic assemblages composed of chlorite, epidote, sphene, calcite, alkali feldspar, and quartz, thus reducing magnetic contrasts among rock types and leveling the magnetic signature to relative flatness. Whatever the nature and source of this putative regional alteration may have been, it occurred before the emplacement of the Paleoproterozoic diabase dikes that transect both the altered north fringe of the Benson block and the quiet zone. The aeromagnetic anomalies associated with the dikes are the same in amplitude within these areas as outside of them, indicating that the magnetic minerals in the dikes were not degraded by regional alteration.

Plutonic transition zone along the south margin

The NICE Working Group (2007) and Van Schmus and others (2007) concluded that the south boundary of the MRV is the Spirit Lake tectonic zone (Fig. 2), south of which plutonic rocks of various geon 17 crystallization ages yield Nd-Sm crustal residence ages (T_{DM} ages, following the model of DePaolo, 1981) that are generally younger than 2.0 Ga. In other words, the magmas from which these intrusions crystallized were derived from and resided within Penokean and/or Yavapai rather than Archean lithosphere. Although the Spirit Lake tectonic zone is clearly defined aeromagnetically, its structural attributes are essentially unknown. Chandler and others (2007), NICE Working Group (2007), and Van Schmus and others (2007) traced the Spirit Lake tectonic zone to the east of the Mesoproterozoic Midcontinent Rift system, where it marks the boundary between geon 18 Penokean terrane (including the dominantly Archean Marshfield terrane) on the north and geon 17 Yavapai terrane on the south.

Approximately the southern fifth of the MRV or roughly the southern half of the Jeffers block is geophysically complex. As seen in the first vertical derivative compilation of the aeromagnetic data (Chandler and Lively, 2007), the convoluted aeromagnetic pattern of compact, gnarled highs and lows that is characteristic of MRV Archean gneiss diminishes southward, giving way to an increasing abundance of smooth, oval highs and lows indicative of discrete mafic to granitic plutons. The transition from dominantly gneissic to dominantly plutonic subcrop is partially obscured by the Sioux Quartzite, which effectively damps out potential-field signals from the underlying rocks. Many of the plutons in this part of the MRV are interpreted to be of Paleoproterozoic age on the basis of geophysical similarity to known Paleoproterozoic intrusions in east-central Minnesota (Boerboom and Holm, 2000; Holm and others, 2005). These plutons of inferred Paleoproterozoic age are further discussed in the "Mafic and ultramafic plugs and small plutons" section.

Terminology and essential characteristics of the Mesoarchean gneisses

It has become customary since the first modern geologic mapping by Lund (1956) to divide the gneissic rocks of the MRV into two regional units—the Montevideo gneiss, which crops out along the northwestern reach of the Minnesota River, and the Morton gneiss, which crops out along the southeastern reach. This informal usage came about because: 1. The two outcrop belts are separated by a river distance of some 16 kilometers (10 miles) in which there are no outcrops; 2. The varieties of gneiss in the two areas, though similar, are not identical; and 3. Geochronologic data were emerging in the 1960s that suggested somewhat different geologic histories for the Montevideo and Morton areas (Goldich and others, 1970). Geochronologic and geologic reports published after 1970 perpetuated this terminology, which tended to accentuate differences rather than similarities between the two gneiss terranes that indeed are very similar, and the terminology has continued to the present day.

The recent high-precision U-Pb dating of gneiss, supracrustal rocks, and intrusions (Table 1; Bickford and others, 2006; Schmitz and others, 2006) has shown the essential synchroneity of geon 31-34 U-Pb ages of orthogneissic components in the Montevideo and Morton blocks and strongly implies that these bodies of rock are pieces of a common Mesoarchean terrane that was subdivided in the Neoarchean era when the Yellow Medicine shear zone developed. Also, it is becoming increasingly clear that imperfectly delineated sequences of supracrustal rocks, now highly deformed and metamorphosed paragneiss, were later deposited upon and infolded with the older orthogneiss complex, and that repeated episodes of partial melting, migmatization, granite emplacement, and deformation affected the whole lithologic package. Grant (1972) recognized this general sequence of events prior to the availability of definitive geochronologic dating, and he interpreted all of the MRV gneisses as constituents of a single unified terrane.

In view of the above, it is useful to subdivide the gneissose rocks of the MRV into three broad categories based on rock type and relative age (Table 2). These are: A. An early-formed (such as Mesoarchean) orthogneiss complex that consists of several types of granitic, intermediate, and mafic protoliths variably intermingled, deformed, and migmatized; B. Somewhat younger, compositionally homogeneous granitoid intrusions of several types and ages that invaded gneissic country rocks prior to circa (ca.) 3,000 Ma and were deformed with them; and C. Stratiform paragneiss of probable supracrustal origin that consists of mafic (amphibolite-granulite), pelitic/psammitic (micaceous schist), and felsic (quartz-feldspar granofels) layers that range from centimeters to tens of meters in thickness. The variably gneissose granitoid intrusions of category B range in composition from granite to diorite and apparently were emplaced episodically over a long time interval (Bickford and others, 2006).

The Mesoarchean orthogneiss complex

The most voluminous lithologies in the older orthogneiss complex are variably layered, foliated, and/or lineated rocks that are mainly tonalitic, trondhjemitic, and granodioritic in bulk composition (Goldich and others, 1980a; Wooden and others, 1980). Together these constitute a TTG (tonalite, trondhjemite, and granodiorite closely intermingled) suite that is characteristic of Archean gneiss complexes worldwide. Commonly these quartzofeldspathic rocks enclose varying amounts of amphibolite, biotite-hornblende schist, and mafic granulite in the form of foliation-parallel lenses or irregularly shaped blocky enclaves. Locally the mafic constituents are abundant enough to define sub-units of gneiss that are mappable in outcrop (Grant, 1972) or regionally by means of geophysical expression (Jirsa and others, 2011). Structurally the TTG rocks range from nearly massive to strongly layered, rather commonly display evidence of incipient to extensive migmatization, and record a complex history of multiple deformation and

Table 2. Gneissose rocks of the MRV, with brief definitions of the five principal rock types that constitute most of the orthogneiss complex in the Morton block.

A: Older Mesoarchean orthogneiss complex.

Principal orthogneiss variants, Morton block

1: Biotite trondhjemite gneiss, relatively massive, coarse-grained, well foliated ("Vicksburg" type).

2: Tonalite/granodiorite gneiss, relatively massive, medium-grained, variably foliated.

3: Tonalite/granodiorite gneiss, modally layered, layers centimeters to decimeters thick.

4: Foliated pegmatite intermingled with finer-grained types of gneissic granitoid rock.

5: Biotite granite gneiss (in part the "adamellite 1" of Goldich and others, 1980b).

B: Foliated, compositionally homogeneous "younger" Mesoarchean granitoid intrusions; compositions range from tonalite to diorite and gabbro.

C: Stratiform paragneiss tentatively interpreted to be of Neoarchean depositional age.

6: Amphibolite and pyroxene granulite.

7: Garnet-biotite schist, garnet-cordierite-anthophyllite schist, and associated high-grade schists of pelitic and psammitic origin.

8: Quartz-feldspar granofels.

metamorphism as described in detail by Bauer (1980) and further elucidated by Bauer and Himmelberg (1993) and Bickford and others (2006).

The orthogneiss complex in the Morton block is divisible on the basis of field criteria into five broad rock types (excluding the mafic enclaves) that are useful in outcrop-scale mapping. These are: 1. Biotite trondhjemite gneiss; 2. Massive tonalite to granodiorite gneiss; 3. Modally layered tonalite to granodiorite gneiss; 4. Foliated pegmatite gneiss; and 5. Biotite granite gneiss or "adamellite 1" (Table 2). The modally layered type of gneiss (category 3) varies sharply from place to place and layer to layer in the modal proportions of plagioclase, K-feldspar, quartz, biotite, and hornblende. Table 3, columns 1 to 5, presents mean compositions of the Morton-block gneisses that are recalculated from major-element chemical analyses published originally by Wooden and others (1980) and Goldich and Fischer (1986). The "wtd average" column is a weighted mean composition of the orthogneiss as a whole in which the mean analyses of rock types 1, 2, and 3 are combined in equal proportions along with 3 percent of rock type 4 and 10 percent of rock type 5. These are the approximate proportions of the constituent rock types estimated from orthogneiss outcrops in the Morton-block reach of the Minnesota River valley. The computed bulk composition in the "wtd average" column is approximately that of a calc-alkalic granodiorite. The major quartzofeldspathic types of orthogneiss in the Montevideo block are essentially the same as those in the Morton block, but have not been as thoroughly characterized.

The recently published U-Pb dates on zircon and monazite corroborate the earlier conclusions of Goldich and Wooden (1980) that the orthogneiss complex was fundamentally assembled by ca. 3,000 Ma and was regionally metamorphosed a final time some 400 m.y. later. The complex would have been compositionally heterogeneous then as now, containing intermingled volumes of various types of quartzofeldspathic gneiss that ranged from meters to tens of kilometers in size. Some of these would have been relatively enriched in K-feldspar and biotite (roughly comparable in normative mineralogy and chemical composition to the layered tonalite and granodiorite gneiss characterized in Table 3) and thus would have been of favorable parent composition for the anatectic production of granite melt upon reaching the necessary temperature. The appropriate pressure and temperature (P-T) conditions for anatexis probably were attained during the 2,600 Ma metamorphic event.

Massive metaplutonic rocks within the Mesoarchean orthogneiss complex

Among the rock types in this category are compositionally massive but tectonically foliated bodies of granite, granodiorite, tonalite, and intermediate to mafic diorite that are surrounded by and incorporated within more heterogeneous and heterolithic constituents of the orthogneiss complex. The granite member of this group includes the textural variants granite, pegmatite, and aplite that Goldich and others (1970, 1980b) collectively termed "adamellite 1" to distinguish them from compositionally similar but undeformed Neoarchean granitic rocks termed "adamellite 2." The "adamellite 1" rocks typically occur as meter-scale bodies that are moderately discordant to essentially concordant with respect to layering in the enclosing gneiss. The bodies of relatively massive granodiorite, tonalite, and diorite vary considerably in fabric development, form, scale, and age. Zircon U-Pb ages of these rocks span several hundred million years of Mesoarchean time (Table 1), indicating a protracted, episodic history of igneous activity within the gneiss complex (Bickford and others, 2006). Massive gneisses derived from intermediate and mafic diorite intrusions are relatively abundant in the Montevideo block near Granite Falls.

Stratiform paragneisses of debatable Mesoarchean or Neoarchean age

These distinctive heterolithic paragneisses appear to be geographically restricted relative to rocks of the orthogneiss complex. The best paragneiss exposures are in the Minnesota River valley at Granite Falls (Figs. 3, 6), where the rocks have been folded into a broad east-plunging antiform. However, the present mapping of the paragneiss in the vicinity of Granite Falls (Himmelberg, 1968; Southwick, 2002) may seriously underestimate the actual extent of this rock type. Reconnaissance mineral-exploration drilling conducted in 2005 (data released in 2010) intersected pelitic and mafic paragneiss at five widely separated locations along a 50-kilometer (31-mile) east–west traverse between the south limb of the Granite Falls antiform and the Yellow Medicine shear zone. The drilling results are interpreted as tentative evidence of a broad paragneiss belt parallel to and north of the Yellow Medicine shear zone, at the south edge of the Montevideo block.

Because of their favorable chemical compositions, the mafic and pelitic layers in the paragneiss at Granite Falls have recorded clear petrologic evidence of granulite-facies metamorphic grade (Himmelberg,

Table 3. Mean major-element compositions of the orthogneiss rock types defined in Table 2.

Rock type	1	standard deviation 1	2	standard deviation 2	3	standard deviation 3	4	5	standard deviation 5	wtd average
SiO_2	74.23	2.25	66.32	3.45	67.53	2.06	71.7	74.80	1.52	69.97
TiO^2	0.22	1.21	0.49	2.07	0.46	0.59	0.3	0.08	1.08	0.35
Al_2O_3	14.27	0.02	17.76	0.13	15.43	0.09	14.8	13.60	0.03	15.57
Fe_2O_3	0.34	0.03	0.68	0.28	1.02	0.46	0.13	0.34	0.25	0.63
FeO	1.22	0.19	1.76	0.16	3.03	0.57	2.12	0.45	0.17	1.85
MnO	0.01	0.01	0.04	0.01	0.07	0.02	0.02	0.01	0.01	0.04
MgO	0.63	0.05	0.86	0.08	1.47	0.35	0.74	0.14	0.06	0.89
CaO	2.33	0.69	3.89	0.74	3.81	0.60	2.49	1.42	0.36	3.12
Na^2O	5.20	0.52	5.89	0.88	4.75	0.40	3.96	3.09	0.55	5.02
K_2O	1.30	0.38	1.62	0.58	1.73	0.48	3.5	5.36	0.55	1.99
P^2O^5	0.04	0.03	0.14	0.10	0.17	0.06	0.1	0.03	0.02	0.11
H^2O^+	0.29	0.08	0.29	0.06	0.35	0.11	0.24	0.14	0.06	0.29
H^2O^-	0.06	0.01	0.06	0.03	0.06	0.01	0.09	0.03	0.02	0.06
CO_2	0.02	0.03	0.03	0.04	0.06	0.05	0.06	0.09	0.05	0.04
F	0.04	0.01	0.05	0.01	0.07	0.01	0.06	0.01	0.01	0.05
Sum	100.19		99.88		100.01		100.31	99.56		99.99
Rb	40.07	5.71	63.40	10.91	79.30	8.63	86.4	111.78	15.72	66.77
Sr	639	176.68	895	406.02	364	12.84	283	357	29.23	594.68
Ba	431	106.13	484	181.91	367	143.58	750	1776	204.65	571.92
FeO^t	1.53		2.38		3.95		2.24	0.75		2.42
Number of samples	3		5		7		1	5		
CIPW norm										
Q	32.57		16.06		22.09		27.76	32.95		24.58
or	7.68		9.57		10.22		20.68	31.67		11.76
ab	44.00		49.84		40.19		33.51	26.15		42.48
an	11.03		17.24		15.6		11.33	6.85		14.07
C	0.27						0.35	0.21		
di			0.72		1.43					0.33
hy	3.18		3.72		7.04		5.17	0.78		4.43
mt	0.49		0.99		1.48		0.19	0.49		0.91
il	0.42		0.93		0.87		0.57	0.15		0.66
ap	0.09		0.33		0.4		0.24	0.07		0.26
fl	0.07		0.08		0.11		0.1			0.08
Total	99.81		99.48		99.51		99.89	99.32		99.57
AN	20.04		25.7		28.05		25.26	20.76		24.89

1: Biotite trondhjemite gneiss, "Vicksburg" type

2: Relatively massive granoblastic tonalite/granodiorite gneiss, fine- to medium-grained

3: Layered tonalite/granodiorite gneiss (layers centimeters to decimeters thick)

4: Foliated pegmatite and associated granodiorite gneiss

5: Biotite granite gneiss (adamellite 1) of Morton area

Notes

Rock types 1-4 defined through field work in June, 2000.

Original analyses from Wooden and others (1980) and Goldich and Fischer (1986) are recompiled into tabulated means 1-4.

The mean reported for rock type 5 is from Wooden and others (1980), Table 13.

Wtd avg = 0.29*column 1 + 0.29*column 2 + 0.29*column 3 + 0.03*column 4 + 0.10*column 5.

1968; Grant, 1972; Perkins and Chipera, 1985; Moecher and others, 1986). Although previous investigators have interpreted the paragneiss to be of Mesoarchean age and a distinctive constituent within the Mesoarchean gneiss complex, there are reasons to question this conclusion. U-Pb dates from monazite (Schmitz and others, 2006) and zircon (Bickford and others, 2006) in the paragneiss cluster near 2.6 Ga (Table 1) and are interpreted to date peak metamorphism rather than depositional age. No older monazite or zircon ages that would delimit provenance or time of deposition have been reported. Furthermore, the monazite in these rocks yields epsilon Nd isotopic compositions that were between +0.15 and +0.30 at the time of its metamorphic growth (2.6 Ga), radiogenic values that suggest a dominantly juvenile volcanosedimentary provenance and relatively young (such as Neoarchean) depositional age (Schmitz and others, 2006). Therefore it is possible that the paragneiss is much younger than the orthogneiss complex and may in fact overlie it unconformably.

Aluminous paragneiss also crops out in the Minnesota River valley about eight kilometers (5 miles) northwest of the village of North Redwood, at a locality known informally as the Delhi area (Fig. 3). The gneiss at this place in the Morton block contains cordierite, anthophyllite, and garnet in addition to biotite, quartz, and feldspar (Grant, 1968, 1972). The bulk compositions of individual layers in the gneiss are within the range of common detrital sedimentary rocks, but they are also within the range of compositions for anatectic restite generated through partial melting of a precursor felsic volcanic or sedimentary rock and removal of the melt fraction (Grant, 1968). Bickford and others (2006) found numerous zircons in the paragneiss at this locality that have abraded Mesoarchean cores (3,150 to 3,520 Ma) and epitaxial overgrowths that are approximately 2,600 Ma. These data imply a sedimentary origin for the gneiss, a sediment source in the Mesoarchean orthogneiss complex, and a high-grade metamorphic event at approximately 2,600 Ma. They also imply the presence of an unconformity beneath the paragneiss that has not yet been identified in the field.

Neoarchean (?) greenstone-belt rocks of the Taunton and St. Leo belts

General description

The informally named Taunton belt is a narrow, fault-bounded septum of metamorphosed Fe-tholeiite, diabase, gabbro, peridotite, iron-formation, and aluminous sedimentary rock that is located at the north edge of the Morton block, immediately south of the Yellow Medicine shear zone (Fig. 6; Southwick and Chandler, 1996). Most of the rocks in the belt constitute a typical Superior Province greenstone-belt assemblage that has been metamorphosed to greenschist or lower amphibolite grade. At the west end of the belt, close to the Minnesota–South Dakota border, the geophysical strike hooks sharply from west–southwest to south–southeast (Figs. 3, 6). A separate subcrop of south–southeast-striking metavolcanic rocks and iron-formation interpreted solely from geophysical expression (Chandler and Lively, 2007) lies farther south; it may be a structurally disrupted extension of the main Taunton belt or an altogether independent entity.

Another small belt of intermediate-grade metavolcanic rocks occurs a few kilometers north of the Yellow Medicine shear zone, more or less along the boundary between Lac Qui Parle and Yellow Medicine Counties northwest of the village of St. Leo (Figs. 3, 6). This west-trending linear belt is directly on strike with granulite-grade paragneisses of debatable Mesoarchean or Neoarchean age in the south limb of the Granite Falls antiform. If future investigations were to confirm a Neoarchean age for the metavolcanic rocks in the St. Leo belt and a geologically viable connection of these rocks to the granulitic paragneisses at Granite Falls, the argument for interpreting the paragneisses to be a Neoarchean sequence would be significantly strengthened. At present, however, no rocks in the Taunton or St. Leo belts have been dated radiometrically.

The age conundrum: Neoarchean, Paleoproterozoic, or both?

Although a Neoarchean age is tentatively favored for most if not all of the rocks in the Taunton belt, a sequence of iron-rich metasedimentary rocks recovered from exploration drilling near Lake Hendricks (Fig. 6) more closely resembles the Paleoproterozoic iron-formation sequences in the mining districts of the Lake Superior region than the Archean iron-formations within greenstone belts (Jirsa, 1986). The drilled section consists of about 113 meters (370 feet) of thinly bedded to laminated, very fine-grained rocks that range in protolithic composition from iron-poor argillite and siltstone to carbonate and silicate iron-formation (Table 4, columns A and D-F). Carbonate and silicate iron-formation are the dominant rock types; these have been altered hydrothermally to oxide and sulfide assemblages along favorable stratigraphic horizons and structures. The Lake Hendricks rocks have been metamorphosed to chlorite- and garnet-bearing assemblages and exhibit deformational fabrics typical of low-grade

Table 4. Chemical analyses of metasedimentary rocks encountered in core drilling near Lake Hendricks, Lincoln County, Minnesota.

Sample number	A E1-798	B E1-941	C E1-957	D E1-963	E E1-901	F E1-1057
SiO_2	64.8	49	47.4	53.2	6.16	11.5
TiO_2	0.22	0.85	0.81	0.46	0.04	0.33
Al_2O_3	8.33	24.8	24	7.97	0.69	1.93
Fe_2O_3	1.97	6.52	3.19	9.73	14.35	26.04
FeO	0.6	0	3.4	10.7	40.5	19.6
MnO	0.06	0.07	0.07	2.06	0.48	4.69
MgO	0.48	2.4	2.26	4.11	2.56	5.24
CaO	10.7	0.33	0.38	0.93	2.39	9.23
Na_2O	0.31	0.27	0.32	0.28	0.26	0.3
K_2O	1.29	10.1	9.73	1.58	0.03	0.49
P_2O_5	0.04	0.2	0.19	0.14	0.62	0.16
CO_2	7.87	0.01	1.52	0.05	27.5	17.4
$H2O^+$	2.3	2.6	2.3	3.3	2.3	1.4
S	1.48	0.43	1.39	2.05	4.28	1.34
Sum	100.45	97.58	96.96	96.56	102.16	99.65
FeO^t	2.37	5.87	6.27	19.46	53.42	43.04
Rb	10	250	240	100	<10	<10
Sr	320	<10	<10	10	30	20
Ba	760	2160	2080	470	260	230
Nb	10	20	<10	20	40	30
Zr	60	20	20	50	<10	<10
Y	10	<10	30	20	<10	<10
Cr	68	4510	5337	400	68	<100
Cu						108
Zn						443

Samples from New Jersey Zinc Corporation drill core E-1:
E1-798: Carbonate-bearing siltstone
E1-941: Chromian muscovite argillite
E1-957: Chromian muscovite phyllite
E1-963: Silicate iron-formation
E1-901: Carbonate iron-formation
E1-1057: Carbonate iron-formation

Analyses A, C, D, E, F from Morey and others (1985), Table 8
Analysis B from Morey and McDonald (1987), Table 12

metamorphism. Nevertheless, some carbonate and silicate iron-formation beds locally exhibit granular or oolitic textures, primary features typically absent from iron-formations within Archean greenstone belts but widely present in Paleoproterozoic iron-formation sequences (Jirsa, 1986).

A green phyllitic argillite interlayered with the iron-formation is composed dominantly of sericitic muscovite along with minor amounts of chlorite and opaque oxides. This anomalous rock is interpreted to be the product of hydrothermal metasomatic processes that affected the iron-formation sequence in the later stages of its deposition on the sea floor. Geochemically it is characterized by strongly elevated contents of chromium, barium, and potassium relative to the flanking iron-formation and diminished contents of iron and manganese (Table 4, columns B and C). The elevated chromium is inferred to reside in the greenish muscovite. Chromian muscovite is a fairly common accessory mineral in the veins and alteration halos of Archean and younger volcanic massive sulfide and vein gold deposits, as at Timmins, Ontario (Bateman and others, 2008; Dinel and others, 2008) or Hellyer, Tasmania (Gemmell and Fulton, 2001).

Most volcanic massive sulfide and vein gold deposits in which chromian muscovite occurs were generated by sea-floor hydrothermal systems that pervaded structurally prepared zones in sequences of mafic and ultramafic volcanic rocks. Trace amounts of chromium in the host volcanics of these deposits were mobilized, along with other chemical species, and redistributed to generally higher parts of the alteration halo where they were incorporated in hydrothermally precipitated sericite. Also, many of these ore-forming hydrothermal systems produced various types of iron-rich crusts in their upper and more distal portions. In the Lake Hendricks case, the hydrothermal fluids responsible for alteration may have traversed mafic volcanic and sub-volcanic rocks that are inferred from aeromagnetic and bouguer gravity signatures to surround and underlie the iron-formation occurrence (Fig. 6). The simplistic geochemical and lithologic analogies made with productive volcanic massive sulfide and vein gold deposits are clearly inadequate to define the Lake Hendricks setting as a viable exploration target. Rather, the point here is to highlight the geologic attributes of the area, as deduced from very limited data, and suggest their possible implications for regional stratigraphic and tectonic interpretations.

The lithologic and alteration patterns observed in the Lake Hendricks core are comparable to those observed in the Cuyuna iron-mining district and other Paleoproterozoic iron-formation occurrences in east-central Minnesota (Schmidt, 1963; McSwiggen and others, 1995; Melcher and others, 1996; Southwick and others, 2005). The North Range of the Cuyuna district is perhaps the closest analog; iron-formations there were affected by hydrothermal metasomatic alteration that involved substantial mobilization of manganese, sodium, and barium, but did not involve chromium, during their deposition and early diagenesis (Melcher and others 1996). In the Cuyuna case, the absence of chromium anomalies in the altered rocks is consistent with the lack of other evidence for volcanic involvement in the alteration process.

It is clear from the foregoing descriptions that the sequence of iron-rich metasedimentary rocks drilled near Lake Hendricks is not a typical Archean iron-formation. It is not the thinly laminated, cherty iron-formation that is characteristic of the Archean greenstone-belt iron deposits in the Superior craton. Furthermore, there is no petrographic, mineralogic, or geochemical evidence of a direct volcanic contribution to the iron-formation sequence, apart from the inferred hydrothermal alteration that may have been driven by volcanic sources of heat and fluids. Thus by analogy with rock sequences in the Cuyuna district and in the absence of geochronologic proof, the weight of the available evidence favors a Paleoproterozoic (Penokean?) age for the Lake Hendricks metasedimentary sequence instead of a Neoarchean one.

A possible Paleoproterozoic age for these rocks at the west end of the Taunton belt has significant implications for the interpretation of tectonic events. If the Taunton belt contains Paleoproterozoic rocks that are tectonically or stratigraphically intermingled with Neoarchean rocks, it would be reasonable to conclude that Paleoproterozoic movement along the Yellow Medicine shear zone played a role in localizing and preserving the supracrustal sequences. Other geologic evidence developed later in this report indicates that the Yellow Medicine shear zone was active in the Paleoproterozoic era. A conclusive demonstration through radiometric dating that Paleoproterozoic strata were indeed preserved and deformed in the shear zone would strengthen the hypothesis that the Yellow Medicine shear zone was a long-lived fundamental feature of the regional tectonic framework.

Neoarchean granitic intrusions

General description

Essentially massive and undeformed granite crops out at several places along the Minnesota River and is inferred to occur widely throughout the MRV (Fig. 3). The most prominent bodies in the Morton block are known informally as the Sacred Heart and Fort Ridgely granites and those in the Benson block as the Odessa and Ortonville granites. Precise U-Pb ages on monazite, xenotime, and zircon from these granites and associated aplite dikes cluster tightly around 2,600 Ma (Table 1; Schmitz and others, 2006). These results agree with the discordant whole-rock Pb-Pb age of 2,605 ± 6 Ma obtained earlier by Doe and Delevaux (1980) for the Sacred Heart granite. Moreover, the date of ca. 2,600 Ma for this regional episode of granite plutonism correlates well with the interpreted time of peak metamorphism in paragneissic portions of the wall-rock terrane into which the granites were emplaced. The Sacred Heart and Fort Ridgely granites are biotite-bearing, medium-grained, generally pink to gray, and massive except near wall-rock contacts where they are moderately flow-foliated and/or compositionally flow-layered. Their normative compositions (Table 5) plot close to the granite minimum trough in the H_2O-saturated

Table 5. Mean major-element and normative compositions of Neoarchean (ca. 2,600 Ma) granites in the Morton and Benson blocks. The analyses recompiled into the group means are from Goldich and others (1970) and Wooden and others (1980).

	A	B	C	D	E	grand mean	standard deviation
SiO_2	72.00	73.20	73.60	74.20	73.40	73.28	0.81
TiO_2	0.28	0.28	0.21	0.13	0.14	0.21	0.07
Al_2O_3	14.00	13.70	13.20	13.10	14.40	13.68	0.54
Fe_2O_3	1.12	0.98	1.05	1.26	1.10	1.10	0.10
FeO	1.19	1.28	1.14	0.99	0.75	1.07	0.21
MnO	0.03	0.02	0.02	0.02	0.02	0.02	0.00
MgO	0.51	0.37	0.30	0.23	0.37	0.36	0.10
CaO	1.71	1.17	1.12	1.10	1.55	1.33	0.28
Na_2O	3.45	3.32	3.16	3.25	3.91	3.42	0.29
K_2O	4.66	5.19	5.31	4.89	4.24	4.86	0.43
P_2O_5	0.10	0.07	0.04	0.05	0.06	0.06	0.02
CO_2	0.14	0.10	0.11			0.12	0.02
H_2O	0.33	0.40	0.30	0.40	0.20	0.33	0.08
F	0.04	0.04	0.03			0.04	0.01
Sum	99.56	100.12	99.59	99.62	100.14	99.87	
Rb	126	168	198	142	165	160	27.44
Sr	402	260	133	368	246	282	106.98
Ba	1745	1365	605	332		1012	655.73
Number of samples	3	6	6	2	2	19	
CIPW norm							
Q	29.67	30.76	31.83	33.75	30.6	31.34	
or	27.54	30.67	31.38	28.9	25.06	28.72	
ab	29.19	28.09	26.74	27.5	33.09	28.94	
an	7.6	5.1	5.1	5.13	7.3	5.95	
C	0.49	0.75	0.38	0.58	0.7	0.61	
hy	2.12	2.04	1.66	1.17	1.2	1.64	
mt	1.62	1.42	1.52	1.83	1.59	1.59	
il	0.53	0.53	0.4	0.25	0.27	0.4	
ap	0.24	0.17	0.09	0.12	0.14	0.14	
fl	0.06	0.07	0.05			0.07	
Total	99.07	99.6	99.17	99.22	99.94	99.41	
AN	20.66	15.36	16.02	15.17	18.07	17.06	

A Mean "adamellite 2", Morton area
B Mean "adamellite 2", North Redwood—Delhi area
C Mean aplite
D Mean Sacred Heart Granite
E Mean granite, Ortonville—Odessa area

Ab-Or-Q system. The Odessa and Ortonville granites include hornblende- and biotite-bearing variants that grade modally toward quartz monzonite and syenogranite and typically are dark red-gray in color. Magmatic flow fabrics defined by aligned feldspar megacrysts are relatively common in the Odessa and Ortonville granites, as are gradationally bounded layers and lenses of pegmatite. The Sacred Heart and Fort Ridgely intrusions and most of the related granite bodies in the Morton block map out as elongated quasi-conformable sheets (Fig. 3). Many of the granite bodies in the Montevideo and Benson blocks are interpreted on geophysical grounds to be more equant in shape.

Outline of granite petrogenesis

It was suggested above that relatively biotite-rich layered gneisses in the Mesoarchean orthogneiss complex could have been the parent material from which the Neoarchean granite masses were derived by anatexis. Many field geologists who have contemplated the features of the flamboyant migmatite that is quarried near the town of Morton and marketed under the descriptive but misleading commercial name "rainbow granite" have entertained this idea informally. The migmatite shows abundant evidence of multiple deformation and partial melting in a tectonically dynamic environment and is thought to encapsulate the fundamental processes of ca. 2,600 Ma granite formation in the Morton block.

Although it is very complex in detail, the Morton migmatite consists fundamentally of three rock types: 1. A highly contorted, modally variable biotite- and hornblende-bearing gray gneiss (bulk composition approximately granodioritic) that consists of layers and irregular small masses of granodioritic, tonalitic, and granitic composition (Goldich and others, 1980b; Wooden and others, 1980); 2. Blocky to lenticular enclaves of amphibolite and pyroxene-bearing amphibolite that are interpreted to be disrupted remnants of former igneous rocks (Nielsen and Weiblen, 1980); and 3. Contorted pink leucosome veins, layers, and lenses of granite, aplite, and pegmatite. The gray granodioritic portion of the gneiss is an earlier-generation migmatite that consists of highly variable proportions of feldspathic leucosome and biotite-hornblende-quartz-feldspar melanosome. This older migmatite is regarded as a coarsely layered, contorted, remobilized variant of general rock type 3 within the orthogneiss complex (Table 2); it contains zircons that have euhedral cores of several Mesoarchean ages and epitaxial overgrowths that are close to 2,600 Ma in age (Bickford and others, 2006).

The amphibolite enclaves in the Morton migmatite contain very sparse accessory zircon. M. Schmitz (unpub. data, 1998) obtained a preliminary concordant U-Pb age of 2,621 ± 12 Ma on a single zircon crystal from a blocky enclave, which agrees approximately with the age of epitaxial zircon rims in the surrounding gray gneiss. The enclaves have been metamorphosed to assemblages of plagioclase + hornblende, plagioclase + hornblende + clinopyroxene, plagioclase + hornblende + orthopyroxene, and plagioclase + hornblende + both pyroxenes (Nielsen and Weiblen, 1980). Metamorphic temperatures estimated for these rocks by the hornblende-plagioclase geothermometer of Blundy and Holland (1990), using previously published mineral compositions (Table 6), fall between 680° and 760° C. These temperatures are interpreted to approximate the peak temperatures attained during regional metamorphism and latest migmatization. They are close to and slightly above the solidus curve for quartzofeldspathic rocks in the presence of H_2O (Winkler, 1976) and therefore would have been high enough to cause partial melting in the granodioritic gray gneiss that is here interpreted as the protolith in the 2,600 Ma migmatization event. The gray gneiss contains approximately 10 to 15 modal percent of combined biotite and hornblende. Dissociation of these hydrous minerals would have facilitated partial melting to some extent even if it did not release water to the point of magmatic saturation. The melt fraction generated in this ca. 2,600 Ma round of anatexis is thought to be preserved in the veins, layers, and lenses of pink granite that permeate the bulk migmatite. Unfortunately, the pink granitic component has not been dated by modern geochronologic methods.

It is likely that regionally widespread and deeper crustal anatexis of the sort illustrated at Morton, followed by large-volume coalescence of the granitic melt fraction, produced some and perhaps most of the 2,600 Ma granite plutons distributed across the MRV. A more rigorous, quantitative test of this simple petrogenetic model is beyond the scope of this review. However, the literature contains well-documented descriptions of field areas where the transition from migmatite to massive granite is firmly established (for example Kisters and others, 2009 and references therein; Reichardt and Weinberg, 2012), and many petrologic and geochemical studies that convincingly demonstrate the feasibility of deriving granitic magma through the partial melting of paragneissic and orthogneissic protoliths (for example Sawyer, 2010 and references therein). It seems reasonable, therefore, to infer a generalized anatectic origin for some and perhaps most of the 2,600 Ma granites in

Table 6. Whole-rock composition of an amphibolite enclave in migmatitic orthogneiss and microprobe analyses of coexisting hornblende, plagioclase, and biotite within it. Analyses are from Nielsen and Weiblen (1980). The hornblende and plagioclase data were used in the calculation of metamorphic temperature.

Sample no. BN-74-11(3)

Mineral	Whole rock	Hornblende	Plagioclase	Biotite
Modal %	-	66.70	31.60	0.50
SiO_2	48.70	44.00	64.05	36.02
TiO_2	1.35	2.88		3.20
Al_2O3	13.70	9.47	20.98	13.82
Fe_2O_3	3.52			
FeO	10.24	19.78		23.08
MnO	0.23	0.25		0.27
MgO	6.07	8.30		10.23
CaO	9.85	10.78	5.19	
Na_2O	3.36	1.31	7.11	
K_2O	1.13	1.01	0.17	9.29
P_2O_5	0.15			
H_2O^+	1.09			
H_2O^-	0.06			
CO_2	0.03			
Cr_2O_3	0.01			
Sum	99.43	97.78	97.50	95.91

CIPW norm			atoms/23 O	atoms/8 O	atoms/22 O
Q		Si	6.644	2.883	5.581
ne	0.03	Al(IV)	1.356	1.114	2.524
or	6.79	Al(VI)	0.330		
ab	27.99	Fe(II)	2.304		2.991
an	19.47	Fe(III)	0.194		
C		Mg	1.868		2.362
di	24.15	Mn	0.032		0.035
hy		Ti	0.327		0.373
wo		Ca	1.744	0.250	
ol	13.06	Na	0.384	0.620	
mt	5.19	K	0.195	0.010	1.836
il	2.61	Sum	15.378	4.877	15.702
ap	0.35				
cr	0.01				
cc	0.07				
Sum	99.72				

BN-74-11(3): Amphibolite 0.5 meter (1.6 feet) from margin of enclave 1.5 meters (4.9 feet) in diameter.

the Morton block of the MRV (such as the Sacred Heart and Fort Ridgely granites plus assorted smaller bodies), and by extension, for some of the Neoarchean granites in the other MRV blocks.

Tonalite plutons

The emplacement of tonalite preceded the emplacement of late- to post-tectonic granite in the MRV. A magmatically foliated biotite tonalite in the subsurface of Watonwan County near the boundary between the Morton and Jeffers blocks yields a discordant U-Pb zircon age of 2,642 ± 57 Ma (age determination by Z. Peterman reported in Southwick, 1994). Similar tonalite is inferred on the basis of geophysical signature to occur in all four blocks of the MRV, although it appears to be less abundant than the younger 2,600 Ma granite. The tonalite has not been sampled widely and its petrologic characteristics are not well known.

PALEOPROTEROZOIC INTRUSIONS

Preliminary discussion

The Paleoproterozoic intrusions within the MRV are generally small in size, varied in composition, and widely but unevenly scattered. To facilitate description and discussion they are here grouped into three categories: 1. Mafic dikes; 2. Plugs and small plutons of gabbro, pyroxenite, peridotite, and diorite; and 3. Plugs and small plutons of granite, granodiorite, quartz monzonite, and related granitic rocks. The mafic dikes are of regional significance because they provide broad time constraints on the movements of the Great lakes tectonic zone, the Appleton shear zone, and the Yellow Medicine shear zone. The temporal relationships among dike-emplacement events and shear-zone movements are developed below.

Mafic dikes

Geologic interpretation of the mafic dikes rests on physical and temporal inferences obtained from geophysical imagery, primarily enhanced presentations of high-resolution aeromagnetic mapping, and previously published geochronologic and geochemical data. The first vertical derivative of the total aeromagnetic anomaly (Chandler and Lively, 2007) was found to be the most useful geophysical image for delineating dikes. The total aeromagnetic anomaly map and the second vertical derivative of the total aeromagnetic anomaly also were utilized as adjuncts to the first derivative map in delineating and classifying subsets of the dike population.

Linear dike anomalies were sorted into four regionally distinct groups defined by strike azimuth and relative ages as determined from crosscutting relationships. Differences in magnetic polarity, such as positive versus negative dike anomalies, also were helpful to the visual sorting process in some situations. The four regional dike groups recognized aeromagnetically are here termed major groups I to IV (Table 7) and are shown in map view in Figure

Table 7. Summary of ages determined on mafic dikes within the MRV, with relevant comments. See text for details. Colors correspond to dike-group colors on Figure 7.

Group symbol	Trend (az.)	Rock type	Age (Ma)	Dating method	Remarks
Major groups					
Group I	070-110	Fe tholeiite	2,080	Hornblende K-Ar	Petrologically very similar to Kenora–Kabetogama/Fort Frances dikes dated 2,076 Ma (badelleyite U-Pb) and presumed to correlate with them.
Franklin dike	110	Fe tholeiite	2,067	Zircon U-Pb	See Schmitz and others (2006) for details on the Franklin dike.
Group II	125-140	Fe tholeiite	< ca. 2,067		Dikes cut group I dikes on aeromagnetic images. Presumed to be a sub-swarm of the Kenora–Kabetogama/Fort Francis swarm.
Group III	075-100	Hornblende ferrodiorite(?)	< ca. 1,772		Cut granites in East-Central Minnesota batholith; inferred to be the same age, composition, as ECMB NW dikes.
ECMB NW	120-130	Hornblende ferrodiorite	< ca. 1,772		Intrude East-Central Minnesota batholith; cut ECMB NE dikes (below).
Group IV	350-020	Hornblende diorite	ca. 1,750?		Tentatively assumed to be comagmatic with Cedar Mountain Complex; inferred rock type and age of dikes based on Cedar Mountain data. Cut dikes of other three major groups.
Minor groups					
Group HA	various	Hornblende andesite	>1,825 <2,067	Bracketed	Disrupted by Section 28 granite dated 1,825 Ma (zircon Pb-Pb); intrude Group I dikes at many localities.
Group OT	various	Olivine tholeiite	unknown		May correlate with olivine tholeiite dikes in ECMB NE group or may be comagmatic with group HA.
ECMB NE	060	Ol and quartz tholeiite	< ca. 1,772		Generally thin dikes that cut granites in the East-Central Minnesota batholith

7. The dikes of group I are inferred to be the oldest, followed in decreasing age by dikes of groups II, III, and IV, respectively. The principal attributes of each major group are summarized in Table 7 and discussed more fully below.

The scheme used here for sorting the major dikes into groups supersedes an earlier one employed in compiling the geologic map of southwestern Minnesota (Southwick, 2002). The magnetic polarity distinctions used in the earlier scheme were found to be of limited value when applied to the larger map area studied here.

Two other sets of dikes that lack aeromagnetic expression are known from outcrop mapping in the Minnesota River valley (Himmelberg, 1968; Manzer, 1978). These are here referred to as minor dike groups OT and HA. The principal attributes of the minor dike groups also are summarized in Table 7 and discussed more fully below.

Dikes of group I

Group I consists of high-Fe tholeiite dikes (Table 8) that range in strike from east–northeast to west–northwest (az. 070 to 110) in the MRV blocks south of the Appleton shear zone and more consistently west–northwest in the Benson block and the adjoining quiet zone of the Wawa subprovince (Fig. 7). Roughly 20 to 25 percent of the dikes generate negative aeromagnetic anomalies and about 75 to 80 percent generate positive anomalies. The intermingling of dikes with positive and negative aeromagnetic signatures is a common feature of major Precambrian dike swarms worldwide that as yet has no satisfactory temporal or petrologic explanation.

Two geochemical subtypes of Fe tholeiite are represented in the group I dikes exposed in the Minnesota River valley (Manzer, 1978; Schmitz and others, 2006). One geochemical type is enriched relative to the other in potassium, titanium, iron, and incompatible trace elements. Manzer (1978) identified the two types through statistical Q-mode clustering of major-element chemical analyses and found that the distinction rested largely on the relative abundance of titanium. He referred to the high-Ti cluster as compositional type T-1 and to the low-Ti cluster as compositional type T-2. Schmitz and others (2006) utilized major- and trace-element data to establish two compositional types based on relative incompatible trace-element (ITE) abundance. Their low-ITE (or more primitive) compositional variant corresponds well with Manzer's low-Ti cluster assignments for dikes that were sampled in both studies.

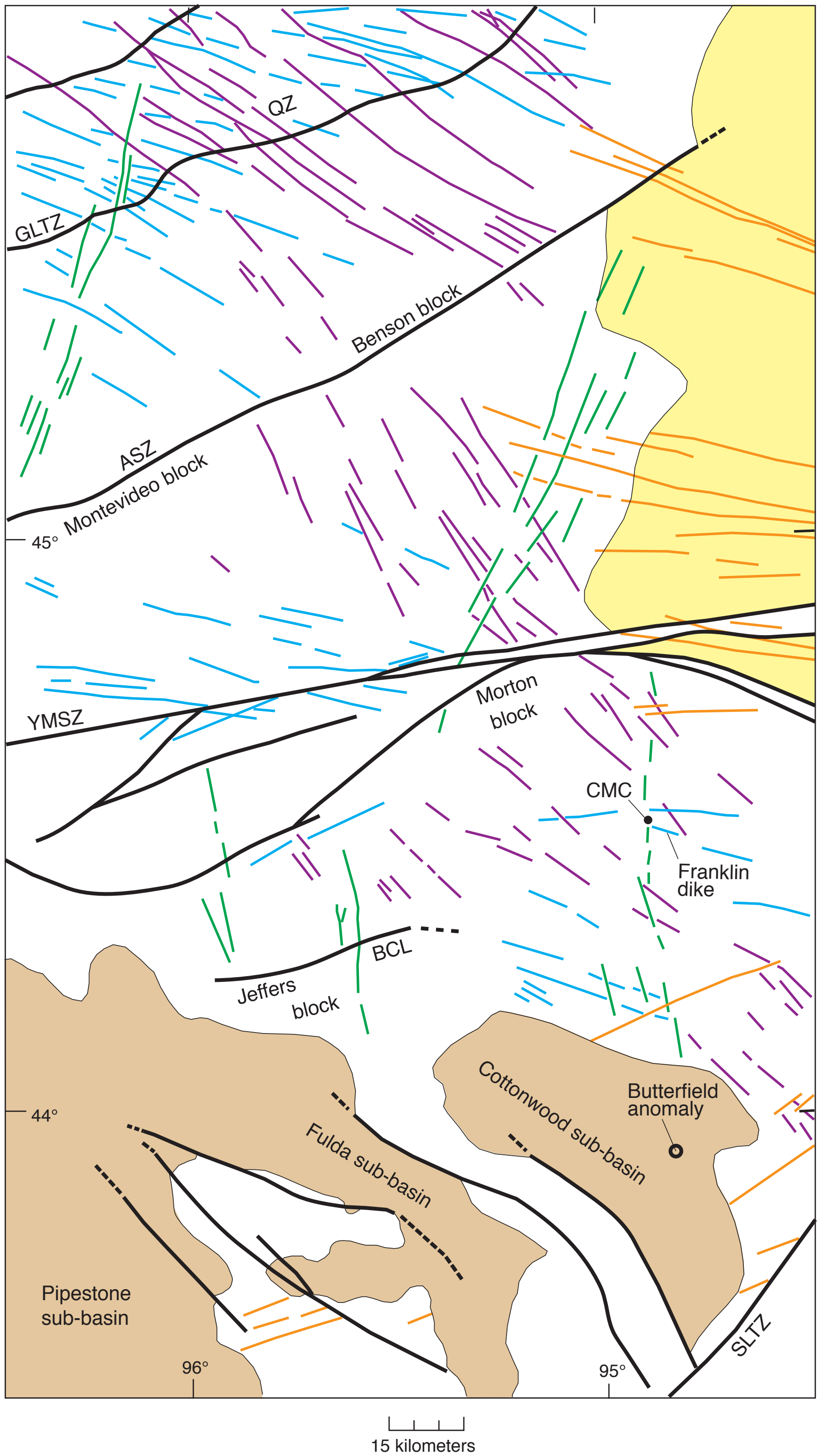

Figure 7. Mafic dikes within the MRV and the "quiet zone" (QZ) of the Wawa subprovince as mapped from a gray-scale image of the first vertical derivative of the aeromagnetic anomaly. Dike color code: blue = group I; purple = group II; orange = group III; green = group IV. CMC represents the Cedar Mountain Complex. The Sioux Quartzite sub-basins are shown in brown. The yellow area includes rocks of the East-Central Minnesota batholith and the Hillman–Little Falls panel of the Penokean orogen. GLTZ = Great Lakes tectonic zone, ASZ = Appleton shear zone, YMSZ = Yellow Medicine shear zone, BCL = Brown County lineament, SLTZ = Spirit Lake tectonic zone.

Table 8. Chemical analyses and CIPW norms of group I Fe tholeiite dikes. Analyses A, B from Schmitz and others (2006); analyses C, D from Daggett (1980); analysis F from Southwick and others (1993); analysis E previously unpublished.

Sample	A	B	C	D	E	F
number	92-6-24-3	MRV-9	MN-79-8	MN-79-21	GF-24A	SWG10-242
Chemical type	low-ITE	low-ITE	low-ITE	low-ITE	high-ITE	high-ITE
SiO_2	50.13	50.62	52.6	55.75	46.7	48.4
TiO_2	1.23	1.33	0.77	0.57	1.73	1.78
Al_2O_3	13.48	13.83	15.82	15.91	14.6	13.5
Fe_2O_3	14.53	13.67	3.73	2.73	3.67	3.22
FeO			5.92	5.44	10.3	11.8
MnO	0.18	0.19	0.15	0.13	0.24	0.24
MgO	6.66	6.97	5.85	5.7	6.49	5.72
CaO	10.55	10.8	8.87	6.86	10.3	8.93
Na_2O	2.3	2.12	2.75	3.11	2.47	1.69
K_2O	0.33	0.36	2.03	2.93	0.7	0.68
P_2O_5	0.11	0.1	0.36	0.32	0.27	0.18
CO_2			0.05	0.03	0.03	0.09
LOI	0.72	0.58	1.01	0.59	1.7	1.5
F						
Sum	100.22	100.57	99.91	100.07	99.20	97.73
Mg# (atomic)	47.60	49.73	50.18	51.09	45.99	40.98
FeO^t	13.08	12.57	9.28	7.90	13.60	14.70
Rb	11	19.2	45	52	37	17
Sr	121	127	604	612	406	121
Ba	47.5	205	675	580	296	103
Sc	44	45.7				
Nb	2.4	3.2			<10	28
Hf	2.05	2.17				
Ta	0.24	0.23				
Zr	71.8	69.7	126	213	79	118
Y	25.7	21.6			<10	23
Cr	122	212			120	183
Ni	71.4	81.8			60	79
Cu					70	76
Zn					122	116
V	332	315			408	403
U	0.5	0.7				
Th	0.41	0.35				
Cs	0.17	0.35				
La	4.7	4.35				
Ce	11.1	11.4				
Nd	17	22				
Sm	3.01	2.83				
Eu	1.07	1.01				
Tb	0.72	0.63				
Yb	2.55	2.33				
Lu	0.37	0.36				
CIPW norm						
Q	1.83	2.75	2.66	3.36	0	4.72
or	1.95	2.13	12	17.31	4.14	4.02
ab	19.46	17.94	23.27	26.32	20.2	14.3
an	25.48	27.16	24.83	20.8	26.68	27.24
di	21.58	21.18	13.6	9.02	18.63	13.21
hy	21.47	21.16	14.8	16.86	10.82	24.19
ol	0	0	0	0	7.07	0
mt	3.96	4.1	5.41	3.96	5.32	4.67
il	2.34	2.53	1.46	1.08	3.29	3.38
ap	0.25	0.23	0.83	0.74	0.63	0.42
Total	98.32	99.17	98.85	99.45	97.47	96.14
AN	56.7	60.22	51.62	44.14	56.08	65.58

Notes:
92-6-24-3: Large dike south of Granite Falls
MRV-9: Franklin dike
MN-79-8: Franklin dike, chilled margin
MN-79-21: Franklin dike, gabbroic interior
GF-24A: Dike south of Granite Falls cut by small faults, Yellow Medicine County
SWG10-242: Dike in drill core near Hanly Falls, Yellow Medicine County

Schmitz and others (2006) reported a precise U-Pb zircon age of 2,067 ± 0.7 Ma for the Franklin dike, a low-ITE dike in group I that is located in the Morton block (Fig. 7). The Franklin dike age of ca. 2,067 Ma agrees, within error, with U-Pb badelleyite/zircon ages of ca. 2,077 and 2,076 Ma obtained from low-ITE dikes in the Kenora–Kabetogama/Fort Frances swarm that crosses the Quetico–Wabigoon subprovince boundary and the Minnesota–Ontario international boundary east of Lake of the Woods (Wirth and others, 1995; Buchan and others, 1996). Moreover, Schmitz and others (1995, 2006) and Wirth and Vervoort (1995) described geochemical and petrologic similarities between the dikes of group I in the MRV and the Kenora–Kabetogama/Fort Frances dikes that strongly imply essential consanguinity of the two dike populations.

Further evidence in favor of this temporal and petrologic connection comes from regional dike patterns revealed in aeromagnetic imagery (Chandler and Lively, 2007) across the 500-kilometer (310-mile) expanse of outcrop-free northwestern Minnesota that separates exposures of the Kenora–Kabetogama/Fort Frances and group I MRV dikes. The Kenora–Kabetogama/Fort Frances swarm in its "type area" contains just one generation of Fe-tholeiite dikes. The dike population includes large master dikes that are as long as 300 kilometers (186 miles) and as thick as 150 meters (492 feet), trend a few degrees west of north, are spaced as closely as a few hundred meters apart, are parallel to one another for many tens of kilometers, are of intermingled high-ITE and low-ITE composition, and show little to no variation in elemental abundance along strike (Southwick and Day, 1983; Southwick and Halls, 1987; Schmitz and others, 1995). High-ITE dikes have not been observed cutting across low-ITE dikes or vice versa. Shorter and thinner dikes of the two compositions are interspersed among the master dikes; these also are intermingled spatially and have not been observed to intersect. Aeromagnetic imagery shows that the Kenora–Kabetogama/Fort Frances swarm is radial in plan view and qualifies as a giant radiating swarm in the terminology of Fahrig (1987) and Ernst and others (1995). Dike trends fan from north–northwest azimuths at the eastern edge, where most of the outcropping dikes are located, to progressively more westerly azimuths further west and south into the covered area. Although the swarm appears to be regionally coherent throughout its extent, there are clear internal differences in its geophysical attributes from northeast to southwest (Chandler and Southwick, 1985). The northeastern sector, which extends west and south from the area of exposed dikes to an indistinct northwest-oriented boundary located geologically in the central part of the Wawa subprovince in northwestern Minnesota, is characterized by positive aeromagnetic anomalies indicative of long, thick, master dikes and intermingled smaller dikes. The southwestern sector of the swarm, which extends from northwestern Minnesota into the map area of southwestern Minnesota shown in Figure 7, contains the aeromagnetic expression of hundreds of dikes but lacks the high-amplitude elongate anomalies associated with master dikes. Furthermore, many of the aeromagnetic anomalies associated with dikes in the southwestern sector are negative, and there is clear aeromagnetic evidence that most of the sector consists of two sub-swarms that differ in strike and relative age. The dike trends in the relatively older sub-swarm merge smoothly northeastward into the radial pattern observed in the northeastern sector, where the only dikes present are this older set.

Based on the temporal, geochemical, and geophysical evidence outlined above, the dikes of group I in the MRV are inferred to be equivalent to dikes in the older of two sub-swarms that make up the southwestern sector of the regional Kenora–Kabetogama/Fort Frances swarm. Furthermore, they are inferred to be temporally and petrogenetically equivalent to the single set of dikes present in the northeastern sector. The dikes that constitute the younger sub-swarm in the southwestern sector of the regional Kenora–Kabetogama/Fort Frances swarm are coextensive with and equivalent to the dikes in the MRV assigned to group II.

Dikes of group II

Group II is composed of tens to hundreds of dikes that strike consistently northwest (az. 125 to 140). Oddly, these dikes have not been identified in the outcrop belt along the Minnesota River despite their apparent presence in the vicinity as interpreted from aeromagnetic imagery. Samples are lacking and therefore the geochemical attributes and precise age of the dikes are unknown. As in group I, about one fourth of the aeromagnetic anomalies indicative of group II dikes are negative and about three fourths are positive. North of the Appleton shear zone and less commonly south of it the aeromagnetic anomalies associated with group II dikes cut across the aeromagnetic expression of group I dikes and therefore are indicative of a younger set of intrusions. This cross-cutting relationship is especially well portrayed in the "quiet zone" of the Wawa subprovince (Fig. 7), where the flat aeromagnetic background of the country rock facilitates remote mapping of the more magnetic dikes. The age difference between the two groups is not known, although it is likely that both groups were emplaced during the extensional phase of the Penokean tectonic cycle, prior to Penokean convergence. Regionally, the group II dikes are interpreted to be the younger of two sub-swarms that make up the giant Kenora–Kabetogama/Fort Frances dike swarm. Precedent for the sub-swarm interpretation comes from the older and much larger Matachewan dike swarm in Canada (age 2.45 to 2.47 Ga), which consists of several sub-swarms of intersecting or overlapping geometry and differing relative ages (West and Ernst, 1991; Phinney and Halls, 2001).

Relationship of dike groups I and II to shear zones in the MRV

The aeromagnetic anomalies associated with dike groups I and II cross the Great Lakes tectonic zone into the MRV without observable deviation or displacement (Fig. 7). The map pattern of dikes within the Benson block is identical to the two-sub-swarm geometry observed in the quiet zone and interior volcanoplutonic zones of the Wawa subprovince. The regular plan-view pattern of these dikes does not continue south of the Benson block, however, and the observed disruption at the northern margin of the Montevideo block implies that movements on the Appleton shear zone and the other MRV shear zones occurred after sub-swarms I and II were emplaced.

This disintegration of well organized sub-swarm geometry appears to coincide with a diminution in the number of group I and group II dikes at the southwestern fringe of the regional Kenora–Kabetogama/Fort Frances swarm, and may be recording the southwestward fading out of the extensional stress field and associated magmatic processes that were responsible for the dike swarm as a whole. The greater crustal thickness and rigidity of the MRV compared to the Wawa subprovince may have been a factor in limiting the southwestward propagation of the Kenora–Kabetogama/Fort Frances dikes.

The dikes in the group II sub-swarm may have developed just a little later than the larger group I sub-swarm in the regional Kenora–Kabetogama/Fort Frances magmatic event, in response to subtle shifts in the tectonomagmatic system. The presumably short time gap between the two periods of dike emplacement envisioned in this scenario has not been determined. Alternatively, the group II dikes may represent an entirely separate episode of pre-Penokean foreland extension and magmatism that emanated from a focal point located south of the one from which the group I sub-swarm emanated. A substantial fraction of the group II dikes trend directly into the area of rift-related rocks in the Penokean foreland mapped by Jirsa and others (2003) and mentioned by Chandler and others (2007) in their discussion of Penokean tectonics. It is conceivable, therefore, that the group II dikes were emplaced in early geon 19, when crustal extension and rift-related volcanism were occurring along much of the foreland belt of the Penokean orogen (Schulz and Cannon, 2007).

Dikes of group III

Dikes in this group strike west–southwest to west–northwest (az. 075 to 100). Most of them produce strongly negative aeromagnetic anomalies, many of which pass from the MRV into the younger rocks of the Hillman–Little Falls panel of the Penokean fold-and-thrust belt and the East-Central Minnesota batholith (Fig. 7). These aeromagnetically mapped dikes, denoted as subgroup ECMB NW in Table 7, are similar in trend and geophysical expression to a west–northwest-trending set of intra-batholith mafic dikes mapped in outcrop near the town of Waite Park (Boerboom and Holm, 2000).

The intra-batholith dikes near Waite Park are chilled against granite and classify modally as pyroxene ferrodiabase or ferrodiorite that contains two or three percent of Fe-Ti oxide phases. They are altered deuterically, but in general their primary igneous textures and minerals are well preserved. This set of intra-batholith dikes produces strong negative aeromagnetic anomalies typical of sources 50 meters (164 feet) or more in width, very similar to the aeromagnetic expression of the group III dikes that intrude the MRV rocks northwest of the batholith contact. The group III dikes within the MRV and their geophysical counterparts within the batholith are inferred to correlate and to consist predominantly of ferrodiabase. Unfortunately, none of the outcropping ferrodiabase dike rock has been chemically analyzed or radiometrically dated.

The dikes of group III are younger than the minimum age of the East-Central Minnesota batholith (Holm and others, 2005) and older than dikes of group IV as inferred from crosscutting relationships observed on aeromagnetic imagery (Fig. 7). Therefore they are bracketed in age between 1,772 and ca. 1,750 Ma.

Dikes of group IV

Dikes in this group occur in four distinct clusters (Fig. 7). Two clusters in the Jeffers, Morton, and

Montevideo blocks of the MRV trend slightly west of north (az. 170 to 180), a third cluster in the western part of the Benson block and the "quiet zone" of the Wawa subprovince trends slightly east of north, and a fourth cluster near the northeast margin of the MRV trends north–northeast. The aeromagnetic anomalies associated with group IV dikes are of high amplitude and are quite broad, indicating that the source dikes are large. The total number of dikes in the group is on the order of a few tens. These dikes cut across the other three dike groups at high angles and are quite clearly the youngest major dike set in the MRV.

Dikes of group IV do not crop out and have not been sampled by drilling. Therefore no data on their composition or age have been obtained directly. However, a strong positive aeromagnetic anomaly indicative of a group IV dike strikes directly into the Cedar Mountain Complex (Fig. 7), a concentrically zoned plug of hornblende diorite and monzonite about 600 meters (1,969 feet) in diameter in the Minnesota River valley that has been studied in some detail (Lund, 1950; Daggett, 1980; Beltrame and others, 1982). It is conceivable that the Cedar Mountain plug and the dike are comagmatic, and if so, petrologic and temporal data obtained on the plug may pertain also to the dike.

The Cedar Mountain Complex consists of: 1. A chilled-margin facies of basaltic andesite and microdiorite; 2. A thick zone of flow-layered melanocratic hornblende diorite; and 3. A central core of weakly flow-layered monzonite and quartz monzonite (Daggett, 1980; Beltrame and others, 1982). The chilled-margin andesite-microdiorite is interpreted to represent the approximate composition of the intruding magma. The hornblende diorite forms the bulk of the intrusion and probably was emplaced as a crystal-liquid mush. The central monzonite core formed from a late pulse of evolved magma that intruded the surrounding diorite after it was solidified and capable of brittle fracturing. The concentric zoning, steep to vertical flow layering, and late intrusion of the monzonite core collectively imply that the Cedar Mountain magma was supplied from a differentiating source at depth and flowed vigorously and repeatedly upward through a pipe-like conduit.

Geophysical modeling (Beltrame and others, 1982) confirms the Cedar Mountain Complex to be a vertical pipe. Moreover, the models reveal the presence of denser, more magnetic rock masses (presumably diorite) at depth beneath the central monzonite core, indicating a carrot-like downward reduction in core volume. The pipe-like shape of the plug and its proximity to the dike support the possibility of the plug having originated as a bud that erupted from and was supplied by the dike in the manner described by Delaney and Pollard (1981). Magnetic susceptibility and density values measured on the Cedar Mountain diorite are appropriate for producing anomalies on the scale of those observed over the group IV dike that is postulated to be a comagmatic equivalent. The principal rock types in the dike are therefore inferred to be hornblende diorite and hornblende andesite analogous to the diorite and andesite of the Cedar Mountain Complex (Table 9).

Biotite and hornblende from the monzonite core of the Cedar Mountain Complex yield essentially identical K-Ar ages of 1,750 Ma (Hanson, 1968). This age, some 20 m.y. younger than the age of the East-Central Minnesota batholith, fits with the relative sequence of dike emplacement inferred from crosscutting relationships of dikes in the four major groups. Modern U-Pb dating of zircon or monazite that would establish more firmly the crystallization age of the Cedar Mountain monzonite (and the inferred emplacement age of dike group IV) would be advantageous.

Minor dikes not discernible on aeromagnetic images

This category consists of two outcropping dike types that differ in modal composition and are demonstrably younger than the Fe-tholeiite dikes of group I (Himmelberg, 1968). Hornblende-bearing diabase dikes of broadly tholeiitic to andesitic composition (Table 10), here designated as group HA, and olivine-phyric diabase dikes of broadly tholeiitic composition, here designated as group OT, crop out within a belt about 10 kilometers (6 miles) wide that crosses the Minnesota River immediately north of the Yellow Medicine shear zone. Neither type has been identified in the Morton block. The dikes range in thickness from less than one to about 10 meters (33 feet); most are less than 5 meters (16 feet) thick. The longer and thicker dikes strike generally northeast but the more abundant short and thin dikes trend in various directions, apparently following nonsystematic brittle fractures in the host rocks. The temporal and petrogenetic relationships between the HA and OT dikes are not firmly established; the contrasting dike types may represent separate magmatic events (Himmelberg, 1968) or they may be the products of a single magmatic episode (Schmitz and others, 2006).

The HA dikes consist of fine-grained hornblende-rich rocks, locally porphyritic, that grade texturally

Table 9. Chemical analyses and CIPW norms of the chilled margin, near-margin microgabbro, and central quartz monzonite of the Cedar Mountain Complex.

Sample number	MN-79-28	MN-79-29	MN-79-27
SiO_2	52.85	51.45	59.35
TiO_2	0.88	0.76	0.56
Al_2O_3	17.46	14.18	18.85
Fe_2O_3	4.31	3.04	2.24
FeO	5.44	6.92	2.58
MnO	0.13	0.16	0.07
MgO	4.25	9.15	1.81
CaO	8.28	8.21	3.71
Na_2O	2.76	2.26	4.94
K_2O	1.98	2.38	3.42
P_2O_5	0.38	0.33	0.35
CO_2	0.07	0.08	0.52
LOI	1.07	1.1	1.58
Sum	99.86	100.02	99.98
Mg# (atomic)	44.86	62.83	41.27
FeOt	9.32	9.66	4.60
Rb	28	40	77
Sr	628	559	413
Ba	695	805	225
Zr	166	179	206
CIPW norm			
Q	5.82		6.91
or	11.7	14.06	20.21
ab	23.35	19.12	41.8
an	29.4	21.52	16.12
C			1.11
di	7.44	13.73	
hy	12.2	19.57	6.6
ol		4.21	
mt	6.25	4.41	3.25
il	1.67	1.44	1.06
ap	0.88	0.76	0.81
Total	98.71	98.82	97.87
AN	55.73	52.95	27.8

Data from Daggett (1980)
MN-79-28: Chilled-margin hornblende andesite
MN-79-29: Hornblende diorite
MN-79-27: hornblende-biotite monzonite, central core

to aphanitic chilled margins at wall-rock contacts. They intrude and are chilled against Archean rocks and the 2.07 Ga tholeiite dikes of group I, and also cut minor shear zones that transect the group I dikes and their gneissic wall rocks (Himmelberg, 1968). Outcrops north of Granite Falls display a hornblende andesite dike that has been invaded and disrupted by a small granite plug that Goldich and others (1970) informally termed the "Section 28 adamellite" and is now called the Section 28 granite. Catanzaro (1963) obtained a zircon-Pb/Pb age of 1,825 Ma on the granite, which, if correct, brackets the emplacement age of the hornblende andesite dikes between 2.07 and 1.82 Ga. In broad terms this interval spans the complete Penokean tectonic cycle.

The dikes of group OT are unaltered basalt and microdiabase composed of microcrystalline plagioclase, granular pyroxene, and dusty opaques plus microphenocrysts of olivine, plagioclase, and augite. The olivine microphenocrysts commonly display reaction rims of colorless amphibole or orthopyroxene + amphibole. Chemical analyses of OT and HA dike rocks are remarkably similar in content of major, minor, and trace elements (Fig. 8; Table 10). This raises the possibility that the OT and HA rocks are comagmatic (Schmitz and others, 2006). Moreover, some analyses of OT rocks are moderately quartz-normative, as the column A analysis in Table 10, and some analyses of HA rocks are olivine-normative, as the column G analysis of a sample from the dike disrupted by the Section 28 granite. The quartz-normative bulk composition of some olivine-bearing dike rocks and the hornblende reaction rims observed on olivine phenocrysts in dike rocks of the OT petrographic type imply that the olivine phenocrysts are incompletely resorbed early-formed crystals. Fractional removal of early olivine from the magma system would tend to drive the composition of remaining melt toward more silica-rich, possibly andesitic, compositions, as would the assimilation of quartz and feldspar from gneissic wall rocks. If the OT and HA rocks are in fact comagmatic (a speculation at this point that requires more sophisticated petrologic research), and accepting provisionally a pre-1,825 Ma age for the HA dikes, it follows that the OT dikes also were emplaced prior to 1,825 Ma.

Several previous investigators, including Schmitz and others (2006), have suggested that the OT dikes in the MRV may correlate with petrographically similar olivine diabase dikes that intrude and are chilled against granitoid rocks of the East-Central Minnesota batholith. The olivine-bearing dikes within the batholith are parallel to and intermingled with quartz tholeiite dikes (Boerboom and Holm, 2000); the olivine and quartz tholeiite dikes together constitute a northeast-trending dike set, denoted as subgroup ECMB NE in Table 7, that is cut by the west–northwest-trending dikes of hornblende ferrodiorite assigned here to group III, subgroup ECMB NW (Table 7). Boerboom and Holm (2000)

Table 10. Chemical analyses and CIPW norms of minor mafic dikes in the MRV and the East-Central Minnesota batholith. Analyses A and C-F are from Schmitz and others (2006); analyses B and G are from Goldich and others (1980a).

	A	B	C	D	E	F	G
Dike group	OT	OT	HA	HA	HA	HA	HA
Sample number	92-6-24-5b	G-775	92-6-24-4a	MRV-4	92-6-24-6a	MRV-5	G-588
SiO^2	52.97	47.2	59.92	52.98	54.69	61.19	47.5
TiO_2	0.6	1.71	0.85	1.04	0.45	0.75	2.5
Al_2O_3	15.64	14.9	15.77	16.74	15.51	15.38	14.1
Fe_2O_3	9.56	2.61	7.17	9.49	8.47	6.96	4.39
FeO		10.88					10.28
MnO	0.13	0.22	0.1	0.14	0.13	0.09	0.36
MgO	7.35	7.03	4.15	5.8	6.7	3.8	5.98
CaO	10.07	11	5.99	8.64	9.43	5.74	8.84
Na_2O	2.16	2.45	3.85	3.09	2.47	3.13	2.76
K_2O	0.98	0.53	1.63	1.42	1.19	2.06	1.47
P_2O_5	0.18	0.26	0.33	0.4	0.19	0.29	0.32
CO_2		0.61					0
LOI	0.68	0.69	1.33	0.87	0.8	0.67	1.1
Sum	100.32	100.07	100.28	100.61	100.02	100.05	99.52
Mg# (atomic)	60.38	48.61	53.43	54.78	61.06	51.98	42.85
FeO^t	8.60	13.23	6.45	8.54	7.62	6.26	14.23
Rb	18.9	11.8	23.3	26.4	24.6	56.2	35.1
Sr	202	494	457	446	254	281	269
Ba	461	360	855	634	513	475	245
Sc	33.6		16.3	26.2	31.2	16	
Nb	3.5		8.8	12.5	3.2	11.5	
Hf	1.72		4.21	4.35	1.82	4.8	
Ta	0.25		0.56	0.68	0.23	0.77	
Zr	68.4	95	168	185	70.9	190	200
Y	14.5		15.7	20.4	13.5	17.8	
Cr	244	25	139	122	247	92.5	45
Ni	115	70	46.9	45.3	106	45.5	120
Cu		40					60
Zn		110					<10
V	182	320	130	184	161	111	380
U	0.62		2.42	1.55	1.02	2.83	
Th	4.41		9.27	6.67	4.4	13.69	
Cs	0.16		0.24	0.29	0.44	1.06	
La	21.4		46.7	50.2	22.9	43	
Ce	39.4		87.7	95.4	42.2	79.2	
Nd	14		33	38	17	31	
Sm	2.54		5.76	6.56	2.94	5.25	
Eu	0.72		1.45	1.63	0.77	1.2	
Tb	0.35		0.57	0.77	0.39	0.62	
Yb	1.64		1.63	2.09	1.65	2.07	
Lu	0.24		0.26	0.32	0.26	0.32	
CIPW norm							
Q	4.19	0	12.44	2.66	6.01	16.77	0
or	5.79	3.13	9.63	8.39	7.03	12.17	8.69
ab	18.28	20.73	32.58	26.15	20.9	26.49	23.35
an	30.09	28.09	20.93	27.61	27.72	21.83	21.74
di	15.17	20.25	5.35	10.26	14.45	3.85	15.47
hy	20.78	7.81	12.56	17.38	18.35	12.45	11.9
ol		11.1					5.26
mt	3.04	3.78	3.51	3.68	2.83	3.26	6.37
il	1.14	3.25	1.61	1.98	0.85	1.42	4.75
ap	0.42	0.62	0.76	0.93	0.44	0.67	0.76
Total	98.9	98.82	99.37	99.04	98.58	98.91	98.61
AN	62.21	57.54	39.12	51.36	57.01	45.18	48.21

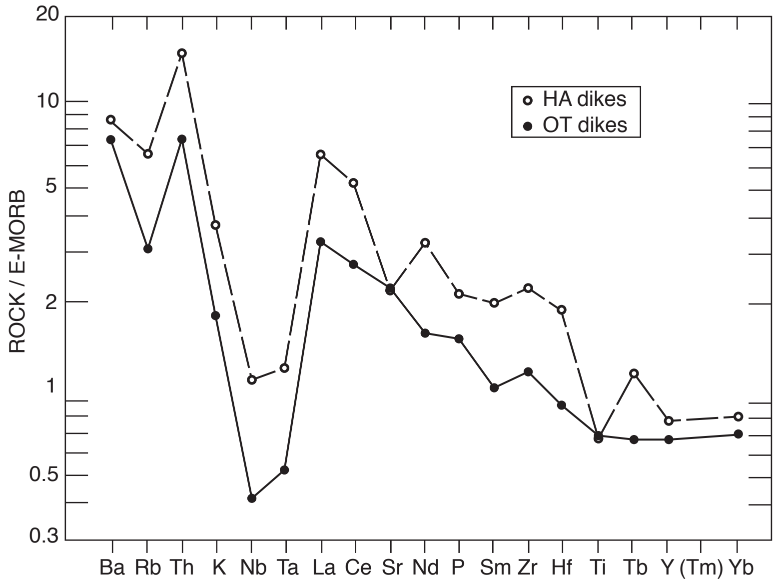

Figure 8. Spider plot of the mean compositions of rocks in dikes classified modally as olivine tholeiite (group OT) and hornblende andesite (group HA). See Table 10 for the analytical data.

argued that textural features at the contact between a quartz tholeiite dike of subgroup ECMB NE and a subparallel dike of microgranite show that the granite dike was still hot when the tholeiite dike was emplaced next to it. The time of quartz tholeiite emplacement therefore is inferred to have been just slightly later than the 1,772 Ma emplacement age of the batholith, and the time of olivine tholeiite emplacement may have been nearly the same.

If the OT dikes in the MRV are indeed comagmatic with the HA dikes and the age of the Section 28 granite is correct, they are at least 55 m.y. older than the olivine tholeiite dikes that intrude the East-Central Minnesota batholith. Alternatively, if the OT and HA dikes are petrologically unrelated, then the correlation of the OT dikes with the intra-batholith olivine tholeiite dikes is a viable possibility. The solution to this age question will eventually come from future petrologic and geochronologic investigations of the dikes and the Section 28 granite.

Mafic and ultramafic plugs and small plutons

Pipe-like plugs

The potential-field images of the MRV and adjacent parts of the Penokean orogen are dotted by many coincident, closed, aeromagnetic and gravity highs that are known to correspond with small plutons of diorite, gabbro, pyroxenite, and peridotite (Table 11). The previously described Cedar Mountain Complex is a member of this group, as is an altered peridotite plug exposed in the Minnesota River Valley northwest of Franklin (Chan, 1990). Several other geophysical anomalies have been confirmed by drilling to consist of gabbro, pyroxenite, or peridotite. A large concentration of these small intrusions is located in the southeastern part of the Morton block. A few are spread south from there into the Jeffers block and north into the Montevideo block (Southwick, 2002), and another large cluster occurs about 60 kilometers (37 miles) northeast of the east end of the Benson block within the Hillman–Little Falls panel of the Penokean fold-and-thrust belt (Boerboom and others, 1995, 1999; Boerboom, 2014). Many of the plugs in the Hillman–Little Falls area consist principally of melanocratic hornblende diorite and closely related rock types. Plugs of this general type also intrude various plutons within the East-Central Minnesota batholith, most abundantly in the northwestern part of the batholith that is closest to the protrusion of Penokean thrust panels into the MRV (Boerboom and others, 1995). This establishes their emplacement age as post-1,772 Ma.

The diorite plugs confirmed by drilling in the Hillman–Little Falls area generate geophysical signatures that are virtually identical to those generated by plugs known to be gabbro or ultramafic rocks (Boerboom, 2014). Plugs of all these compositions are inferred from their geophysical signatures to be subcircular, oval, or hook-shaped in plan, typically 1 to 3 kilometers (0.6 to 1.9 miles) in diameter, and pipe-like in the depth dimension as determined from geophysical modeling (Beltrame and others, 1982; Southwick and Chandler, 1987). Their dimensions, clustered distribution, pipe-like form, and occurrence within an Archean craton are analogous to the first-order attributes of kimberlite and lamproite pipes in the diamond fields of South Africa and elsewhere.

Table 11. Chemical analyses and CIPW norms of mafic and ultramafic rocks in pipe-like plugs that intrude Archean rocks in the MRV (columns A-C) and the Little Falls Formation within the Penokean orogen (columns D-E). Analysis A from Southwick and others (1993); analysis E from Southwick and Chandler (1987); others from Minnesota Geological Survey unpublished files.

Sample number	A YB89-8	B MRV-1	C MRV-2	D EX-C1-299	E P-14b
SiO_2	52.9	42.49	54.96	42.46	43.4
TiO_2	0.58	0.21	0.07	0.18	0.19
Al_2O_3	17.7	4.05	2.08	2.8	4.46
Fe_2O_3	3.87	0	0	0	4.8
FeO	4.7	8.37	4.23	8.92	5.2
MnO	0.14	0.13	0.11	0.15	0.16
MgO	5.73	32.58	17.46	29.53	25.5
CaO	9.31	2.78	7.25	5.35	7.22
Na_2O	3.49	0.44	0	0.3	0.66
K_2O	0.48	0.06	0	0.39	0.56
P_2O^5	0.23	0.02	0.02	0.06	0.04
LOI	0.8	8.41	12.49	8.43	7.81
Sum	99.93	100.47	99.13	99.57	100
FeO^t	8.18	8.37	4.23	8.92	9.52
FeOt/MgO	1.43	0.26	0.24	0.30	0.37
Mg#(atomic)	55.54	87.41	88.04	85.52	82.70
Rb	17	3.38	2.27	13.17	14
Sr	885	29.47	24.04	81.86	120
Ba	329	86.73	16.57	124.98	103
Sc					36
Nb	10				
Zr	32	14.47	7.8	12.37	36
Y	13	2.44	0	2.27	10
Cr	123	2086	1074	3343	2800
Ni	47	1884	1286	944	770
Cu	8	89.05	44.46	41.28	15.5
Zn	91	93.88	33.04	82.98	66
V	156	54.69	0	78.89	91
La		2.58	2.11	4.07	
Ce		4.36	3.3	8.68	
Pr		0.68	0.5	1.29	
Nd		1.2	0.24	4.04	
Sm		0.63	0.33	1.21	
Eu		0.19	0.09	0.36	
Tb		0.12	0.01	0.15	
Dy		0.95	0.34	0.94	
Ho		0.11	0	0.13	
Er		0.6	0.17	0.57	
Tm		0.11	0.03	0.08	
Yb		0.49	0.08	0.49	
Lu		0.09	0.03	0.08	
CIPW norm*					
Q	3.72		20.8		
or	2.84	0.41		2.54	3.6
ab	29.79	4.06		2.79	6.09
an	31.51	9.75	6.58	5.73	8.17
di	10.87	3.97	27.55	18.42	23.89
hy	13.96	28.41	42.75	20.52	17.69
ol		50.52		47.17	32.52
mt	5.65	2.51	2.29	2.46	7.55
il	1.12	0.44	0.15	0.38	0.4
ap	0.53	0.05	0.05	0.16	0.09
Total	99.99	100.12	100.15	100.18	100.01
AN	51.41	70.6	100	67.25	57.29

* Norms are calculated from analyses that have been normalized volatile-free.

YB89-8: Gabbro from plug near Cobden, Brown County

MRV-1: Serpentinized peridotite from plug south of Franklin, Renville County

MRV-2: Silicified peridotite from Franklin plug

EX-C1-299: Serpentinized peridotite from plug near Albany, Stearns County

P-14B: Phlogopite-olivine pyroxenite, plug near Little Falls, Morrison County

However, neither true kimberlite inclusions nor kimberlite indicator minerals have been found in the Minnesota pipes or superjacent sedimentary strata, and the area has been largely dismissed as prospective for diamonds.

The Garvin anomaly: Inferred source and associated skarn

The Garvin anomaly, located in the Jeffers block near its northern boundary, is a prominent football-shaped feature of the gravity and aeromagnetic fields that is unusual because it is a congruent combination of a weak aeromagnetic low with a strong gravitational high. The combination of low or moderate magnetic susceptibility with high density is not characteristic of common igneous rocks. The position of the anomaly in geologic context is represented in Figure 3 by an igneous intrusion and contact aureole interpreted from the geophysical signatures. The inverse correlation between magnetic and gravity anomalies is especially clear in the first vertical derivative of the magnetic field and the second vertical derivative of the Bouguer gravity field (Fig. 9). Near the center of the aeromagnetic low is a secondary magnetic anomaly of small diameter that is strongly positive (Fig. 9A) and similar in size and shape to anomalies associated with the pipe-like mafic intrusions discussed above.

Core drilling into the inverse anomalies about a kilometer (0.6 mile) from the central magnetic peak encountered a complex suite of metamorphic and metasomatic rock types provisionally interpreted to be a contact skarn (Southwick and others, 1993). The central aeromagnetic peak was not tested by drilling. The rock types that together constitute the contact skarn are: 1. A fine-grained plagioclase-hornblende hornfels that is modally layered on the scale of meters; 2. Conformable calc-silicate marble layers typically 5 to 15 centimeters (2 to 6 inches) thick that are composed chiefly of calcite but also contain variable amounts of grossular, diopside, plagioclase, scapolite, vesuvianite, hornblende, and sphene; and 3. Compositionally zoned, boudinaged, and ptygmatically folded calc-silicate veins a few centimeters thick that traverse both the hornfels and marble. The mineral assemblages, mineral compositions, and zoning patterns in the calc-silicate veins (details presented in Southwick and others, 1993) are highly suggestive of metasomatic reactions between a streaming fluid phase and the confining wall rock. The fluid probably was aqueous, with elevated concentrations of CO_2 and the alkalis, especially potassium. Such a fluid and the heat required to drive metasomatic reactions may have emanated from a magmatic body, possibly a lamproite or lamproite-carbonatite, located deeper beneath the inversely correlated aeromagnetic and gravity anomalies. No other geophysical anomalies like the Garvin or occurrences of lamproite have been identified elsewhere in the MRV or neighboring terranes. The Garvin anomaly therefore seems to be an isolated phenomenon and its petrologic origin remains obscure.

The plutonic body inferred to underlie the Garvin anomaly may be akin to the small plugs of kimberlite, lamproite, carbonatite, and ultra-alkalic syenite that are scattered across the Midcontinent and the Front Range of the Rocky Mountains, such as the Elk Creek carbonatite in southeastern Nebraska (Carlson and Treves, 2005). These compositionally diverse intrusions range in age from Proterozoic to Mesozoic. Some of them are significantly enriched in rare-earth minerals, and given the renewed national interest in developing domestic sources of rare earths for use in electronics and other high-technology applications, a few have become targets for further economic evaluation (Long and others, 2010). The Garvin anomaly warrants reconnaissance-level mineral exploration in this regard.

Mafic intrusions in the southern part of the Montevideo block

Geophysical anomalies interpreted to indicate three discrete gabbro plutons and one diorite pluton are distributed across the southern fourth of the Montevideo block about 10 kilometers (6 miles) north of the Yellow Medicine shear zone (Figs. 3, 6; Southwick, 2002). The westernmost of these, located in the St. Leo metavolcanic belt, has been sampled by drilling and is a massive to weakly flow-foliated olivine ferrogabbro (Table 12; Southwick and others, 1993). Two anomalies located north of Granite Falls have not been drilled but are very similar to the St. Leo anomaly in form and amplitude and are therefore interpreted to have a gabbro source. The easternmost anomaly (Fig. 6), interpreted to derive from a diorite pluton, is similar in form to the St. Leo anomaly but lower in magnetic amplitude. The two gabbro anomalies north of Granite Falls have pronounced aeromagnetic lows near their centers which suggest the presence of granitic cores in the source plutons that may be similar to the monzonite core of the much smaller Cedar Mountain Complex of mid-geon 17 age.

These gabbro and diorite plutons are of more than passing interest because of their possible bearing on other aspects of the regional geology. Goldich and others (1961) obtained K-Ar ages of 1,750 to

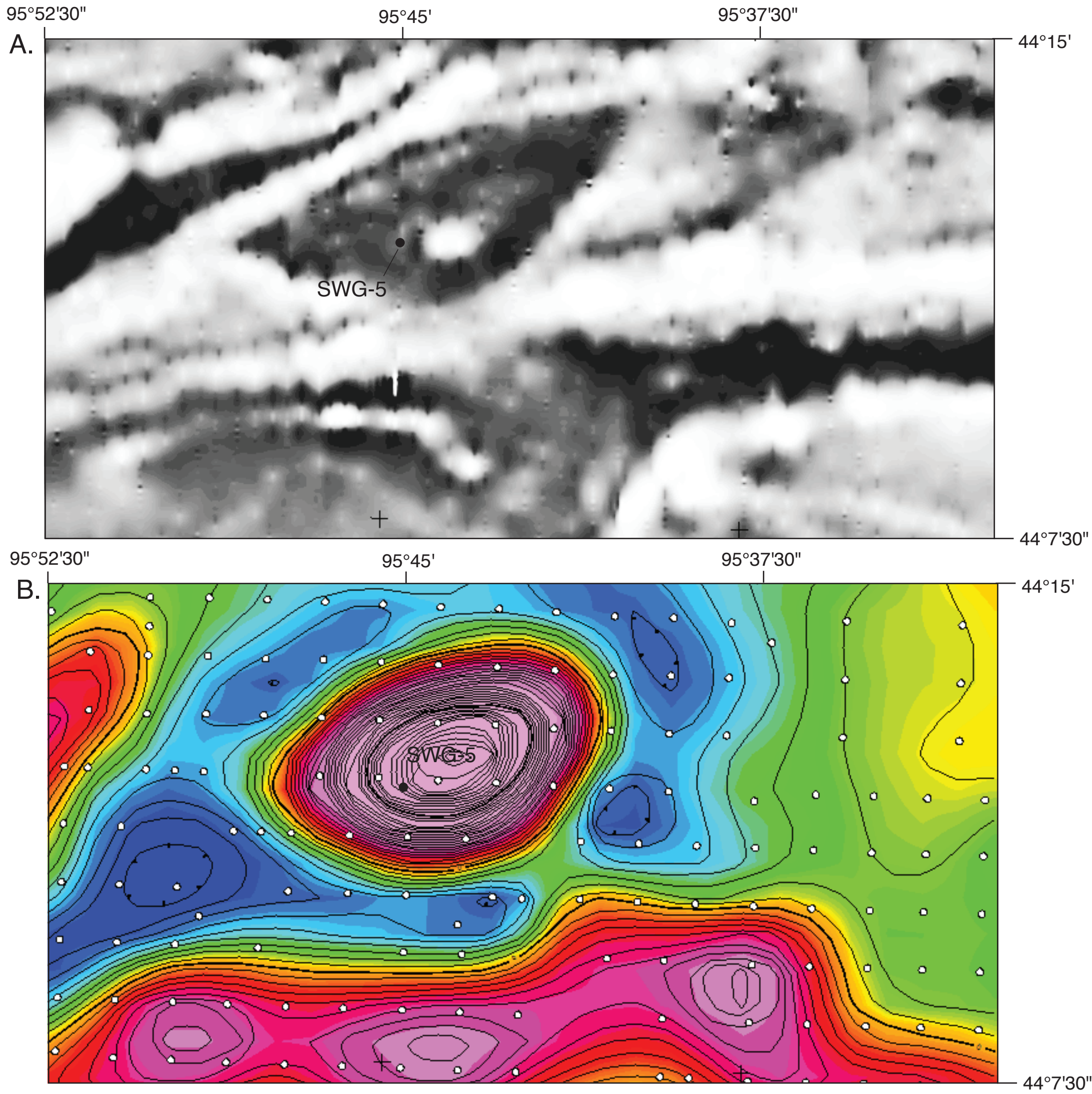

Figure 9. Geophysical images of the Garvin area. Core from drill hole SWG-5 is the source of lithologic descriptions summarized in the text.

A. Gray-scale image of the first vertical derivative of the aeromagnetic map. The Garvin anomaly stands out as a pronounced ovoid low. Approximate range: +500 to -200 nT/km^2 (lightest to darkest shades).

B. Color image of the second derivative of the Bouguer gravity field. The Garvin anomaly stands out as a pronounced ovoid high. Approximate range: +1.5 to -1.5 mgal/km^2 (lightest to darkest shades).

1,850 Ma (mean 1,770 Ma) on biotite, amphibole, and whole-rock samples from Archean rocks north of the Yellow Medicine shear zone and K-Ar ages of 2,400 to 2,500 Ma (mean 2,470 Ma) from Archean rocks south of the Yellow Medicine shear zone. The ca. 2,470 Ma K-Ar ages characteristic of the Morton block, though younger than the emplacement age of 2,600 Ma for the regionally voluminous Neoarchean granite (Schmitz and others, 2006), probably reflect the crustal heating and cooling cycle associated with that episode of granite intrusion. The ca. 1,770 Ma ages characteristic of the Montevideo block indicate a regional resetting of K-Ar systematics in response to a crustal heating-cooling cycle of debatable origin. Southwick and Chandler (1996) proposed that deeper, hotter rocks of the Montevideo block were elevated by a component of reverse-slip movement on the Yellow Medicine shear zone and then cooled beneath the K-Ar blocking temperature in early geon 17.

Table 12. Chemical analyses and CIPW norms of gabbro from the Paleoproterozoic pluton north of St. Leo that intrudes Neoarchean (?) metavolcanic rocks of the St. Leo volcanic belt. Samples are from cores drilled at three different locations within the pluton.

Sample number	ML1-111	ML1-253	YB89-2A
SiO_2	51.1	47.3	45.4
TiO_2	0.39	1.63	4.56
Al_2O_3	7.43	12.8	15.6
Fe_2O_3	1.9	4.1	4.92
FeO	10.8	9.7	9.8
MnO	0.22	0.18	0.17
MgO	16	8.95	4.88
CaO	8.79	9.8	9.82
Na_2O	1.06	2.15	2.59
K_2O	0.14	0.54	0.27
P_2O_5	0.06	0.24	0.52
CO_2	0.92	0.35	
H_2O	0.7	0.8	0.7
S	0.52	0.22	
Sum	100.03	98.76	99.23
FeO^t	12.51	13.39	14.23
FeOt/MgO	0.78	1.50	2.92
Mg#(atomic)	69.53	54.39	37.96
Rb	20	20	8
Sr	140	240	397
Ba	90	160	139
Nb	10	20	18
Zr	<10	30	56
Y	<10	20	13
Cr	1600	300	18
Ni			29
Cu	322		60
Zn	11		94
V			313
CIPW norm			
Q	0	0	2.71
or	0.85	3.28	1.62
ab	9.16	18.68	22.24
an	15.43	24.32	30.59
C	0	0	0
di	23.19	19.47	12.5
hy	46.97	20.62	13.07
ol	0.69	3.77	0
mt	2.81	6.1	7.24
il	0.76	3.18	8.79
ap	0.14	0.58	1.25
Total	100	100	100.01
AN	62.75	56.56	57.90

Alternatively, geon 17 magmatism, especially mafic magmatism, may have been instrumental in conveying heat into mid-crustal levels of the Montevideo block and resetting the K-Ar systematics of the rocks prior to uplift. The gabbro plutons just north of the Yellow Medicine shear zone are direct evidence of mafic magmatic activity but are not by themselves of sufficient volume to have produced a regional-scale thermal impact. Barton and Hanson (1989) have shown that an intrusion density approaching 50 percent of the volume of affected crust is required to engender regional low-grade metamorphism. However, Southwick and Chandler (1996) noted that the Montevideo block as a whole stands out as a broad positive anomaly on regional maps of the Bouguer gravity field. The gravity contrast with the Morton block across the Yellow Medicine shear zone is very evident (Fig. 10). The elevated gravity signature of the Montevideo block relative to that of the Morton block indicates the presence of relatively more dense rock at depth; the nature of this denser material is not known, but large quasi-stratiform intrusions of gabbro, diorite, or ultramafic rocks are a possibility. Such intrusions, if in fact they are present and of geon 17 age, may have contributed substantially to the heating of the Montevideo block. Movement on the Yellow Medicine shear zone (reverse-slip, strike-slip, or both) is inferred to have brought intrusion-heated rocks of the Montevideo block into contact with rocks of the Morton block that were not reheated by early geon 17 magmatism.

The validity of the intrusion-heating hypothesis hinges in part on establishing an early geon 17 age for the causative mafic plutons. Ideally the age question could be addressed directly by drilling the magnetic lows located centrally in two of the gabbro plutons north of the Yellow Medicine shear zone and obtaining precise U-Pb zircon dates on the predicted core granite or monzonite (Fig. 6). An indirect approach to the problem would include: 1. Geophysical modeling to determine the extent of mafic underplating in the Montevideo block, particularly in the vicinity of Granite Falls; and 2. Modern petrologic and geochemical study of the Section 28 granite and its various mafic inclusions to determine whether or not it is plausible to link it petrogenetically to the nearby gabbro intrusions. If the results of these investigations should turn out positive, it would then be worthwhile to obtain a high-precision U-Pb date or series of dates from the Section 28 granite to establish its emplacement age

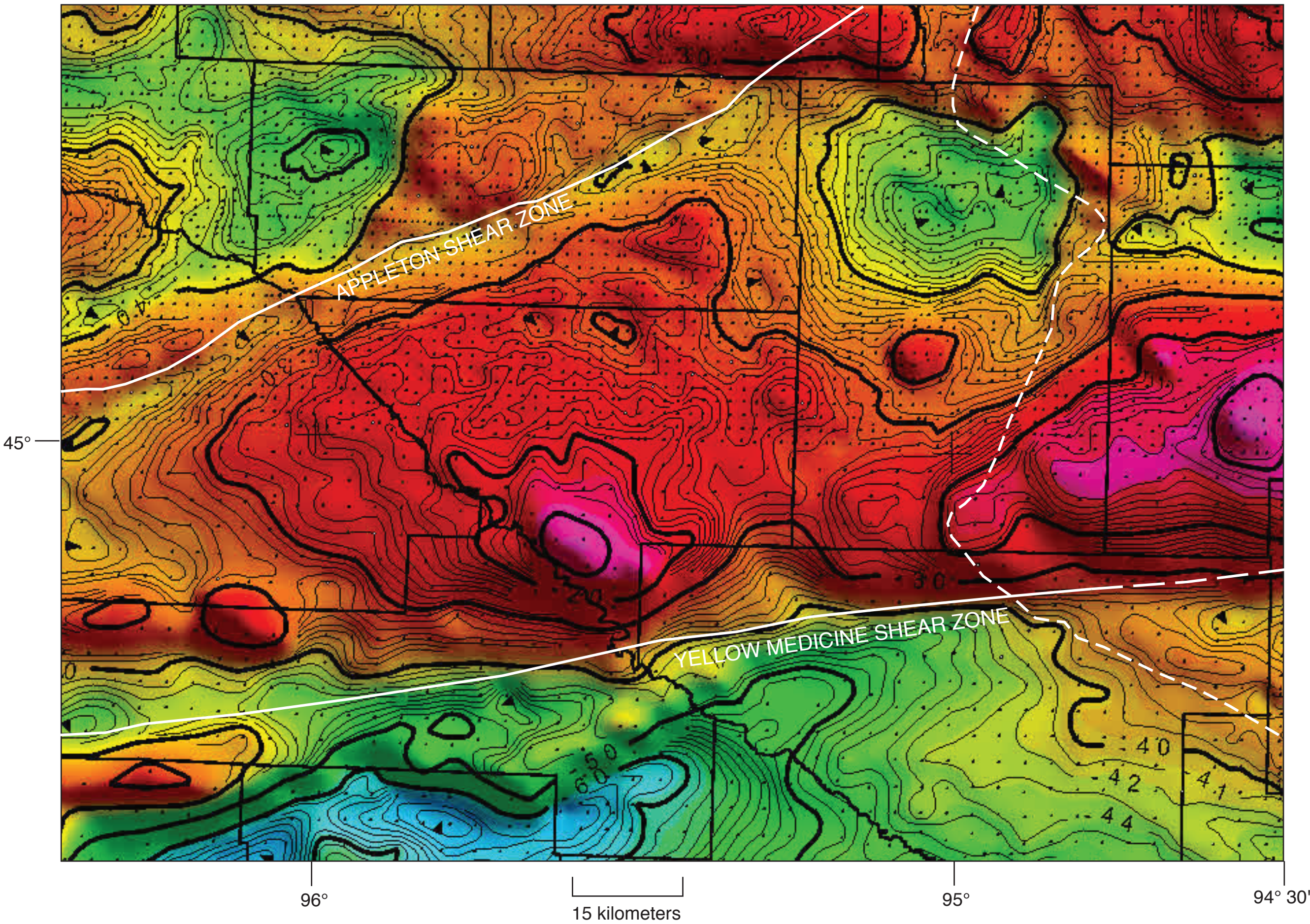

Figure 10. Bouguer gravity map of the Montevideo block and adjacent portions of the Morton and Benson blocks. Contour interval is 10 mgal. Note the pronounced contrast in gravity signature between the Montevideo Block (high; anomaly values consistently greater than -30 mgal) and the Morton block (low; anomaly values consistently lower than -40 mgal). The Yellow Medicine shear zone aligns with the regional east–northeast-trending gravity gradient. The dashed line indicates the approximate contact between the MRV and Paleoproterozoic rocks of the Penokean orogen and the East-Central Minnesota batholith. The area south of 45° N. and west of 94° 30' W. corresponds to the northern part of Figure 3.

and evaluate the possibility of zircon inheritance from the Archean wall rocks. Inherited zircon may have caused the Pb/Pb zircon date of 1,825 Ma obtained by classical multi-grain techniques (Catanzaro, 1963) to be erroneously old.

Plutonic rocks in the south half of the Jeffers block

As mentioned previously, the southern fringe of the MRV (roughly the south half of the Jeffers block) is a transition zone in which the proportion of plutonic rocks increases southward. The plutons so far sampled by drilling range from gabbro to granite in composition (Table 13). The only pluton in this zone that has been radiometrically dated is quartz monzonite (Fig. 3); its U-Pb zircon crystallization age is 1,792 ± 31 Ma and its Sm-Nd TDM age is 2.2 Ga (Van Schmus and others, 2007). These data are consistent with values obtained from various intrusions within the East-Central Minnesota batholith (Holm and others, 2005). Overall, the geophysical, geochemical, and petrographic characteristics of the south Jeffers plutons closely resemble those of the various rock types within the East-Central Minnesota batholith and among the nearby pre-batholithic intrusions (Boerboom and Holm, 2000; Holm and others, 2005).

STRUCTURAL AND TECTONIC CONSIDERATIONS

Penokean structural setting

The tightest bend in the tectonic strike of the Penokean orogen (or its apex, in the terminology of Macedo and Marshak, 1999) is the northwest-facing salient (terminology of Weil and Sussman, 2004) located in east-central Minnesota (Fig. 2). Chandler and others (2007) referred to this salient as the Becker embayment. The cratonic foreland outboard of the Becker salient consists mainly of the Neoarchean Wawa greenstone-granite terrane, whereas the foreland outboard of the companion recess south of the apex (terminology of Weil and Sussman, 2004) consists mainly of the MRV. Chandler and others (2007) interpreted the east-facing recess south of the Becker salient to have been shaped by an east-facing promontory in the pre-Penokean passive margin; likewise, the northwest-facing Becker salient may have been shaped by a passive-margin reentrant developed in thinner and rheologically weaker greenstone-granite crust.

The kinematics involved in the production of curved orogens is complex and challenging to understand from both geologic and mechanical perspectives. The subject has a long research history (for example Weil and Sussman, 2004, and references therein) throughout which the emphasis has been mainly on the origin of curvature within the deforming fold-and-thrust mass. The foreland response to convergent tectonism has been considered mainly in terms of vertical crustal flexure caused by orogenic loading and its role in producing foreland basins and bulges (for example Beaumont, 1981; MacKenzie and Jackson, 2002). For the most part, crustal flexure has been analyzed as a purely geophysical problem in which the crustal deflections are modeled from a number of physical parameters of the lithosphere and the applied loads. Relatively few studies have taken into account the complicating effects of basement structures on flexural profiles in either cross sectional or plan view (for example Lacomb and Mouthereau, 2002; Catuneanu, 2004).

Schulz and Cannon (2007) concluded that closure of the pre-Penokean ocean and subsequent Penokean accretion were directed toward the north–northwest, in which case the crust of the MRV block would have experienced minimal loading. The principal loading would have occurred farther north, where imbricated fold-and-thrust panels were stacked upon a foreland that consisted principally of the Wawa subprovince (Fig. 2). Although the MRV was largely unaffected by convergent Paleoproterozoic tectonism, two west-

Table 13. Chemical analyses and CIPW norms of mafic rocks from intrusions in the southern part of the Jeffers block. These intrusions are inferred to be of geon 17 age.

Sample number	SK1-1080	SK1-1131	RL2-904	SWG3-733	SWG3-738
SiO_2	49.9	47.1	51.2	51.1	51
TiO_2	1.34	1.05	1.08	0.27	0.24
Al_2O_3	15.2	14.9	15.8	17.7	20.7
Fe_2O_3	5.3	5.5	3.69	1.61	1.1
FeO	6.3	7.1	7.1	4.4	3.5
MnO	0.2	0.21	0.18	0.12	0.1
MgO	5.36	6.11	6.08	7.21	5.65
CaO	8	11	6.87	12	12.1
Na_2O	3.56	2.21	3.53	2.55	2.58
K_2O	1.16	1.33	1.43	0.6	0.85
P_2O_5	0.41	0.15	0.26	0.04	0.04
CO_2	0.48	0.56			
H_2O	1	1	1.9	2.2	1.6
S	0.23	0.04			
Sum	98.44	98.26	99.12	99.80	99.46
FeO^t	11.07	12.05	10.42	5.85	4.49
Mg# (atomic)	46.35	47.50	51.00	68.74	69.18
Rb	10	20	60	29	19
Sr	670	340	486	193	208
Ba	400	280	569	124	159
Nb	30	20	14	8	7
Zr	180	80	114	40	37
Y	30	10	15	10	18
Cr	100	400	62	86	57
Ni			64	137	104
Cu			28	144	3
Zn			111	57	53
V			202	130	89
CIPW norm					
Q	1.62	0	0.28	0	0
or	7.09	8.13	8.69	3.63	5.13
ab	31.14	19.35	30.73	22.11	22.31
an	22.82	27.74	23.7	35.94	43.32
C	0	0	0	0	0
di	12.43	22.4	7.81	19.91	14.27
hy	13.35	10.16	20.57	15.07	12.34
ol	0	1.56	0	0.25	0.44
mt	7.94	8.25	5.5	2.39	1.63
il	2.63	2.06	2.11	0.53	0.47
ap	1	0.37	0.63	0.1	0.1
Total	100.02	100.02	100.02	99.93	100.01
AN	42.29	58.91	43.54	61.91	66.01

SK1-1080: St. Killian hornblende diorite; Amselco ddh SK1, Nobles County, Minnesota (Morey and others, 1985, Table 8)

SK1-1131: St.Killian granofels inclusion in granite; Amselco ddh SK1, Nobles County, Minnesota (Morey and others, 1985, Table 8)

RL2-904: Round Lake metadiabase; EXXON ddh RL2, Nobles County, Minnesota (Morey and others, 1985, Table 8)

SWG3-733: Adrian metadiabase; Minnesota Geological Survey ddh SWG3, Nobles County, Minnesota (Southwick and others, 1993, Table 2)

SWG3-738: Adrian metagabbro; Minnesota Geological Survey ddh SWG3, Nobles County, Minnesota (Southwick and others, 1993, Table 2) facing protrusions of Paleoproterozoic rocks into the MRV coincide with the position of the Appleton shear zone and the Yellow Medicine shear zone. This indicates the probable influence of structurally weak regions of MRV crust on the detailed form of the Penokean tectonic front (Chandler and others, 2007). The protrusion of Penokean fold-and-thrust panels onto the MRV in the immediate vicinity of the Appleton shear zone indicates a west-directed component of compressional stress during Penokean convergence. Furthermore, the westward invasion of the East-Central Minnesota batholith along and north of the Yellow Medicine shear zone indicates the probable influence of the old shear zone on the ease of magma emplacement during Yavapai tectonism.

Paleoproterozoic reactivation of major MRV shear zones

General considerations

In this section it is argued that the Great Lakes tectonic zone and the block-bounding shear zones within the MRV were reactivated to varying degrees during Penokean and younger orogenesis. There is little direct evidence available on the nature or magnitude of shear displacements that occurred in the Penokean tectonic cycle. The argument for Penokean reactivation is based on the geometric relationship of the shear zones to the inferred direction of Penokean tectonic transport, and analogy with Penokean-age reactivation of Neoarchean shear zones in other parts of the Superior craton. The evidence for post-Penokean shear displacement is more direct. It includes observed geophysical prolongations of shear zones into Penokean rocks within the Becker salient and Yavapai-age rocks of the East-Central Minnesota batholith, temporal deductions from dike swarms of different relative ages that are disrupted at the shear zones, and small-scale shear phenomena observed in outcrop. The main post-Penokean shear-zone reactivation is inferred to have occurred in geon 17, probably in conjunction with Yavapai orogenesis and subsequent crustal extension and collapse.

The four major shear zones were pre-existing zones of weakness in stiff Archean crust that was tectonic foreland with respect to Penokean convergence and accretion. The shear zones are oriented at a high angle to the Penokean structural front south of the Becker salient but are nearly normal to the inferred north–northwest direction of pre-Penokean crustal extension and Penokean tectonic convergence (Fig. 2; Schulz and Cannon, 2007). Even though the MRV was largely unaffected by penetrative Penokean deformation, it is quite likely that crustal-scale stresses involved in the Penokean tectonic cycle were transmitted into the foreland and that shear components of the regional stress field were resolved onto the shear zones. The regional stress field during the Penokean cycle probably was transtensional (early) and transpressional (later) with respect to the shear zones. Components of subhorizontal shear stress may have been sufficient to cause dip-slip, reverse-slip, strike-slip, or oblique-slip fault displacements at various times. West-directed Penokean thrusts at the east margin of the MRV near the Appleton shear zone (Boerboom and others, 1995; Jirsa and others, 2003) heighten the probability that the Appleton shear zone, specifically, did experience a component of strike-slip deformation during Penokean convergence.

Reactivation of crustal-scale Neoarchean shear zones within the time frame of the Penokean tectonic cycle has been documented in other areas of the Superior craton. Peterman and Day (1989) obtained Rb/Sr dates of about 1.95 Ga from pseudotachylite veins within the Rainy Lake–Seine River and Quetico fault zones in the border zone between the Quetico and Wabigoon subprovinces (Fig. 4). These major transcurrent faults are late-stage manifestations of Neoarchean transpressional deformation associated with southward growth of the craton at ca. 2.68 to 2.69 Ga (Davis and others, 1989); they apparently were reactivated some 700 m.y. later. Rb/Sr dates for fault-zone rocks and neoblastic minerals at several other localities in Canada range from 2.35 to 2.18 Ga, indicating that Paleoproterozoic faulting and fault reactivation were relatively common in much and perhaps most of the Superior craton (Kamineni and others, 1990). Peterman and Day (1989) and Kamineni and others (1990) interpreted the Paleoproterozoic fault movements to be the result of tectonic convergence of Paleoproterozoic orogens (including the Penokean) against the margins of the Superior craton during the formation of the supercontinent Laurentia (Hoffman, 1988).

Although the Rainy Lake–Seine River and Quetico faults developed earlier in Archean time than the Great Lakes tectonic zone and the shear zones within the MRV, their scale and general orientation are comparable to the MRV shears. Therefore, by analogy, it is quite probable that the MRV shear zones also were reactivated in response to Penokean tectonism, and that they moved episodically and in different ways in response to later tectonic events.

Displacements on the Appleton and Yellow Medicine shear zones

The strong geophysical expression of the Appleton shear zone becomes much less distinct east

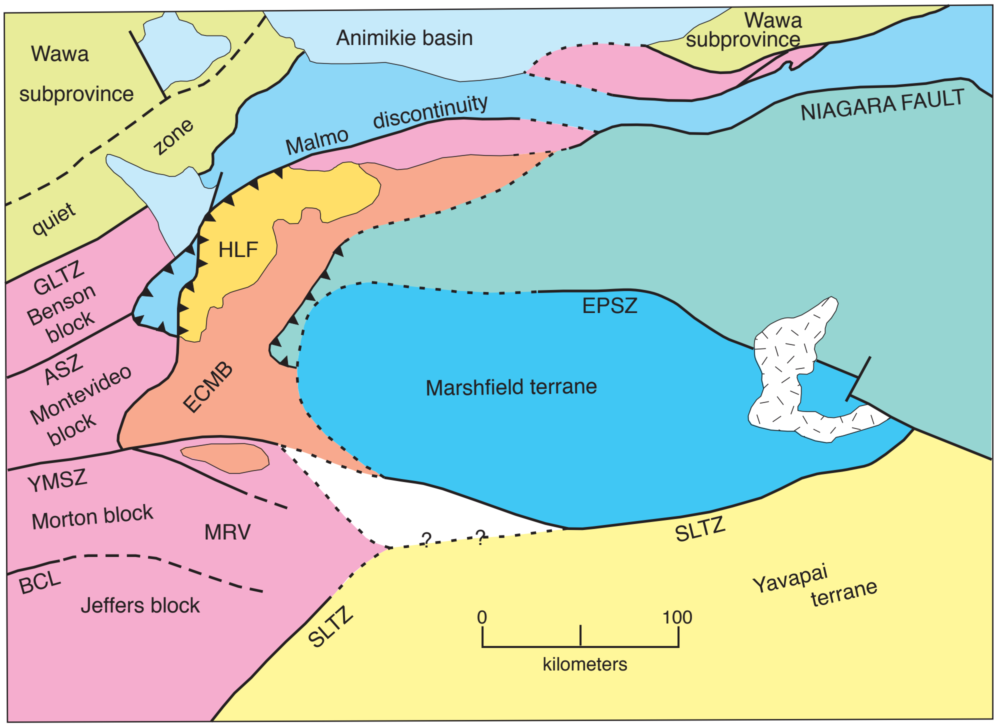

EXPLANATION

- Undifferentiated complex terrane of igneous and metamorphic rocks inferred to have been emplaced and deformed in geon 17.
- Granitic rocks of the East-Central Minnesota batholith (ECMB).
- Tonalite, granodiorite, and high-grade schist of the Hillman–Little Falls (HLF) structural panel. Inlcudes plutonic rocks emplaced at ca. 1,865 and 1,797 Ma.
- Metagraywacke and allied metasedimentary rocks of the Penokean foreland basin.
- Metamorphosed volcanic and sedimentary rocks of the Penokean fold-and-thrust belt.
- Metavolcanic and associated plutonic rocks of island-arc affinity that constitute the Penokean Pembine-Wausau terrane.
- Granite of Penokean age that transects the Eau Pleine shear zone.
- Archean gneiss and superjacent Penokean-age metavolcanic rocks of the Marshfield terrane. Penokean-age fabrics are present in all rock types.
- Neoarchean greenstone-granite terrane of the Wawa subprovince of the Superior craton.
- Mesoarchean and Neoarchean quartzofeldspathic gneiss of the Minnesota River valley subprovince of the Superior craton. Small areas of Archean gneiss involoved in the Penokan fold-and-thrust belt may or may not be MRV equivalents.

Figure 11. Generalized paleotectonic map of eastern Minnesota and western Wisconsin that shows the arrangement of major crustal components prior to the opening of the crosscutting Midcontinent rift in the Mesoproterozoic era; modified from Chandler and others (2007). GLTZ = Great Lakes tectonic zone, ASZ = Appleton shear zone, YMSZ = Yellow Medicine shear zone, BCL = Brown County lineament, EPSZ = Eau Pleine shear zone, SLTZ= Spirit Lake tectonic zone. The present arrangement and location of tectonic elements, including the Midcontinent rift, are shown in Figure 2.

of longitude 95° W., where the zone becomes involved with a complex web of thrust faults interpreted to have formed along the leading edge of the Penokean orogen during its northwest-directed accretion to the Archean foreland (Fig. 11; Boerboom and others, 1995; Jirsa and others, 1995). A major northeast-striking fault mapped by Jirsa and Chandler (1997) that aligns with the Appleton shear zone and defines a 40-kilometer (25-mile) long contact between Penokean supracrustal rocks on the southeast and Archean rocks on the northwest may be a manifestation of foreland block-boundary adjustments along the eastward prolongation of the Appleton shear zone. This fault brings rocks in the Hillman–Little Falls terrane (or its equivalents) that are inferred to be of geon 19 or early to mid-geon 18 age into contact with Archean rocks of the Benson block; moreover, it projects eastward into the Malmo discontinuity, an enigmatic geophysical feature within the Penokean fold-and-thrust belt that has been interpreted to be a deep thrust on which Archean rocks of the McGrath dome moved to a structurally higher position (Southwick and others, 1988). These relationships to structures in the Penokean fold-and-thrust belt strongly suggest the possibility of coincident Penokean movement on the Appleton shear zone west of the Penokean tectonic front.

More concrete evidence of Penokean and post-Penokean displacements on the Appleton shear zone (and also on the Yellow Medicine shear zone, discussed further on) comes from the changes in orientation and abundance of diabase dikes that occur at these block boundaries (Fig. 7). As previously noted, the group I diabase dikes in the MRV (ca. 2.07 Ga) are interpreted to be part of the larger and older sub-swarm of the radial Kenora–Kabetogama/Fort Frances dike swarm. The somewhat younger group II dikes are viewed as an areally smaller sub-swarm of the Kenora–Kabetogama/Fort Frances swarm. The Kenora–Kabetogama/Fort Frances intrusive event is generally interpreted to be a manifestation of plume-driven crustal extension in late geon 20 that was a precursor to or a consequence of the opening of a pre-Penokean ocean basin that closed during convergent Penokean tectonism in mid-geon 18. The well-organized radial pattern of the Kenora–Kabetogama/Fort Frances dikes (both sub-swarms) persists across the southern part of the Wawa subprovince and the Benson block of the MRV but does not continue south of the Appleton shear zone (Fig. 7). This may mean that the southern three blocks of the MRV responded differently to the extensional stress regime responsible for the radial geometry of most of the dike swarm, or that the original dike pattern in those blocks was disrupted by later tectonic events.

The regional dike map (Fig. 7) shows that dikes of all orientations and imputed ages cross the Minnesota segment of the Great Lakes tectonic zone without visible displacement. This indicates that the Neoarchean tectonic weld between the MRV and the rest of the Superior craton held fast through multiple episodes of crustal extension and dike emplacement. Many of the dikes in groups I and II terminate abruptly or are deflected in strike at the Appleton shear zone. These occur in diminished number and somewhat different orientations south of the Appleton shear zone, and appear to have been largely obliterated within the shear zone itself. Dikes of group III, inferred to have been emplaced between 1,772 and 1,750 Ma (Table 7), cross the northeast end of the Appleton shear zone without visible displacement or truncation. The group III dikes also transect supracrustal strata in the outboard structural panels of the Penokean orogen and the granitic plutons of the East-Central Minnesota batholith. These relationships indicate that the Appleton shear zone was a zone of active faulting after 2.07 Ga and before some unspecified late-geon 17 date. This inferred time bracket would admit pre-Penokean, Penokean, and Yavapai reactivation of the Appleton shear zone, including movement that may have coincided approximately with the ca. 1.95 Ga displacement recognized on the Rainy Lake–Seine River fault system far to the north. The Appleton shear zone probably was reactivated more than once in response to changing stress regimes associated with Penokean and Yavapai tectonism. The same is true for the Yellow Medicine shear zone.

The geophysical trace of the Yellow Medicine shear zone curves gradually from east–northeast to east–southeast and more than doubles in width in the vicinity of the Penokean front (Figs. 3, 11). Lozenge-shaped kilometer-scale bodies of rock inferred to be fault-bounded blocks of granite or granodiorite akin to the East-Central Minnesota batholith in composition and age are caught up in this flared portion of the shear zone, which implies that shearing continued past the ca. 1,772 Ma crystallization age of the batholith and related intrusions. Moreover, the southward curvature of the shear zone may indicate that shearing was deflected around the mechanically resistant core of the batholith after its solidification. Aeromagnetic anomalies indicative of group III and IV diabase dikes cross the granitic lozenges and flanking threads of the Yellow Medicine shear zone without deviation (Fig. 7); displacement therefore ceased prior to dike emplacement at an unknown time that was later than roughly 1,772 Ma and earlier than ca. 1,750 Ma, the inferred age of the group IV dikes. In summary, both the Yellow Medicine shear zone and the Appleton shear zone were active zones of foreland deformation in the Paleoproterozoic, whereas the Minnesota segment of the Great Lakes tectonic zone was not.

Further structural details observed in outcrop illustrate the geologic complexity of the Yellow Medicine shear zone on the one hand, and raise perplexing structural questions on the other. Numerous small faults occur in all of the rock types exposed within about 5 kilometers (3 miles) of the Yellow Medicine shear zone, including the 2.07 Ga dikes of group I (Lund, 1956; Himmelberg, 1968; Grant, 1972). Morphologically these faults grade from brittle-ductile shear zones that are less than a meter thick to sharp, slickensided brittle fractures, and it is quite likely that they developed over a span of Proterozoic and perhaps post-Proterozoic time. A single roadcut outcrop of mafic gneiss about 50 meters (164 feet) long located south of Granite Falls contains 22 subvertical shear zones that strike close to az. 070 and contain pseudotachylite seams. Craddock and Magloughlin (2005) have identified and measured a suite of kinematic indicators in these shear zones that record a complex movement history. S-C structures in the country rock and fault drag indicators along shear zone margins indicate predominantly right-lateral displacement (that is, the northwest block is displaced to the northeast). Porphyroclast imbrication within the pseudotachylite seams indicates a shear sense that is dominantly up and easterly. Strains deduced from calcite twinning indicate flattening normal to the seams and near-vertical extension in the shear plane. Magnetic fabric measurements give Kmax vertical and Kmin subhorizontal and zone-normal. Taken together, these data are consistent with a movement plan that involved early right-lateral slip followed by somewhat later subvertical slip during which the pseudotachylite seams developed. Obviously, it would be helpful to have geochronologic confirmation of this inferred movement history, but as yet neither the pseudotachylite veins nor shear-zone minerals have been dated.

Two-dimensional models computed from aeromagnetic and Bouguer gravity data yield a best-fit profile across the Yellow Medicine shear zone in which the primary fault surface dips north–northwest at about 45° and extends downward from the ground surface to depths of more than 5 kilometers (3 miles; Southwick and Chandler, 1996). Inclined faults are very rare in outcrops close to the Yellow Medicine shear zone, whereas vertical and subvertical faults are quite abundant. Although most of the faults and shear zones observed in the field appear to involve no more than a few meters of displacement, the total displacement across tens or hundreds of such faults could easily reach a kilometer or more over the width of the Yellow Medicine shear zone. The vertical and subvertical faults locally cut 2.07 Ga diabase dikes and therefore are Proterozoic structures that presumably offset the more fundamental north–northwest-dipping Neoarchean shears at depth. This inference remains unverified. Unfortunately, the main deformed zone of the Yellow Medicine shear zone is not exposed and cannot be studied directly.

Finally, the previously discussed disparity in K-Ar whole-rock and mineral ages across the Yellow Medicine shear zone is further evidence of geon 17 fault movement. The overall deformation plan at this stage is interpreted to have been extensional and the Montevideo block is interpreted to have moved up relative to the Morton block.

Possible connections across the Midcontinent Rift

Chandler and others (2007) presented a restored geologic map that shows the probable juxtaposition of rock units and structures in the Penokean orogen before their separation by the crosscutting Mesoproterozoic Midcontinent rift (Fig. 11). The rift was closed graphically by converging the opposing sides approximately 60 kilometers (37 miles) in a northwest–southeast direction. This manipulation brings the Marshfield terrane of south-central Wisconsin, which consists dominantly of Archean gneiss and remnants of overlying Paleoproterozoic metavolcanic and metasedimentary rocks, into near alignment with the Montevideo block and Taunton belt in the MRV. In this scenario, the Spirit Lake tectonic zone at the south boundary aligns roughly with the Yellow Medicine shear zone (Fig. 11).

Geologic and geochronologic evidence convincingly supports the conclusion that the Archean rocks in the Marshfield terrane were intimately involved in geon 18 Penokean tectonism (Sims and others, 1989; Sims and Schulz, 1996; Schulz and Cannon, 2007). Furthermore, research on all aspects of the Penokean orogen over the past forty years has led to a robust tectonic model in which the Marshfield gneisses are interpreted to be an exotic fragment of Archean crust caught up in geon 18 accretionary events (Schulz and Cannon, 2007). Apart from their close proximity, there is no evidence that the MRV and the Marshfield terrane were separate pieces of a once continuous cratonic mass, and there is considerable evidence that they were not. Chandler and others

(2007) pointed out that the sigmoidal pattern of potential-field anomalies in the Marshfield terrane is distinctly different from the pattern of broad magnetic and gravity highs associated with the MRV. Moreover, the U-Pb zircon ages between 3,000 and 2,800 Ma for the Marshfield gneisses (Sims, 1989) are significantly younger than the 3,500 to 3,100 Ma ages of various rock types in the MRV orthogneiss complex. It would seem, therefore, that the MRV and Marshfield terrane are not cogenetic and that their near juxtaposition is a fortuitous consequence of complicated Penokean tectonism. The Marshfield terrane probably originated an unknown distance southeast of the MRV and developed independently in the late Mesoarchean era.

A more intriguing feature of the pre-rift reconstruction is the near alignment of the Yellow Medicine shear zone and the Spirit Lake tectonic zone. This alignment obviously does not imply a common origin for the aligned structures, in that the Yellow Medicine shear zone most probably developed during late Neoarchean assembly of the Superior craton (geon 26 or 25), whereas the Spirit Lake tectonic zone is inferred to be a Yavapai (geon 17) suture. Rather, the positioning of these structures appears to have been largely (if not entirely) a random result of Paleoproterozoic deformational events. Even though the Yellow Medicine shear zone and the Spirit Lake tectonic zone formed at different times and by different processes, once the shear zones were aligned they may well have acted as a composite structural zone of weakness that became the locus of post-Penokean faulting. The Yellow Medicine shear zone slices into the south end of the East-Central Minnesota batholith and therefore moved after 1,770 Ma. The Spirit Lake tectonic zone, as a putative Yavapai terrane boundary, is also likely to have been active after 1,770 Ma. Future determinations of fault-zone mineral ages along the Yellow Medicine shear zone in Minnesota and the Spirit Lake tectonic zone in Wisconsin would be most helpful in evaluating the tentative tectonic correlation of these prominent Paleoproterozoic structures.

Summary

The observations and inferences presented above indicate a north-to-south gradation in the duration of shear-zone activity during the Paleoproterozoic era. The Minnesota segment of the Great Lakes tectonic zone, the northernmost of the zones under discussion, apparently moved little if any in response to Penokean or Yavapai tectonism. The Appleton shear zone projects beneath the fold-and-thrust belt of the Penokean orogen and may have to some extent guided the development of regional structures there. Motion on the Appleton shear zone disrupted the orientation and population density of 2.07 Ga diabase dike swarms and did not disrupt dikes emplaced ca. 1.77 Ga. It appears therefore that the major Paleoproterozoic activity on the Appleton shear zone occurred during the Penokean orogenic cycle with perhaps some rejuvenation occurring in Yavapai time. The Yellow Medicine shear zone transects the south end of the East-Central Minnesota batholith and therefore was active in Yavapai and possibly post-Yavapai time. The alignment of the Yellow Medicine shear zone with the Wisconsin segment of the Spirit Lake tectonic zone prior to the intervention of the Midcontinent rift suggests a possible kinetic connection of the two during Yavapai tectonism. This tentative hypothesis merits further consideration and research.

SIOUX QUARTZITE

Regional generalizations

The Sioux Quartzite is a tightly cemented supermature quartz arenite (quartzite) formation that unconformably overlies the Archean and Paleoproterozoic rocks of southwestern Minnesota and adjacent parts of South Dakota and Iowa. Its depositional age is bracketed between 1,729 Ma, the youngest Pb-Pb age so far determined on detrital zircon (Holm and others, 1998), and 1,615 Ma, the oldest Ar/Ar age so far determined on diagenetic muscovite (Hanly and others, 2006). The Sioux Quartzite therefore falls within the Baraboo interval of quartzite deposition (Dott, 1983; Medaris and others, 2003) and is broadly correlative, but not necessarily precisely correlative, with similar sequences of supermature quartzite in Wisconsin. Furthermore, the Sioux Quartzite and the rest of the quartzite units in the southern Lake Superior region appear to be broadly correlative with supermature quartzite sequences in the southwestern United States (Jones and others, 2008) and possibly with some quartzite units on other continents (Karlstrom and others, 2001). Altogether these widely dispersed quartzite occurrences are thought to mark a prolonged interval of tectonic quiescence, intense continental weathering, and polycyclic deposition of chemically mature quartz sand and aluminous, clay-rich mud in sedimentary environments that ranged from fluvial to estuarine to shallow marine (Dott, 1983, 2003; Ojakangas and Weber, 1984; Soegaard and Eriksson, 1985; Southwick and others, 1986; Medaris and others, 2003). Eolian processes may have prevailed at times; Morey (1983) reported the presence of frosted sand grains in the arenite-catlinite sequence of Sioux Quartzite at the Pipestone National Monument in southwest Minnesota. This prolonged quiet time followed Yavapai orogenesis (early- to mid-geon 17) and preceded Mazatzal orogenesis (mid-geon 16). In the Lake Superior region, the quartzite units located farthest southeast (the Baraboo, Waterloo, and other quartzites of south-central Wisconsin) were folded and moderately metamorphosed in the convergent phase of Mazatzal deformation (Holm and others, 1998; Czeck and Ormand, 2007), whereas those located farther northwest (the Barron Quartzite of west-central Wisconsin and the Sioux Quartzite) were not folded, penetratively deformed, or metamorphosed beyond diagenetic grade at any time after their deposition.

Tectonic framework

The Sioux Quartzite most probably was deposited on a south-facing passive continental margin that developed in the rifting stage of the Mazatzal tectonic cycle. It escaped tectonic shortening due to its greater distance from the principal axis of Mazatzal convergence, and perhaps more important, due to its foreland position atop the tectonically strong and thick MRV crustal block.

The poorly constrained depositional age of the Sioux Quartzite overlaps the tightly constrained depositional ages of the quasi-correlative quartzite units of New Mexico and Arizona. Two age groups of quartzite are recognized in the southwestern United States, one having been deposited about 1,705 to 1,695 Ma and the other about 1,665 to 1,660 Ma (Williams, 2003; Jones and others, 2008). Convergent deformation, metamorphism, and plutonism that marked the culmination of Mazatzal tectonic activity occurred between 1,665 and 1,660 Ma. Jones and others (2008) concluded that the quartzite units in the southwestern United States were deposited in local syntectonic basins that opened by tectonic stretching and subsequently closed by thrusting; they further concluded that the structural history and relatively short lifespans of the basins are consistent with a slab-rollback origin during outboard subduction, and that the supermature characteristics of the basin fill were caused by intense diagenetic alteration rather than a prolonged period of subaerial weathering of the source terrain. The tectonic environment inferred for the quartzite units in the southwestern United States is significantly different from that envisioned for the quartzite units of the southern Lake Superior region, including the Sioux Quartzite. However, in both places mature quartz arenite accumulated within tectonic regimes that were fundamentally extensional, and in both places diagenetic alteration was involved in producing the presently observable chemical and mineralogic attributes of the quartzite successions.

If most of the Sioux Quartzite was deposited around 1,700 Ma, say in the interval between 1,710 and 1,695 Ma, then the extending continental margin on which deposition occurred must have begun to develop before 1,710 Ma and possibly as early as 1,730 Ma. Normal faulting and the eventual development of fault-block topography would be expected consequences of this cratonic stretching. Fault-bounded topographic lows, such as graben and half-graben depressions, would have influenced drainage and sedimentation patterns in the subaerial portions of the continental margin where fluviatile processes were dominant. Evidence derived from geologic mapping and topical studies over the past half century that supports this contention is summarized in the following points:

- Master bedding in the Sioux Quartzite is gently tilted (Baldwin, 1951; Ojakangas and Weber, 1984; Southwick and others, 1986). Generally southward dips of about 2° to 10° may include a component of primary depositional slope, but the measured dip values exceed the usual range of primary dips and therefore are regarded as chiefly tectonic, probably the result of normal faulting and block tilting toward the axis of crustal extension. Paleocurrent indicators (manly cross-bedding) show that sediment was transported south and southeastward from sources that lay north to northwest of the present Sioux Quartzite occurrences (Ojakangas and Weber, 1984; Southwick and others, 1986).
- Beds of supermature polymict conglomerate in which the lithic clasts are vein quartz, red and purple quartzite, red chert, iron-formation, and rare silica-rich rhyolite are interstratified with quartzite in the lower part of the stratigraphic succession and occur much less commonly at higher stratigraphic levels (Table 14; also see Baldwin, 1951; Miller, 1961; Ojakangas and Weber, 1984; Southwick, 1994). Zircons from silica-rich rhyolite pebbles in a conglomerate bed in the Pipestone basin yield a discordant U-Pb age of 1,902 ± 55 Ma (Wallin and Van Schmus, 1988), a pre-Penokean age that Van Schmus and others (2007) subsequently revised downward to ca. 1,850 Ma. The rhyolite pebbles are undeformed and display delicate relict textures typical of the glassy, high-silica rhyolite found in modern intracratonic settings. They have been strongly

Table 14. Pebble types and their approximate proportions near the base of the Sioux Quartzite in the New Ulm outlier, Nicollet County, about 2 kilometers (1.2 miles) east–northeast of New Ulm. Field modes are based on outcrop intercept measurements along linear traverses normal to bedding.

	Traverse 1	Traverse 2	Traverse 3	Traverse 4	Sum all four
Intercept, centimeters					
Matrix	62.0	53.3	137.2	123.4	375.9
Vein quartz	19.3	15.2	9.4	13.5	57.4
Red chert	18.8	19.3	14.0	10.2	62.2
Red quartzite	0.0	0.0	7.4	9.4	16.8
Total length	100.1	87.9	167.9	156.5	512.3
Percent					
Matrix	61.9	60.7	81.7	78.9	73.4
Vein quartz	19.3	17.3	5.6	8.6	11.2
Red chert	18.8	22.0	8.3	6.5	12.1
Red quartzite	0.0	0.0	4.4	6.0	3.3
Sum	100.0	100.0	100.0	100.0	100.0

Notes:

- Traverses 1 and 2 measured 36 centimeters (14 inches) apart on outcrop approximately 42 meters (138 feet) south of old Highway 14.
- Traverses 3 and 4 measured 91 centimeters (36 inches) apart on outcrop approximately 162 meters (531 feet) south of old Highway 14.
- Matrix is tightly cemented medium- to very coarse-grained quartz arenite.
- Measured pebble and cobble intercepts are on particles greater than 1 centimeter diameter.

depleted in the alkalis while in the conglomerate, presumably during diagenetic alteration of the entire quartzite section.

- The northern limit of the Sioux Quartzite subcrop in Minnesota is the Yellow Medicine shear zone (Figs. 3, 7). The northern limit in South Dakota is approximately the weakly defined westward projection of the Yellow Medicine shear zone. As previously discussed, K-Ar cooling-age differences across the Yellow Medicine shear zone are consistent with north-side-up fault displacement in mid-geon 17, following the main pulse of Yavapai plutonism. This displacement may have generated topographic highlands north of the Yellow Medicine shear zone that shed detritus southward.
- In Minnesota, the belt of Sioux Quartzite consists of three sub-basins (Fig. 7) that are separated by basement highs, and a small remnant outlier located about 5 kilometers (3 miles) east of the Figure 7 map boundary on the eastern outskirts of New Ulm. These are informally named the Pipestone, Fulda, and Cottonwood sub-basins and the New Ulm outlier. The three sub-basins are elongated northwest–southwest, roughly parallel to geophysical discontinuities interpreted to mark basement faults. Some of these inferred faults are located at or close to basin margins. The erosional remnant at New Ulm is equant in shape and is not related spatially to inferred faults. Northwest-oriented zones of brittle faults mapped within quartzite in the Pipestone and Cottonwood basins (Fig. 3; Southwick, 2002) are interpreted to be manifestations of post-depositional movement on buried basement faults.
- The residual eroded thickness of the quartzite ranges from a few tens of meters (New Ulm outlier) to a kilometer (0.6 mile) or more. Direct measurements of residual thickness from drilling are very sparse and most of the few drill holes completed to basement are located near basin margins, where the preserved quartzite section is thin. A hole drilled to basement in Charles Mix County, South Dakota intersected 1,054 meters (3,458 feet) of quartzite at a location far from basin margins (South Dakota Geological Survey well record 10170101). This is the longest recorded drilling intersection of the Sioux Quartzite and is less than the true original thickness by an unknown amount.

- The basement highs between the sub-basins in Minnesota presently stand at topographic elevations of about 200 to 300 meters (656 to 984 feet) above mean sea level, whereas the elevation of the basal Sioux Quartzite unconformity is locally and perhaps widely as deep as 1,000 meters (3,281 feet) below mean sea level in the Pipestone basin and contiguous areas in South Dakota. Thus the present topographic relief on the sub-Sioux Quartzite basement surface is at least 1,200 to 1,300 meters (3,937 to 4,265 feet). This implies that the basement surface was dissected by valleys (possibly fault-controlled) prior to deposition of the Sioux Quartzite, or that it was displaced by syn- or post-depositional normal faulting into several grabens (or half-grabens) and intervening horsts, or that these processes combined to produce the present basement-surface relief.

Hydrothermal alteration and diagenesis

The Sioux Quartzite contains small but widely distributed amounts of the secondary aluminous minerals kaolinite (or dickite) and diaspore along with abundant secondary quartz (chiefly as epitaxial overgrowths on detrital grains) and minor secondary hematite. Secondary muscovite, illite, and pyrophyllite occur less widely. All the secondary minerals are interstitial to framework quartz in the volumetrically dominant quartz arenite and form a very fine-grained microcrystalline aggregate in the volumetrically minor interbeds of argillite. The timing of secondary mineral growth (variously termed metamorphism, hydrothermal alteration, or diagenesis) has been difficult to determine and confusing to interpret. Vander Horck (1984) and Hanly and others (2006) recognized morphologic subtypes of diaspore and kaolinite (dickite) and independently deduced a paragenetic sequence of mineral formation in the quartz arenite cement that is based on petrographic observations and scanning electron microscope imaging. In much of the arenite, hematite grain coatings and epitaxial quartz overgrowths were deposited first, followed paragenetically by the deposition of early diaspore (two morphotypes), dickite (two morphotypes), illite, and late diaspore (two morphotypes). Paragenetically later muscovite and pyrophyllite are relatively rare, the muscovite occurring mainly in the lowermost few meters of section just above the basal unconformity and the pyrophyllite occurring mainly in the western parts of the Pipestone sub-basin in Minnesota and South Dakota. The paragenetic sequence appears to indicate successive stages of mineral growth under varying conditions of fluid chemistry and temperature rather than a single cement-forming alteration event.

Hanly and others (2006) obtained Ar/Ar ages ranging from 1,615 to 1,543 Ma on muscovite grains in the quartz arenite that they interpreted from textural criteria to be diagenetic or metamorphic (not detrital) in origin. These ages are significantly older than the Ar/Ar plateau ages of 1,370 ± 10 and 1,280 ± 13 Ma that Medaris and others (2003) obtained from two whole-rock samples of pyrophyllite-bearing argillite (pipestone). Altogether the argon dates appear to indicate a lengthy period of diagenetic alteration that occurred later than the well-documented Mazatzal-age metamorphism and deformation recorded in the Baraboo Quartzite and other quartzites in Wisconsin. However, as Medaris and others have pointed out, some of the scatter in the Ar/Ar results may be attributable to grain-size differences and other variables within analyzed samples that influenced Ar diffusion rates and thus the measured isotope ratios.

The temperatures that prevailed during alteration of the Sioux Quartzite are also difficult to ascertain and interpret. Chemographic analysis constrained by equilibrium dehydration reactions among the aluminous phases in the presence of excess quartz and H_2O indicates crystallization temperatures in pyrophyllite- and muscovite-bearing assemblages that reached 305° to 345° C at P=1 kilobar (Medaris and others, 2003). However, fine grain size is known to influence reaction kinetics and mineral equilibria among kaolinite, diaspore, gibbsite, and pyrophyllite, and the presence of ferric iron in these phases (common in natural materials) adds further uncertainty to temperature estimates derived from calculated phase diagrams (for example Tardy and Nahon, 1985; Trolard and Tardy, 1987). Bauxite formed under ambient weathering conditions commonly contains assemblages of aluminum and iron hydroxides, including diaspore, that would be interpreted as having equilibrated at considerably higher temperatures on the basis of thermodynamic data measured or calculated in the laboratory. A large body of geochemical, mineralogic, and soil science research points to grain size effects in ultra-fine-grained aggregates as the primary cause of this discrepancy. It is possible, therefore, that the estimated temperatures of formation for the fine-grained mineral assemblages in the arenite cements and argillite layers of the Sioux Quartzite are too high by some unknown amount. Nonetheless, the temperature estimates published by Medaris and others (2003) are the best data presently available and must therefore be taken into account in alteration models pertaining to the Sioux Quartzite.

The alteration temperature of greater than 300° C inferred from mineral equilibria that involve pyrophyllite or muscovite is about 100° above the generally accepted range of diagenetic temperatures. The Ar/Ar mineral ages of secondary muscovite and whole-rock argillite indicate a time span of about 330 m.y. during which alteration occurred. Therefore either an abnormally hot thermal regime persisted for a very long time, or a cooler, more normal diagenetic regime was warmed locally by external heat sources.

Three external sources of heat may have affected the Sioux Quartzite basin at different times during its history. These are: 1. Mantle upwelling and rising crustal geotherms that accompanied syndepositional crustal extension (for example Wickham and Oxburgh, 1985); 2. Higher than average radioactive heat production from abundant high-K Yavapai-age intrusions in the sub-Sioux Quartzite basement rocks; and 3. A crustal heat flux generated by intrusions and associated igneous phenomena during and following the geon 14 transcontinental igneous event (Anderson, 1983; Bickford and Anderson, 1993; Medaris and others, 2003). Thermal inputs from extension-related mantle upwelling and decay of radioactive isotopes in basement granites may have contributed to the heating of circulating ground water throughout the physical extent and temporal lifespan of the Sioux Quartzite basin. It is unlikely that this heating was sufficient to boost geothermal temperatures beyond the normal range of diagenesis, however, and low-temperature mineral assemblages of quartz, diaspore, kaolinite (dickite), and illite would be the predicted alteration products during and after the extensional stage of basin development.

Magmatic heat advected from geon 14 intrusions is the most straightforward explanation for boosting the thermal regime into the stability fields of pyrophyllite and muscovite (Medaris and others, 2003). Geon 14 intrusions are well documented in the vicinity of the Baraboo Quartzite in Wisconsin (Anderson and others, 1980) but have not been identified in the vicinity of the Sioux Quartzite. The apparent absence of local geon 14-12 magmatic sources prompted Medaris and others (2003) to develop a far-field hypothesis for heating the Sioux Quartzite to ca. 300° C in the geon 14-12 time interval. In brief, their proposed scenario postulates: 1. The existence of an efficient hydraulic connection between strata located close to the Mazatzal deformational front and the distal foreland strata of the Sioux Quartzite, that is, a hydrologic setup analogous to that in a miogeoclinal foreland basin; 2. Deep circulation of hot ground-water brine through the system that was driven from the south by a combination of a gravitational head in the Mazatzal mountains, continuing tectonic compression, and sediment compaction, that is, the "orogenic" ground-water flow mechanism of Bethke and Marshak (1990); and 3. The re-energizing of the ground-water system in mid-geon 14 when the igneous rocks of the transcontinental magmatic belt were emplaced along the approximate trend of the earlier Mazatzal orogen (Fig. 2).

Although the regional paleohydrogeologic model proposed by Medaris and others (2003) is plausible, a less elaborate alternative for a late-diagenetic thermal pulse is here proposed that is based on two key points. First, pyrophyllite-bearing mineral assemblages are restricted to the western part of the Pipestone sub-basin in Minnesota (Vander Horck, 1984) and the adjoining area of eastern South Dakota. Second, there definitely was post-Sioux Quartzite igneous activity within the area where pyrophyllite occurs. An intrusion of alkali olivine diabase (Sklar, 1982) crops out near Corson, in eastern South Dakota. The diabase clearly transects bedding in the Sioux Quartzite and has metamorphosed nearby silty argillite layers into a gray-black hornfels that contains abundant "schimmer-aggregat" spots interpreted to be pseudomorphic after andalusite. A ground magnetic survey of the outcrop area and information derived from exploration drilling indicate that the diabase at Corson is more or less sill-like in form and occupies an area of several square kilometers in the subsurface. The magnetic survey indicates the probable presence of another subsurface diabase body about 5.5 kilometers (3.4 miles) west of the body that crops out. In addition, essentially identical alkali olivine diabase occurs in an abandoned quarry in East Sioux Falls, about 13 kilometers (8 miles) southwest of the Corson outcrop area, and has been recovered from a depth of 77 meters (253 feet) in a drill hole near Colton, South Dakota, about 33 kilometers (21 miles) northwest of the outcrop locality (Sklar, 1982). It appears, therefore, that alkali olivine diabase intruded the Sioux Quartzite within a broad area of eastern South Dakota. The full geographic extent of this magmatic event, and its age, remain unknown.

There are no geophysical indications of Corson-like intrusions in the Pipestone or Fulda sub-basins in Minnesota. The only documented evidence of igneous rocks invading Sioux Quartzite is in a report by Sardeson (1908) that briefly mentioned mafic dikes that intrude the Sioux Quartzite in the eastern part of the New Ulm outlier. The dikes

Sardeson observed are no longer available for study, the outcrops having been removed to make way for a housing development. Therefore neither the petrologic attributes nor the age of the dikes can be established, but there is no reason to doubt Sardeson's basic observations.

Small intrusions like those known in the Corson area of South Dakota or presumed to be present in the New Ulm outlier in Minnesota would not have been adequate sources of heat by themselves for producing regionally significant thermal anomalies. If, however, there are other as yet unrecognized intrusions of post-Sioux Quartzite age scattered about in deeper levels of the Sioux Quartzite and its underlying basement, or in basement terrane that was formerly covered by the Sioux Quartzite, the combination of these may have generated broader geothermal anomalies that were sufficient to drive pyrophyllite- and muscovite-forming reactions in the argillite layers and the intergranular cement of the quartz arenite. In this connection, coincident aeromagnetic and gravity anomalies indicate the presence of small, subcircular mafic intrusions in the southern part of the Cottonwood sub-basin that could be analogs of the Corson occurrences. The geophysical anomalies do not unequivocally establish a within-Sioux Quartzite or sub-Sioux Quartzite depth for the source rocks and therefore do not resolve the geologic issue of relative age. However, the relatively high amplitude and steep marginal gradients of one anomaly (the Butterfield anomaly on Fig. 7) indicate a relatively shallow source and thus are suggestive of an intrusion that has penetrated the Sioux Quartzite. This interpretation will not be verified until the Butterfield anomaly is drilled.

The validity of this scenario obviously depends on establishing the age of the Corson diabase and/or its contact aureole and finding more intrusions of the same age. The previously discussed hornfels and skarn associated with the Garvin geophysical anomaly would be interesting geochronologic targets in this connection, inasmuch as the causative intrusion at Garvin may be a unique rock type that is located in basement terrane once covered by quartzite (Fig. 3). Other targets are the assorted intrusions mapped between the Pipestone and Fulda sub-basins, a few of which have been drilled and sampled (Southwick, 2002). These are provisionally interpreted to be mainly if not entirely of Yavapai age, but the possibility remains that some are younger. A reconnaissance geochronology program using available samples of these plutonic rocks could yield age data that are relevant to the alteration scenario here proposed.

Regardless of the specific sources of fluids and heat, the alteration history of the Sioux Quartzite is inferred to have progressed in two distinct phases. The earlier and longer phase was the end result of a sedimentary history that involved deep subaerial weathering of a predominantly quartzofeldspathic source area (such as the Archean and older Paleoproterozoic rocks of the MRV); the accumulation of supermature weathering residue in a depositional environment dominated by fluvial braided-stream processes; the continued weathering and reworking of sediment during transport and temporary lodgment in the depositional system; the ultimate accumulation of a thick sedimentary apron on a subsiding continental margin; and deep circulation of ground water driven more or less down-slope by gravity. In this phase the ground water was heated geothermally in the deeper parts of the sediment pile. The geothermal gradient may have been steepened by heating related to crustal extension and mantle upwelling and to the decay of radioelements in basement granitoids that at the time of Sioux Quartzite sedimentation would have been relatively young. The assemblage of fine-grained detrital minerals derived through prolonged, intense chemical weathering would have included kaolinite, gibbsite, aluminum goethite, boehmite, and ultra-fine-grained quartz. Over time these reacted in the warm ground-water environment to secondary assemblages of dickite, diaspore, hematite, and recrystallized quartz that filled much of the pore space in the quartz arenite and became major constituents of the aluminous mudrock interbeds. The second alteration phase occurred at a higher temperature, which was sufficient to stabilize the formation of pyrophyllite and muscovite. The second heating cycle may have been driven by intrabasinal and subbasinal igneous activity (here viewed as most likely), or by far-field tectonic events that propelled hot ground-water from deep basinal environments into shallower settings near the basin margin. The late dickite and diaspore recognized petrographically in arenite (Vander Horck, 1984; Hanly and others, 2006) may have formed in the cooling stage of the second-phase hydrothermal alteration.

SUMMARY AND CONCLUSIONS

1. The Mesoarchean history of the MRV was long and complicated. The principal product of repeated plutonism and deformation was an orthogneiss complex in which the various lithologic components and deformational events range in age between ca. 3,500 and 3,100 Ma (Bickford and others, 2006). The bulk composition

of the orthogneiss complex is approximately granodioritic.

2. The Neoarchean history of the MRV involved the widespread and voluminous intrusion of granitic plutons at ca. 2,600 Ma (Schmitz and others, 2006). An episode of high-grade metamorphism occurred at about the same time. The emplacement of granite and the high-grade regional metamorphism are probably related, and together mark the effective end of Neoarchean convergent tectonism. The fundamental crustal architecture of the MRV was established by ca. 2,600 Ma.
3. The sequences of gneissic rocks that most clearly records the 2,600 Ma metamorphic event are of probable supracrustal origin (Himmelberg, 1968; Grant, 1972; Perkins and Chipera, 1985; Moecher and others, 1986). Their depositional ages are not known and their geologic relationships to the underlying orthogneiss complex have not been established. A Neoarchean depositional age (rather than Mesoarchean) for these paragneiss sequences cannot be ruled out.
4. Metavolcanic and metasedimentary rocks of upper greenschist and lower amphibolite grade occupy the fault-bounded Taunton belt and two subsidiary belts that are tentatively regarded as infolded synformal keels. Except for the metasedimentary sequence of iron-formation and argillite encountered in drill core at Lake Hendricks, near the west end of the Taunton belt, the rock types within these belts constitute a typical Archean greenstone-belt association. The Lake Hendricks rocks are inferred to be of possible Paleoproterozoic age, based largely on analogy with the rock types and alteration history in the Cuyuna district, and therefore the Taunton belt may include an undetermined fraction of Paleoproterozoic (Penokean?) rock throughout its length. The St. Leo metavolcanic belt, located north of the Taunton belt, is close to and directly on strike with one of the enigmatic paragneiss sequences mentioned in conclusion 3. The alignment and proximity of these rocks suggest the possibility of a temporal correlation that can be demonstrated (or disproved) by future geochronologic investigations.
5. An episode of epidote-chlorite hydrothermal alteration affected the northern margin of the MRV and the southern margin of the Wawa subprovince following Neoarchean suturing of the MRV to the Superior craton. The fluids responsible for the alteration may have been channeled along the Great Lakes tectonic zone and subsidiary fracture systems. The alteration preceded the emplacement of the Kenora–Kabetogama/Fort Frances diabase dikes.
6. The southwestern sector of the Kenora–Kabetogama/Fort Frances diabase dike swarm consists of two sub-swarms of differing relative ages. The older sub-swarm, composed of dikes classed as group I in the MRV, includes the Franklin dike dated at ca. 2,067 Ma; the Franklin dike and the other dikes in group I are interpreted to be at the southwestern fringe of the Kenora–Kabetogama/Fort Frances dike swarm as originally defined and described in its type area some 500 to 600 kilometers (311 to 373 miles) to the northeast. The younger sub-swarm consists of group II dikes in the MRV; it may represent a late phase of the main Kenora–Kabetogama/Fort Frances intrusive event (2,077 to 2,067 Ma), or it may represent a separate episode of crustal extension and magmatism.
7. Dikes of groups I and II cross the Great Lakes tectonic zone without visible disruption, displacement, or reorientation. This indicates that the Minnesota portion of the Great Lakes tectonic zone was not significantly involved in Penokean or later tectonic adjustments.
8. Many of the dikes in groups I and II terminate abruptly or are deflected in strike at the Appleton shear zone. The west–northwest-trending dikes of group III cross the Appleton shear zone and the Yellow Medicine shear zone without visible disruption, displacement, or reorientation and intrude the ca. 1.77 Ga East-Central Minnesota batholith. The Yellow Medicine shear zone itself transects the south end of the East-Central Minnesota batholith. The Appleton shear zone therefore was reactivated in the Paleoproterozoic era between 2,077 Ma and the post-batholith emplacement age of the group III dikes, probably as a foreland response to Penokean (geon 18) or Yavapai (geon 17) tectonism, or both. The Yellow Medicine shear zone was activated most recently after the emplacement of the batholith and before the emplacement of the post-batholith group III dikes, during Yavapai tectonism.
9. Movement on the bounding shear zones uplifted the Montevideo block of the MRV in mid-geon 17. This horst-like uplift may have produced a topographic highland that was a major but not exclusive contributor of sediment to the Sioux Quartzite. The crustal mechanisms responsible for uplift are not well understood and pose interesting questions for future research.

10. The south edge of the MRV is full of granitic, intermediate, and mafic plutons. Based on the similarity of their aeromagnetic and gravity signatures to those of geon 17 plutons in east-central Minnesota, plus a small number of direct geon 17 age determinations (Van Schmus and others, 2007), these plutons are inferred to be predominantly of geon 17 age and to indicate an increasing degree of MRV involvement with Yavapai tectonism close to the Spirit Lake shear zone.
11. Deposition of supermature quartz arenite, lithic conglomerate, and mudstone (precursors of the Sioux Quartzite) onto a south-sloping passive continental margin may have begun as early as ca. 1.73 Ga. Fault-bounded depressions influenced local sedimentation patterns, and some depressions became depocenters that are partially preserved as northwest-oriented sub-basins. The sedimentary deposits were lithified and hydrothermally altered in two or more steps over a time span measured in hundreds of millions of years. The first and longest-lasting step was red-bed diagenesis that began as soon as sediment had accumulated to the required thickness and hydrogeochemical conditions were appropriate. Subsequently, igneous activity within and beneath the sediment pile caused the temperature of the hydrothermal system to rise locally from the diagenetic range to ca. 300° to 350° C, within the stability field of pyrophyllite. Argon dates obtained from pyrophyllite-bearing rocks are interpreted to indicate a geon 16 to geon 12 time frame for this superimposed alteration.
12. The deformational style in the MRV in geons 17 and 16 was chiefly extensional and transtensional, involving the reactivation of earlier faults in older Paleoproterozoic and Archean basement and the formation of new faults in the basement and its quartzite cover. The igneous activity during that span of time was mainly "anorogenic." Mafic and intermediate dikes, mafic to ultramafic plugs and pipes, and larger intrusions of a broad compositional range that lack deformational fabrics were emplaced under relatively relaxed crustal conditions. It is possible that extensional tectonism played a much larger role in the middle-Paleoproterozoic cratonization of Laurentia than has been recognized generally. Data that might provide further evidence of widespread extensional tectonism are sparse in the critical covered areas of the central United States. Nevertheless, the ideas on this topic put forward by Bickford and Hill (2007) merit careful consideration and critical evaluation.

ACKNOWLEDGEMENTS

The author is grateful for many years of close collaboration at the Minnesota Geological Survey with G.B. Morey, V.W. Chandler, T.J. Boerboom, M.A. Jirsa, and P.W. Weiblen. Their contributions to this geologic synthesis go well beyond the listed citations of their published work. Morey's thorough review of an early typescript led to significant improvements in content and clarity, and Chandler's critique of the geophysical aspects of the paper led to further improvements.

REFERENCES

Anderson, J.L., 1983, Proterozoic anorogenic granite plutonism of North America, *in* Medaris, L.G., Jr., Byers, C.W., Mickelson, D.M., and Shanks, W.C., eds., Proterozoic geology: Selected papers from an international symposium: Geological Society of America Memoir 161, p. 133-154.

Anderson, J.L., Cullers, R.L., and Van Schmus, W.R., 1980, Anorogenic metaluminous and peraluminous granite plutonism in the Mid-Proterozoic of Wisconsin, U.S.A.: Contributions to Mineralogy and Petrology, v. 74, p. 311-328.

Baldwin, W.B., 1951, Geology of the Sioux Formation: New York, Columbia University, Ph.D. dissertation, 161 p.

Barton, M.D., and Hanson, R.B., 1989, Magmatism and the development of low-pressure metamorphic belts: Implications from the western United States and thermal modeling: Geological Society of America Bulletin, v. 101, p. 1051-1065. Doi: 10.1130/0016-7606(1989)101<1051:MATDOL>2.3.CO;2.

Bateman, R., Ayer, J.A., and Dube, B., 2008, The Timmins-Porcupine gold camp, Ontario: Anatomy of an Archean greenstone belt and ontogeny of gold mineralization: Economic Geology, v. 103, p. 1285-1308. Doi: 10.2113/gsecongeo.103.6.1285.

Bauer, R.L., 1980, Multiphase deformation in the Granite Falls–Montevideo area, Minnesota River valley, *in* Morey, G.B., and Hanson, G.N., eds., Selected studies of Archean gneisses and lower Proterozoic rocks, southern Canadian Shield: Geological Society of America Special Paper 182, p. 1-17.

Bauer, R.L., and Himmelberg, G.R., 1993, Minnesota River valley, *in* The Lake Superior region and

Trans-Hudson orogen, chapter 2 *of* Reed, J.C., Jr., ed., Precambrian: Conterminous U.S.: Geological Society of America, The Geology of North America, v. C-2, p. 31-38.

Beaumont, C., 1981, Foreland basins: Geological Journal of the Royal Astronomical Society, v. 65, p. 291-329.

Beltrame, R.J., Chandler, V.W., and Gulbranson, B.L., 1982, Geophysical investigation of the Cedar Mountain Complex, Redwood County, Minnesota: Minnesota Geological Survey Report of Investigations 27, 20 p.

Bethke, C.M., and Marshak, S., 1990, Brine migrations across North America—The plate tectonics of groundwater: Annual Reviews of Earth and Planetary Sciences, v. 18, p. 287-315.

Bickford, M.E., and Anderson, J.L., 1993, Middle Proterozoic magmatism, *in* Reed, J.C., Jr., ed., Precambrian: Conterminous U.S.: Geological Society of America, The Geology of North America, v. C-2, p. 281-292.

Bickford, M.E., and Hill, B.M., 2007, Does the arc accretion model adequately explain the Paleoproterozoic evolution of southern Laurentia? An expanded interpretation: Geology, v. 35, p. 167-170.

Bickford, M.E., Wooden, J.L., and Bauer, R.L., 2006, SHRIMP study of zircons from early Archean rocks of the Minnesota River valley: Implications for the tectonic history of the Superior Province: Geological Society of America Bulletin, v. 118, p. 94-108.

Blundy, J.D., and Holland, T.J.B., 1990, Calcic amphibole equilibria and a new amphibole-plagioclase geothermometer: Contributions to Mineralogy and Petrology, v. 104, p. 208-224.

Boerboom, T.J., 2007, Bedrock geology, pl. 2 *of* Setterholm, D.R., project manager, Geologic atlas of Todd County, Minnesota: Minnesota Geological Survey County Atlas C-18, scale 1:200,000.

———2014, Bedrock geology, pl. 2 *of* Setterholm, D.R., project manager, Geologic atlas of Morrison County, Minnesota: Minnesota Geological Survey County Atlas C-31, scale 1:100,000.

Boerboom, T.J., and Holm, D.K., 2000, Paleoproterozoic intrusive igneous rocks of southeastern Stearns County, Minnesota: Minnesota Geological Survey Report of Investigations 56, 36 p.

Boerboom, T.J., Setterholm, D.R., and Chandler, V.W., 1995, Bedrock geology, pl. 2 *of* Meyer, G.N., project manager, Geologic atlas of Stearns County, Minnesota: Minnesota Geological Survey County Atlas C-10, pt. A, scale 1:200,000.

Boerboom, T.J., Southwick, D.L., and Severson, M.J., 1999, Bedrock geology of the Mille Lacs Lake 30 x 60 minute quadrangle, east-central Minnesota: Minnesota Geological Survey Miscellaneous Map M-100, scale 1:100,000.

Boyd, N.K., and Smithson, S.B., 1993, Moho in the Archean Minnesota gneiss terrane: Fossil alteration or layered intrusion?: Geology, v. 21, p. 1131-1134.

Buchan, K.L., Halls, H.C., and Mortensen, J.K., 1996, Paleomagnetism, U-Pb geochronology, and geochemistry of Marathon dykes, Superior Province, and comparison with the Fort Frances swarm: Canadian Journal of Earth Sciences, v. 33, p. 1583-1595.

Card, K.D., 1990, A review of the Superior Province of the Canadian Shield, a product of Archean accretion: Precambrian Research, v. 48, p. 99-156.

Carlson, M.P., and Treves, S.B., 2005, The Elk Creek carbonatite, southeast Nebraska—An overview: Natural Resources Research, v. 14, p. 39-45.

Catanzaro, E.J., 1963, Zircon ages in southwestern Minnesota: Journal of Geophysical Research, v. 68, p. 2045-2048.

Catuneanu, O., 2004, Basement control on flexural profiles and the distribution of foreland facies: The Dwyka Group of the Karoo basin, South Africa: Geology, v. 32, p. 517-520.

Chan, Chien-Lu, 1990, The Minnesota River valley peridotites and other selected mantle materials: Minneapolis, University of Minnesota, Ph.D. dissertation, 193 p.

Chandler, V.W., and Lively, R.S., 2007, Aeromagnetic data for Minnesota, final report, black and white first vertical derivative magnetic anomaly map: Minnesota Geological Survey Open-File Report OFR 07-06.

Chandler, V.W, Boerboom, T.J., and Jirsa, M.A., 2007, Penokean tectonics along a promontory-embayment margin in east-central Minnesota: Precambrian Research, v. 157, p. 26-49. Doi: 10.1016/j.precamres.2007.02..009.

Chandler, V.W., and Southwick, D.L., 1985, Regional characteristics of the Kenora–Kabetogama dike swarm, Minnesota and Ontario [abs.], *in* Mafic dyke swarms—International Conference, University of Toronto, Canada, June 4-7, 1985, Abstracts: Sponsored by the International Lithosphere Programme, IUGS Commission on

Tectonics, Geological Survey of Canada, Canadian Geological Foundation, Geological Association of Canada, and Canadian Geophysical Union, p. 29.

Chulick, G.S., and Mooney, W.D., 2002, Seismic structure of the crust and uppermost mantle of North America and adjacent ocean basins: A synthesis: Seismological Society of America Bulletin, v. 92, p. 2478-2492.

Craddock, J.P., and Magloughlin, J.F., 2005, Calcite strains, kinematic indicators, and magnetic flow fabric of a Proterozoic pseudotachylyte swarm, Minnesota River valley, USA: Tectonophysics, v. 402, p. 153-168.

Czeck, D.M., and Ormand, C.J., 2007, Geometry and folding history of the Baraboo syncline: Implications for the Mazatzal orogeny in the north-central U.S.: Precambrian Research, v. 157, p. 203-213. Doi: 10.1016/j.precamres.2007.02.017.

Daggett, M.D., III, 1980, The structure and petrology of the Cedar Mountain Complex, Redwood County, Minnesota: Minneapolis, University of Minnesota, M.S. thesis, 85 p.

Davis, D.W., Poulsen, K.H., and Kamo, S.L., 1989, New insights into the Archean crustal development from geochronology in the Rainy Lake area, Superior Province, Canada: Journal of Geology, v. 97, p. 379-398.

Delaney, P.T., and Pollard, D.D., 1981, Deformation of host rocks and flow of magma during growth of minette dikes and breccia-bearing intrusions near Ship Rock, New Mexico: U.S. Geological Survey Professional Paper 1202, 61 p.

DePaolo, D.J., 1981, A neodymium and strontium isotopic study of the Mesozoic calc-alkaline granitic batholiths of the Sierra Nevada and Peninsular Ranges, California: Journal of Geophysical Research, v. 86, p. 10470-10488.

Dinel, E., Fowler, A.D., Still, A., Tylee, K., and Barr, E., 2008, Lithogeochemical and stratigraphic controls on gold mineralization within the metavolcanic rocks of the Hoyle Pond mine, Timmins, Ontario: Economic Geology, v. 1203, p. 1341-1363. Doi: 10.2113/gsecongeo.103.6.1341.

Doe, B.R., and Delevaux, M.H., 1980, Lead-isotope investigations in the Minnesota River valley—Late-tectonic and post-tectonic granites, *in* Morey, G.B., and Hanson, G.N., eds., Selected studies of Archean gneisses and lower Proterozoic rocks, southern Canadian Shield: Geological Society of America Special Paper 182, p. 105-112.

Dott, R.H., Jr., 1983, The Proterozoic red quartzite enigma in the north-central U.S.—Resolved by plate collision?, *in* Medaris, L.G., Jr., ed., Early Proterozoic geology of the Great Lakes region: Geological Society of America Memoir 160, p. 129-141.

———2003, The importance of eolian abrasion in supermature quartz sandstones and the paradox of weathering on vegetation-free landscapes: Journal of Geology, v. 111, p. 387-405. Doi: 10.1086/375286.

Ernst, R.E., Buchan, K.L., and Palmer, H.C., 1995, Giant dyke swarms: Characteristics, distribution and geotectonic applications, *in* Baer, G., and Heimann, A., eds., Physics and chemistry of dykes: Rotterdam, Balkema, p. 3-21.

Fahrig, W.F., 1987, The tectonic setting of continental mafic dyke swarms: Failed arm and early passive margin, *in* Halls, H.C., and Fahrig, W.F., eds., Mafic dyke swarms: Geological Association of Canada Special Paper 34, p. 331-348.

Gemmell, J.B., and Fulton, R., 2001, Geology, genesis, and exploration implications of the footwall and hanging-wall alteration associated with the Hellyer volcanic-hosted massive sulfide deposit, Tasmania, Australia: Economic Geology, v. 96, p. 1003-1035. Doi: 10.2113/96.5.1003.

Gibbs, A.K., Payne, B., Setzer, T., Brown, L.D., Oliver, J.E., and Kaufman, S., 1984, Seismic-reflection study of the Precambrian crust of central Minnesota: Geological Society of America Bulletin, v. 95, p. 280-294.

Goldich, S.S., and Fischer, L.B., 1986, Air-abrasion experiments in U-Pb dating of zircon: Chemical Geology, v. 58, p. 195-215.

Goldich, S.S., Hedge, C.E., and Stern, T.W., 1970, Age of the Morton and Montevideo gneisses and related rocks, southwestern Minnesota: Geological Society of America Bulletin, v. 81, p. 3671-3696.

Goldich, S.S., Hedge, C.E., Stern, T.W., Wooden, J.L., Bodkin, J.B., and North, R.M., 1980a, Archean rocks of the Granite Falls area, southwestern Minnesota, *in* Morey, G.B., and Hanson, G.N., eds., Selected studies of Archean gneisses and lower Proterozoic rocks, southern Canadian Shield: Geological Society of America Special Paper 182, p. 19-43.

Goldich, S.S., and Wooden, J.L., 1980, Origin of the Morton Gneiss, southwestern Minnesota: Part 3, Geochronology, *in* Morey, G.B., and Hanson, G.N., eds., Selected studies of Archean gneisses and lower Proterozoic rocks, southern Canadian Shield: Geological Society of America Special Paper 182, p. 77-94.

Goldich, S.S., Wooden, J.L., Ankenbauer, G.A., Jr., Levey, T.M., and Suda, R.U., 1980b, Origin of the Morton Gneiss, southwestern Minnesota: Part 1, Lithology, *in* Morey, G.B., and Hanson, G.N., eds., Selected studies of Archean gneiss and lower Proterozoic rocks, southern Canadian Shield: Geological Society of America Special Paper 182, p. 45-56.

Grant, J.A., 1968, Partial melting of common rocks as a possible source of cordierite-anthophyllite-bearing assemblages: American Journal of Science, v. 266, p. 908-931.

———1972, Minnesota River Valley, southwestern Minnesota, *in* Sims, P.K., and Morey, G.B., eds., Geology of Minnesota: A centennial volume: Minnesota Geological Survey, p. 177-196.

Hanly, A.J., Kyser, T.K., Hiatt, E.E., Marlatt, J., and Foster, S., 2006, The uranium mineralization potential of the Paleoproterozoic Sioux basin and its relationship to other basins in the southern Lake Superior region: Precambrian Research, v. 148, p. 125-144. Doi: 10.1016/j.precamres.2006.03.007.

Hanson, G.N., 1968, K-Ar ages for hornblende from granites and gneisses and for basaltic intrusives in Minnesota: Minnesota Geological Survey Report of Investigations 8, 20 p.

Hanson, G.N., and Himmelberg, G.R., 1967, Ages of mafic dikes near Granite Falls, Minnesota: Geological Society of America Bulletin, v. 78, p. 1429-1432.

Himmelberg, G.R., 1968, Geology of Precambrian rocks, Granite Falls–Montevideo area, southwestern Minnesota: Minnesota Geological Survey Special Publication SP-5, 33 p.

Hoffman., P.F., 1988, United plates of America, the birth of a craton—Early Proterozoic assembly and growth of Laurentia: Annual Reviews of Earth and Planetary Sciences, v. 16, p. 543-603.

Holm, D.K., Schneider, D., and Coath, C.D., 1998, Age and deformation of Early Proterozoic quartzites in the southern Lake Superior region: Implications for extent of foreland deformation during final assembly of Laurentia: Geology, v. 26, p. 907-910.

Holm, D.K., Schneider, D.A., Rose, S., Mancuso, C., McKenzie, M., Foland, K.A., and Hodges, K.V., 2007, Proterozoic metamorphism and cooling in the southern Lake Superior region, North America and its bearing on crustal evolution: Precambrian Research, v. 157, p. 106-126. Doi: 10.1016/j.precamres.2007.02.012.

Holm, D.K., Van Schmus, W.R., MacNeil, L.C., Boerboom, T.J., Schweitzer, D., and Schneider, D., 2005, U-Pb zircon geochronology of Paleoproterozoic plutons from the northern mid-continent, U.S.A.: Evidence for subduction flip and continued convergence after geon 18 Penokean orogenesis: Geological Society of America Bulletin, v. 117, p. 259-275.

Jirsa, M.A., 1986, Iron-formations in the subsurface of southwestern Minnesota: Institute on Lake Superior Geology, 32nd Annual Meeting, Wisconsin Rapids, Wis., Program and Abstracts, p. 34.

Jirsa, M.A., Boerboom, T.J., Chandler, V.W., Mossler, J.H., Runkel, A.C., and Setterholm, D.R., 2011, Geologic map of Minnesota—Bedrock geology: Minnesota Geological Survey State Map S-21, scale 1:500,000.

Jirsa, M.A., and Chandler, V.W., 1997, Scientific test drilling and mapping in east-central Minnesota, 1994-1995: Summary of lithologic results: Minnesota Geological Survey Information Circular 42, 105 p.

Jirsa, M.A., Chandler, V.W., Cleland, J.M., and Meints, J.P., 1995, Bedrock geologic map of east-central Minnesota: Minnesota Geological Survey Open-File Report 95-1, scale 1:100,000.

Jirsa, M.A., Chandler, V.W., Lively, R.S., and Boerboom, T.J., 2003, Maps of the bedrock geology and superimposed magnetic on gravity (SMOG) anomaly for east-central Minnesota: Minnesota Geological Survey Miscellaneous Map M-132, scale 1:100,000.

Jones, J.V., III, Connelly, J.N., Karlstrom, K.E., Williams, M.L., and Doe, M.F., 2008, Age provenance, and tectonic setting of Paleoproterozoic quartzite successions in the southwestern United States: Geological Society of America Bulletin, v. 121, nos. 1-2, p. 247-264. Doi: 10.1130/B26351.1.

Kamineni, D.C., Stone, D., and Peterman, Z.E., 1990, Early Proterozoic deformation in the western Superior province, Canadian Shield: Geological Society of America Bulletin, v. 102, p. 1623-1634.

Karlstrom, K.E., Ahall, K.I., Harlan, S.S., Williams, M.L., McLelland, J., and Geissman, J.W., 2001, Long-lived (1.8-1.0 Ga) convergent orogeny in southern Laurentia, its extensions into Australia and Baltica, and implications for refining Rodinia: Precambrian Research, v. 111, p. 5-30. Doi: 10.1016/S0301-9268(01)00154-1.

Kisters, A.F.M., Ward, R.A., Anthonissen, C.J., and Vietze, M.E., 2009, Melt segregation and far-field melt transfer in the mid-crust: Journal of the Geological Society, London, v. 166, p. 905-918. Doi: 10.1144/0016-76492009-012.

Lacomb, O., and Mouthereau, F., 2002, Basement-involved shortening and deep detachment tectonics in forelands of orogens: Insights from recent collision belts (Taiwan, Western Alps, Pyrenees): Tectonics, v. 21, no. 4, p. 12.1-12.22. Doi: 10.1029/2001TC901018.

Long, K.R., Van Gosen, B.S., Foley, N.K., and Cordier, D., 2010, The principal rare earth elements deposits of the United States—A summary of domestic deposits and a global perspective: U.S. Geological Survey Scientific Investigations Report 2010-5220, 96 p.

Lund, E.H., 1950, Igneous and metamorphic rocks of the Minnesota River Valley: Minneapolis, University of Minnesota, Ph.D. dissertation, 88 p.

———1956, Igneous and metamorphic rocks of the Minnesota River Valley: Geological Society of America Bulletin, v. 67, p. 1475-1490.

Macedo, J., and Marshak, S., 1999, Controls on the geometry of fold-thrust belt salients: Geological Society of America Bulletin, v. 111, p. 1808-1822.

MacKenzie, D., and Jackson, J., 2002, Conditions for flow in the continental crust: Tectonics, v. 21, no. 6, p. 5.1-5.7. Doi: 10.1029/2002TC001394.

Manzer, G.K., 1978, Petrology and geochemistry of Precambrian mafic dikes, Minnesota and their bearing on the secular variations in Precambrian basaltic magmas: Houston, Tex., Rice University, Ph.D. dissertation, 217 p.

McSwiggen, P.L., Morey, G.B., and Cleland, J.M., 1995, Iron-formation protolith and genesis, Cuyuna range, Minnesota: Minnesota Geological Survey Report of Investigations 45, 54 p.

Medaris , L.G., Jr., Singer, B.S., Dott, R.H., Jr., Naymark, A., Johnson, C.M., and Schott, R.C., 2003, Late Paleoproterozoic climate, tectonics, and metamorphism in the southern Lake Superior region and proto-North America: Evidence from Baraboo interval quartzites: Journal of Geology, v. 111, p. 243-257. Doi: 10.1086/373967.

Melcher, F., Morey, G.B., McSwiggen, P.W., Cleland, J.M., and Brink, S.E., 1996, Hydrothermal systems in manganese-rich iron-formation of the Cuyuna North range, Minnesota: Geochemical and mineralogical study of the Gloria drill core: Minnesota Geological Survey Report of Investigations 46, 59 p.

Miller, T.P., 1961, A study of the Sioux Formation of the New Ulm area: Minneapolis, University of Minnesota, M.S. thesis, 75 p.

Moecher, D.P., Perkins, D., III, Leier-Englehardt, P.J., and Medaris, L.D., Jr., 1986, Metamorphic conditions of late Archean high-grade gneisses, Minnesota River valley, U.S.A.: Canadian Journal of Earth Sciences, v. 23, p. 633-645.

Morey, G.B., 1983, Evaluation of catlinite resources, Pipestone National Monument, Minnesota: Omaha, U.S. National Park Service, Midwest Regional Office Research/Resources Management Report MWR-4, 48 p.

Morey, G.B., and McDonald, L.L., 1987, Analytical results of the public geologic sample program, 1985-1987 biennium: Minnesota Geological Survey Information Circular 25, 59 p.

Morey, G.B., McSwiggen, P.L., Kuhns, M.J.P., and Jirsa, M.A., 1985, Analytical results of the public geologic sample program, 1983-1985 biennium: Minnesota Geological Survey Information Circular 22, 56 p.

Morey, G.B., and Sims, P.K., 1976, Boundary between two Precambrian W terranes in Minnesota and its geologic significance: Geological Society of America Bulletin, v. 87, p. 141-152.

NICE Working Group, 2007, Reinterpretation of Paleoproterozoic accretionary boundaries of the north-central United States based on a new aeromagnetic-geologic compilation: Precambrian Research, v. 157, p. 71-79. Doi: 10.1016/j.precamres.2007.02..023.

Nielsen, B.V., and Weiblen, P.W., 1980, Mineral and rock compositions of mafic enclaves in the Morton Gneiss, *in* Morey, G.B., and Hanson, G.N., eds., Selected studies of Archean gneisses and lower Proterozoic rocks in the southern Canadian Shield: Geological society of America Special Paper 182, p. 95-103.

Ojakangas, R.W., and Weber, R.E., 1984, Petrography and paleocurrents of the Lower Proterozoic Sioux Quartzite, Minnesota and South Dakota, *in* Southwick, D.L., ed., Shorter contributions to the geology of the Sioux Quartzite (Early Proterozoic), southwestern Minnesota: Minnesota Geological Survey Report of Investigations 32, p. 1-15.

Perkins, D., III, and Chipera, S.J., 1985, Garnet-orthopyroxene-plagioclase-quartz barometry: Refinement and application in the English River subprovince and the Minnesota River valley: Contributions to Mineralogy and Petrology, v. 89, p. 69-80.

Peterman, Z.E., and Day, W., 1989, Early Proterozoic activity on Archean faults in the western Superior province—Evidence from pseudotachylite: Geology, v. 17, p. 1089-1092.

Phinney, W.C., and Halls, H.C., 2001, Petrogenesis of the Early Proterozoic Matachewan dike swarm, Canada, and implications for magma emplacement and subsequent deformation: Canadian Journal of Earth Sciences, v. 38, p. 1541-1563.

Reichardt, H., and Weinberg, R.F., 2012, The dike swarm of the Karakoram shear zone, Ladakh, NW India: Linking granite source to batholith: Geological Society of America Bulletin, v. 124, p. 89-103. Doi: 10.1130/B30394.1.

Sardeson, F.W., 1908, Geological history of the Redstone quartzite: Geological Society of America Bulletin, v. 19, p. 221-242.

Sawyer, E.W., 2010, Migmatites formed by water-fluxed partial melting of a leucogranodiorite protolith: Microstructures in the residual rocks and source of the fluid: Lithos, v. 116, p. 273-286. Doi: 10.1016/j.lithos.2009.07.003.

Schaap, B.D., 1989, The geology and crustal structure of southwestern Minnesota using gravity and magnetic data: Minneapolis, University of Minnesota, M.S. thesis, 78 p.

Schmidt, R.G., 1963, Geology and ore deposits of Cuyuna North range, Minnesota: U.S. Geological Survey Professional Paper 407, 96 p.

Schmitz M.D., Bowring, S.A., Southwick, D.L., Boerboom, T.J, and Wirth, K.R., 2006, High-precision U-Pb geochronology in the Minnesota River valley subprovince and its bearing on the Neoarchean to Paleoproterozoic evolution of the southern Superior Province: Geological Society of America Bulletin, v. 118, p. 82-93.

Schmitz, M.D., Wirth, K.R., and Craddock, J.P., 1995, Major and trace element geochemistry of early Proterozoic dykes of northern Minnesota and southern Ontario, *in* Baer, G., and Heimann, A., eds., Physics and chemistry of dykes: Rotterdam, Balkema, p. 219-233.

Schulz, K.J., and Cannon, W.F., 2007, The Penokean orogeny in the Lake Superior region: Precambrian Research, v. 157, p. 4-25. Doi: 10.1016/j.precamres.2007.02.022.

Sims, P.K., 1989, Geologic map of Precambrian rocks of Rice Lake 1° x 2° quadrangle, northern Wisconsin: U.S. Geological Survey Miscellaneous Investigations Map I-1924, scale 1:250,000.

Sims, P.K., and Day, W.C., 1993, The Great Lakes tectonic zone—Revisited: U.S. Geological Survey Bulletin 1904-S, 11 p.

Sims, P.K., Kisvarsani, E.B., and Morey, G.B., 1987, Geology and metallogeny of Archean and Proterozoic basement terranes in the northern mid-continent, U.S.A.—An overview: U.S. Geological Survey Bulletin 1815, 51 p.

Sims, P.K., and Schulz, K.J., 1996, Wisconsin magmatic terranes, *in* Sims, P.K., ed., Archean and Proterozoic geology of the Lake Superior Region, U.S.A. 1993: U.S. Geological Survey Professional Paper 1556, p. 51-56.

Sims, P.K., Van Schmus, W.R., and Peterman, Z.E., 1989, Tectonostratigraphic evolution of the Early Proterozoic Wisconsin magmatic terranes of the Penokean orogeny: Canadian Journal of Earth Sciences, v. 26, p. 2145-2158.

Sklar, P.J., 1982, Petrologic, petrographic, and paleotectonic investigation of Precambrian mafic intrusives in eastern South Dakota: Iowa City, Iowa, University of Iowa, M.S. thesis, 98 p.

Smithson, S.B., Johnson, R.A., and Hurich, C.A., 1986, Crustal reflections and crustal structure, *in* Barazangi, M., and Brown, L., eds., Reflection seismology: The continental crust: American Geophysical Union Geodynamics Series 14, p. 21-32.

Soegaard , K., and Eriksson, K.A., 1985 , Evidence of tide, storm, and wave interaction on a Precambrian siliclastic shelf: The 1,700 m.y. Ortega Group, New Mexico: Journal of Sedimentary Petrology, v. 55, p. 672-684.

Southwick, D.L., 1994, Assorted geochronologic studies of Precambrian terranes in Minnesota: A potpourri of timely information, *in* Southwick, D.L., ed., Short contributions to the geology of Minnesota, 1994: Minnesota Geological Survey, Report of Investigations 43, p. 1-19.

———2002, Geologic map of pre-Cretaceous bedrock in southwestern Minnesota: Minnesota Geological Survey Miscellaneous Map M-121, scale 1:250,000.

Southwick, D.L., and Chandler, V.W., 1987, Mica-bearing olivine pyroxenite of possible lamproite-kimberlite affinity in central Minnesota: Economic Geology, v. 82, no. 1, p. 212-217.

———1996, Block and shear-zone architecture of the Minnesota River valley subprovince: Implications for late Archean accretionary tectonics: Canadian Journal of Earth Sciences, v. 33, p. 831-847.

Southwick, D.L., and Day, W.C., 1983, Geology and petrology of Proterozoic mafic dikes, north-central Minnesota and western Ontario: Canadian Journal of Earth Sciences, v. 20, p. 622-638.

Southwick, D.L., and Halls, H.C., 1987, Compositional characteristics of the Kenora–Kabetogama dyke swarm (Early Proterozoic), Minnesota and Ontario: Canadian Journal of Earth Sciences, v. 24, p. 2197-2205.

Southwick, D.L., Morey, G.B., Christopher, J.M., McSwiggen, P.L., and Boerboom, T.J., 2005, Preliminary description and interpretation of the "Hattenberger" deep test well, Carlton County, Minnesota: Minnesota Geological Survey Report of Investigations 63, 63 p.

Southwick, D.L., Morey, G.B., and McSwiggen, P.L., 1988, Geologic map (scale 1:250,000) of the Penokean orogen, central and eastern Minnesota, and accompanying text: Minnesota Geological Survey Report of Investigations 37, 25 p.

Southwick, D.L., Morey, G.B., and Mossler, J.H., 1986, Fluvial origin of the Lower Proterozoic Sioux Quartzite, southwestern Minnesota: Geological Society of America Bulletin, v. 97, p. 1432-1441.

Southwick, D.L., Setterholm, D.R., Runkel, A.C., Patterson, C.J., and Chandler, V.W., 1993, Scientific test drilling, 1989-1992: Descriptions and interpretations pertinent to the bedrock geology and quaternary hydrogeology of southwestern Minnesota: Minnesota Geological Survey Information Circular 39, 63 p.

Tardy, Y., and Nahon, D., 1985, Geochemistry of laterites. Stability of Al-goethite, Al-hematite and Fe^{+3}- kaolinite in bauxites and ferricretes. An approach to the mechanism of concretion formation: American Journal of Science, v. 285, p. 865-903.

Tohver, E., Holm, D.K., van der Pluijm, B.A., Essene, E.J., and Cambray, F.W., 2007, Late Paleoproterozoic (geon 18 and 17) reactivation of the Neoarchean Great Lakes tectonic zone, northern Michigan, USA: Evidence from kinematic analysis, thermobarometry and 40Ar/39Ar geochronology: Precambrian Research, v. 57, p. 144-168. Doi: 10.1016/j.precamres.2007.02.014.

Trolard, F., and Tardy, Y., 1987, The stabilities of boehmite, aluminous goethites and aluminous hematites in bauxites, ferricretes and laterites as a function of water activity, temperature and particle size: Geochimica et Cosmochimica Acta, v. 51, p. 945-957.

Vander Horck, M.P., 1984, Diagenesis in the Sioux Quartzite: Minneapolis, University of Minnesota, M.S. thesis, 101 p.

Van Schmus, W.R., Schneider, D.A., Holm, D.K., Dodson, S., and Nelson, B.K., 2007, New insights into the southern margin of the Archean-Proterozoic boundary in the north-central United States based on U-Pb, Sm-Nd, and Ar-Ar geochronology: Precambrian Research, v. 157, p. 80-105. Doi: 10.1016/j.precamres.2007.02.011.

Wallin, E.R., and Van Schmus, W.R., 1988, Geochronological studies of the Archean–Proterozoic transition, north-central United States: Geological Society of America Abstracts and Programs, v. 20, p. 131.

Weil, A.B., and Sussman, A.J., 2004, Classifying curved orogens based on timing relationships between structural development and vertical-axis rotations, *in* Sussman, A.J., and Weil, A.B., eds., Orogenic curvature: Integrating paleomagnetic and structural analyses: Geological Society of America Special Paper 383, p. 1-15.

West, G.F., and Ernst, R.E., 1991, Evidence from aeromagnetics on the configuration of Matachewan dykes and the tectonic evolution of the Kapuskasing structural zone, Ontario, Canada: Canadian Journal of Earth Sciences, v. 28, p. 1797-1811.

Wickham, S.M., and Oxburgh, E.R., 1985, Continental rifts as a setting for regional metamorphism: Nature, v. 318, p. 330-333.

Williams, M.L., 2003 [abs.], Proterozoic rhyolite-quartzite sequences of the Southwest: Syntectonic "cover" and stratigraphic breaks (~1,695 and ~1,660 Ma) between orogenic pulses: Geological Society of America Abstracts with Programs, v. 35, no. 5, p. 42.

Winchell, N.H., and Upham, W., 1888, Volume 2 of the final report, 1882-1885: Minnesota Geological and Natural History Survey, 695 p.

Winkler, H.G.F., 1976, Anatexis, formation of migmatites, and origin of granitic magmas, *in* Winkler, H.G.F., Petrogenesis of metamorphic rocks, 4th ed.: New York, Springer-Verlag, p. 278-324.

Wirth, K.R., Vervoort, J.D., and Heaman, L.M., 1995, Nd isotopic constraints on mantle and crustal contributions to 2.08 Ga diabase dykes of the southern Superior Province: Proceedings of the 3rd International Dyke Conference, Jerusalem, Program and Abstracts, p. 84.

Wooden, J.L., Goldich, S.S., and Suhr, N.H., 1980, Origin of the Morton Gneiss, southwestern Minnesota: Part 2, Geochemistry, *in* Morey, G.B., and Hanson, G.N., eds., Selected studies of Archean gneiss and lower Proterozoic rocks, southern Canadian Shield: Geological Society of America Special Paper 182, p. 57-75.